NOAA Technical Report ERL 383-AOML 25

Oceanographic Variations Across the Gulf Stream Off Charleston, South Carolina, During 1965 and 1966

John B. Hazelworth

September 1976

U.S. DEPARTMENT OF COMMERCE
National Oceanic and Atmospheric Administration
Environmental Research Laboratories

NOAA Technical Report ERL 383-AOML 25

Oceanographic Variations Across the Gulf Stream Off Charleston, South Carolina, During 1965 and 1966

John B. Hazelworth

Atlantic Oceanographic and Meteorological Laboratories
Miami, Florida

September 1976

U.S. DEPARTMENT OF COMMERCE
Elliot Richardson, Secretary
National Oceanic and Atmospheric Administration
Robert M. White, Administrator
Environmental Research Laboratories
Wilmot Hess, Director

Boulder, Colorado

Notice

Mention of a commercial company or product does not constitute an endorsement by NOAA Environmental Research Laboratories. Use for publicity or advertising purposes of information from this publication concerning proprietary products or the tests of such products is not authorized.

CONTENTS

OCEANOGRAPHIC VARIATIONS ACROSS THE GULF STREAM OFF CHARLESTON, SOUTH CAROLINA, DURING 1965 AND 1966

John B. Hazelworth

The ship Peirce of the United States Coast and Geodetic Survey (U.S.C.&G.S.), now the National Ocean Survey (NOS) of the National Oceanic and Atmospheric Administration (NOAA), conducted a physical oceanographic program across the Gulf Stream off Charleston, South Carolina. The project consisted of a series of cruises, one every two weeks, from August 1965 to July 1966. The primary objectives of the program were to investigate the variability of the physical properties and to record the dynamic variability of the Gulf Stream over a period of one year. This report describes the measurements taken and the methods applied to correct and analyze the hydrographic station data. Cross-sections of each physical property for each cruise are presented. Geostrophic currents and volume transport calculations are presented. Results of water mass analysis by use of the T/S curve and also by use of the oxygen-density relationship are given.

1. INTRODUCTION

The Gulf Stream (specifically the Florida Current) was first described by Ponce de Leon in 1513. Since then numerous men have made observations describing it, and others have advanced theories explaining it. Stommel (1965) has an excellent historical summary in which he states that "even now, after many years of effort, our concept of the Gulf Stream is incomplete." He further states "even today we do not have nearly as much accurate synoptic information about the Gulf Stream as we desire".

With this need in mind, oceanographers from several oceanographic laboratories designated 1965 and 1966 as a period of intense study of the Gulf Stream. The U.S.C.&G.S. planned three projects and designated the ships Explorer and Peirce to carry them out.

The Explorer carried out a series of cruises tracking and monitoring the position of the Gulf Stream meanders northeast of Cape Hatteras. The results of this work have been reported by Hansen (1970)

During the same period, the Peirce was assigned the responsibility of obtaining, as nearly as possible, synoptic data across the Gulf Stream by a series of hydrographic casts. To obtain as accurate and detailed information as possible, the Nansen bottles were spaced relatively close together and the distance between stations was relatively short.

A third project, reported by Wunsch et al. (1969), investigated fluctuations of the Florida Current inferred from sea level tide records.

2. FIELD OPERATIONS

The field operations for the Peirce Gulf Stream project lasted one year. Twenty-seven cruises were planned, one every two weeks. Each cruise lasted three to four days. Cruises 13 and 17 were canceled because of bad weather. Cruises 3, 11, and 19 were shortened for the same reason. Table 1 lists the dates of the cruises and the National Oceanographic Data Center (NODC) cruise numbers.

Table 1. Cruise Dates and NODC Cruise Numbers

Cruise No.	Date	Season	NODC Cruise No.
1	3-8 August 1965	summer	718
2	19-23 August 1965	summer	953
3	1-2 September 1965	summer	515
4	15-18 September 1965	summer	705
5	30 September-3 Oct 1965	fall	718
6	12-15 October 1965	fall	721
7	27-31 October 1965	fall	953
8	11-14 November 1965	fall	980
9	1-4 December 1965	fall	721
10	15-18 December 1965	fall	725
11	5-6 January 1966	winter	953
12	11-14 January 1966	winter	961
14	2-5 February 1966	winter	989
15	16-19 February 1966	winter	766
16	3-6 March 1966	winter	766
18	22-25 March 1966	spring	782
19	5-6 April 1966	spring	723
20	18-21 April 1966	spring	782
21	4-7 May 1966	spring	693
22	18-20 May 1966	spring	737
23	1-3 June 1966	spring	694
24	15-17 June 1966	spring	737
25	28-30 June 1966	summer	737
26	12-15 July 1966	summer	769
27	26-28 July 1966	summer	813

According to the original cruise plan, the ship was to go to about 32°22'N and 79°14'W. At that point the direction of the Gulf Stream was to be determined by means of a parachute current drogue. The cruise track was then laid out at right angles to the current direction. During each cruise, 16 oceanographic stations were taken at 10-mile intervals along a 150-mile track line. After taking station 16, the ship would return to station 13 and reoccupy it as station 17. The ship would then proceed towards shore reoccupying each station, for a total of 29 stations. Approximate station locations are given in Table 2. Starting with cruise 20, the track line was revised as shown in Figure 1. The track line described by the odd numbered stations was the approximate track line for the first 19 cruises. The number within the station identification circle indicates the station number for cruise 1 through 19. Also starting with cruise 20, a near-surface parachute current drogue was set out at each even numbered station from 2 to 20. Each drogue was followed for about 30 minutes to one hour and the average current was computed.

Table 2. Approximate Locations of Gulf Stream Stations

Station No.	Latitude	Longitude
1	32°21'N	79°13'W
2	32°12'N	79°10'W
3	32°05'N	79°03'W
4	31°57'N	78°56'W
5	31°48'N	78°50'W
6	31°38'N	78°44'W
7	31°30'N	78°38'W
8	31°20'N	78°32'W
9	31°11'N	78°26'W
10	31°02'N	78°20'W
11	30°53'N	78°14'W
12	30°44'N	78°08'W
13	30°35'N	78°01'W
14	30°26'N	77°55'W
15	30°17'N	77°50'W
16	30°08'N	77°42'W

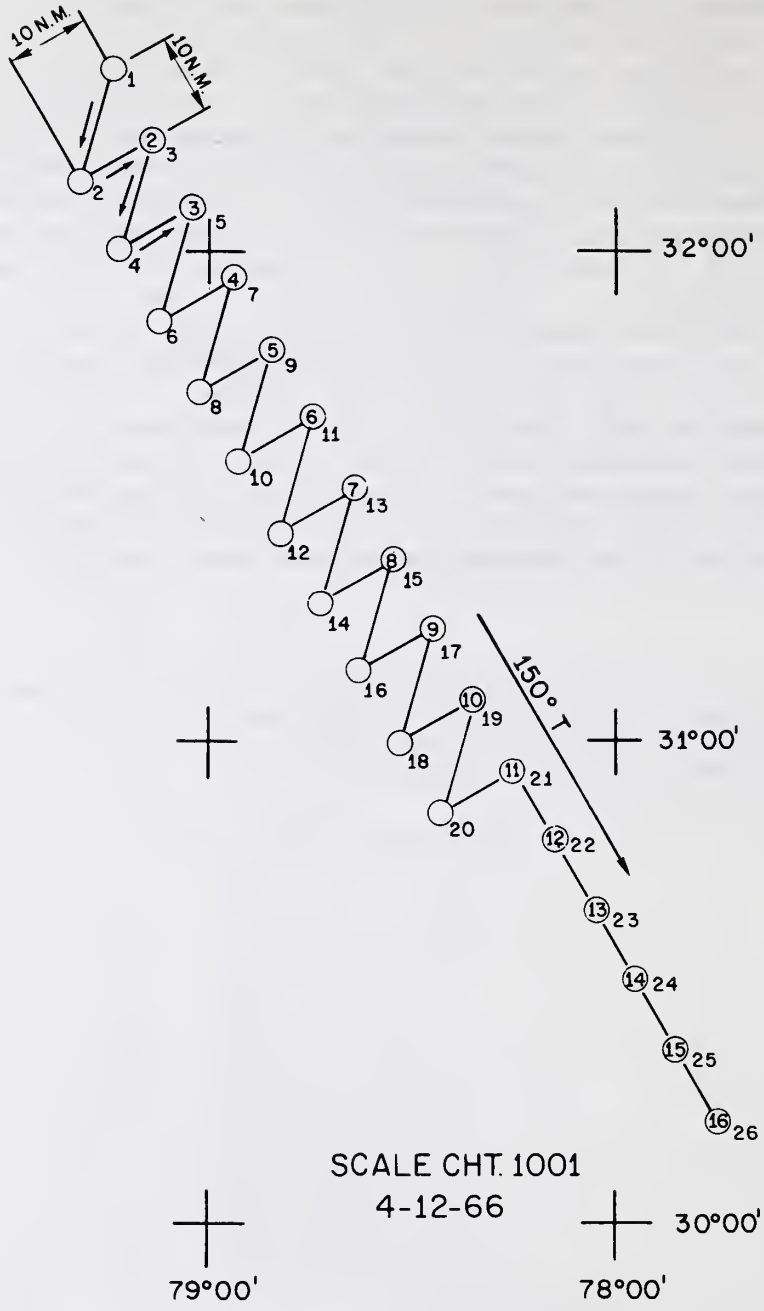

Figure 1. Amended station array, Project OPR-458 Gulf Stream investigation, ship Peirce, 1965-66.

A Nansen cast was taken at each station. Bottles were spaced at 10-m intervals from 0 to 60 m, at 20-m intervals from 60 to 300 m, at 50-m intervals from 300 to 500 m, and at 100-m intervals from 500 m to the bottom. If the station was in water deeper than about 180 m, it was necessary to make two casts.

Primary position locations were determined by LORAN A. Nearshore determinations also were made by HIFIX. Relative positions of the parachute drogues also were made by HIFIX.

Each Nansen bottle held two protected reversing thermometers. In addition an unprotected reversing thermometer was placed on each bottle below 100 m.

3. STATION DATA PROCESSING

Standard thermometer corrections, thermometric depths, and sigma-t values were calculated aboard the ship on a PDP-8 computer. Salinities were determined by using a HYTECH inductive salinometer. Oxygen values were determined by the Winkler method.

At the conclusion of each cruise, the data were processed using standard techniques as outlined by the U.S. Navy Hydrographic Office (1951, 1955). For cruises 1 through 20, the temperature vs. depth, salinity vs. depth, sigma-t vs. depth, oxygen vs. depth and the temperature vs. salinity graphs were hand drawn. Starting with cruise 21, the graphs were drawn by a Cal Comp plotter.

For each cruise, a composite temperature-salinity (T-S) graph was drawn, and individual station observations were compared with it.

When the processing of the serial station data was completed and checked for a cruise, data were sent to the NODC. The NODC calculated sigma-t, specific volume anomaly, dynamic depth, and sound velocity at each observed and standard depth. Temperature, salinity, and oxygen interpolated values also were computed at standard depths.

Before a final computer serial data list was printed, a preliminary listing was reviewed. Sigma-t values were plotted as a check, and hand interpolations of temperature, salinity, and oxygen values at standard depths were made where the computer-calculated values were unacceptable. Final listings were then produced by the NODC.

Unless questioned, the depths of the individual observations are considered to be accurate within 5 m, the temperatures to $\pm$ 0.02°C, and the salinities to $\pm$ 0.01°/oo. When two protected thermometers were used on a Nansen bottle, the average of the two readings was accepted, unless the readings differed by more than 0.05°C. In that case, the more reasonable value was accepted.

One of the following analyses involves seasonal summations of the various oceanographic parameters by station. In these cases, a constant position for each station is assumed. Originally it was intended that station 1 was to be at the same position for all cruises. Successive stations would be located at ten-mile intervals along a straight line at right angles to the current direction. Thus, owing to variation in current direction, the position of a station varied slightly from cruise to cruise. A plot of all stations showed that station 1 varied for all cruises less than one mile. However, the position of each succeeding station ranged over a slightly larger area. Finally station 16 ranged up and down stream from the position given in Figure 1 by as much as 10 miles. It is the opinion of the author that this position variation does not seriously affect the particular analysis, as the position variation for any given station is generally up and down stream and not cross-stream. Also, the greatest position variations occurred at the eastern end of the track line where the parameter variations were the least.

4. COMPUTER COMPUTATION AND PLOTTING

Data sorting and computation of seasonal mean values for each parameter were made by computer. For these mean values, observed data at varying depths could not be used. Rather the interpolated values at standard depths were used. The data were sorted by station and by season, and means were then computed at each standard depth for each oceanographic parameter.

The contour cross-sections were drawn by a Stromberg-Carlson 4020 plotter for each oceanographic parameter for each cruise as well as for seasonal cross-sections. The contour computer program required data at all points of a square matrix. Ideally the points should be equal distances apart. As the data fell far short of these requirements, they had to be manipulated by interpolation procedures. The first interpolation was the computation of standard depths by the NODC. Both observed and standard depth values were used in the matrix computation for the individual cruise cross-sections unless the two were within five meters of each other. Then only the observed values was used. The second interpolation was vertical and linear filling in all points of a 16 x 50 matrix. A third interpolation by weighted means was performed to put the data into a 20 x 20 square matrix. This still was not a true square matrix, as the horizontal distance was 150 miles and the vertical distance was 1000 m.

In spite of the several interpolations, the finished contoured cross-sections agreed quite well with hand drawn ones as long as a sufficient amount of observed data was available. In some cases, holidays occurred. Then interpolation processes took over and the results may be unreliable.

For this reason, on the individual cruise cross-sections each observed data point is indicated by a symbol. The contours also were quite unreliable in the vicinity of a very steep bottom gradient, notably between stations 2 and 3. Station 2 had observed data down to about 50 m and then extrapolated values to 200 m. These values were contoured with the observed values to 200 m at station 3. The results, particularly notable on the water temperature cross-sections, were unacceptable.

The 4020 plots were checked against the original data. Where found to be unreliable the plots were redrawn by hand to fit the original data and then the final contour cross-section plots were drafted.

5. VARIATIONS OF PHYSICAL PROPERTIES

5.1 Temperature

The yearly mean temperature cross-section (Fig. 2) shows that the warmest water appears at the surface in the vicinity of the core of the Gulf Stream. Farther seaward the surface temperature averages about 1°C cooler, while the nearshore end of the time, being somewhat under the environmental influence of the nearby land mass, averaged 3 to 3 1/2°C colder. Water temperature decreased with increased depth. Minimum temperature for the entire cross-section of less than 8°C was observed at stations 3 and 4 in 300 to 350 m. In fact, the water temperature was colder at those stations than at stations 12 through 16 in over 800 m.

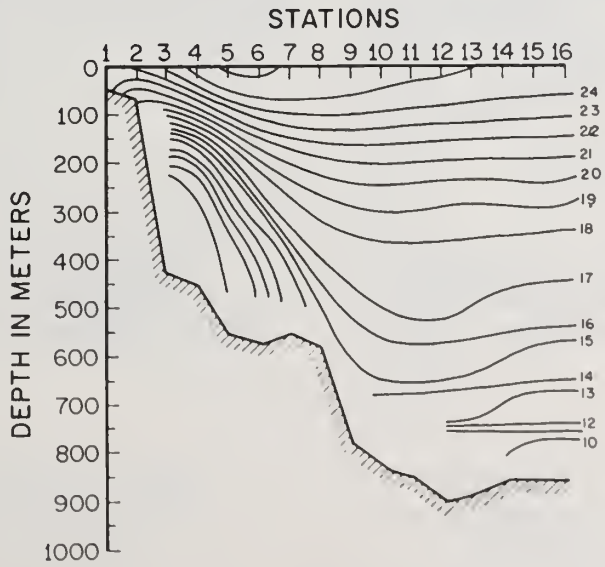

Figure 2. Mean of all cruises water temperature (°C) cross-section.

Throughout the near surface regions (Figs. 3, 4, 5, and 6) seasonal temperature variations were noted. Individual cruise cross-sections are given as Figures 7 through 29. Temperatures were warmest during summer and coldest during winter. The largest seasonal temperature variations were recorded at the nearshore stations. For example, the largest temperature range during the entire year was 9.65°C with a standard deviation of 2.93°C. This was recorded at the surface at station 3. The surface temperature range at station 4 was almost as large, yet the smallest range was found at the next station in the core of the Gulf Stream.

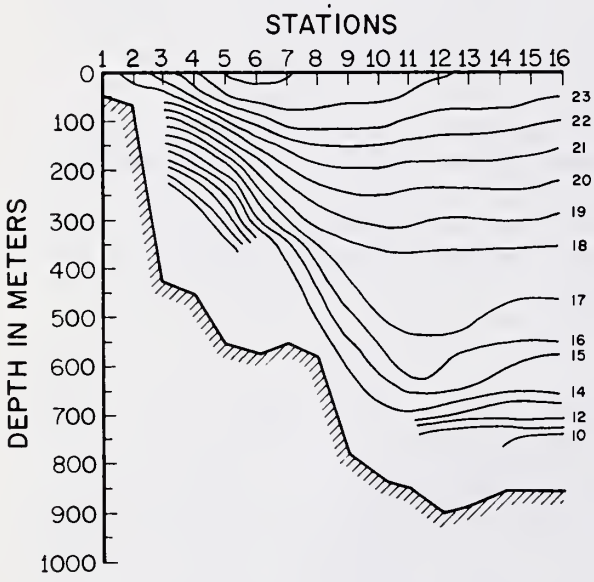

Figure 3. Mean of spring cruises water temperature (°C) cross-section.

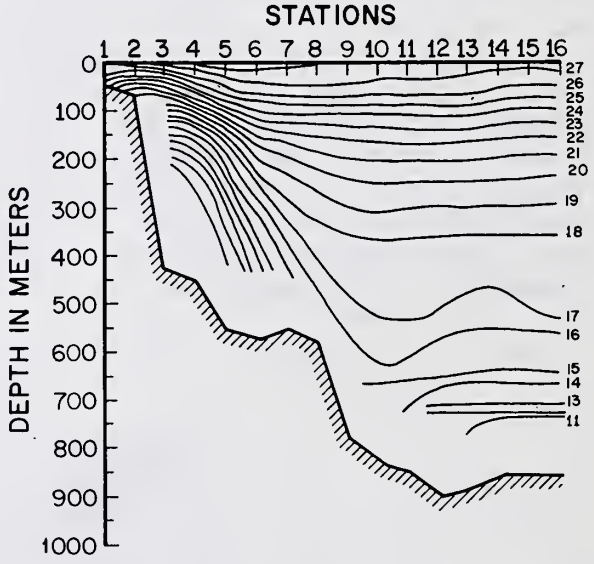

Figure 4. Mean of summer cruises water temperature (°C) cross-section.

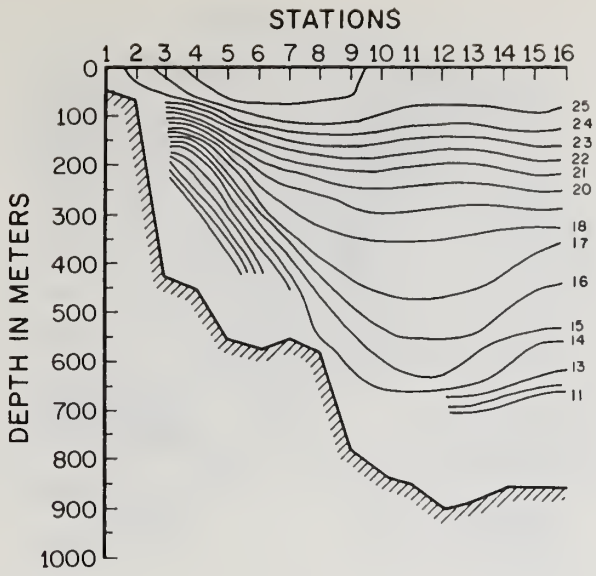

Figure 5. Mean of fall cruises water temperature (°C) cross-section.

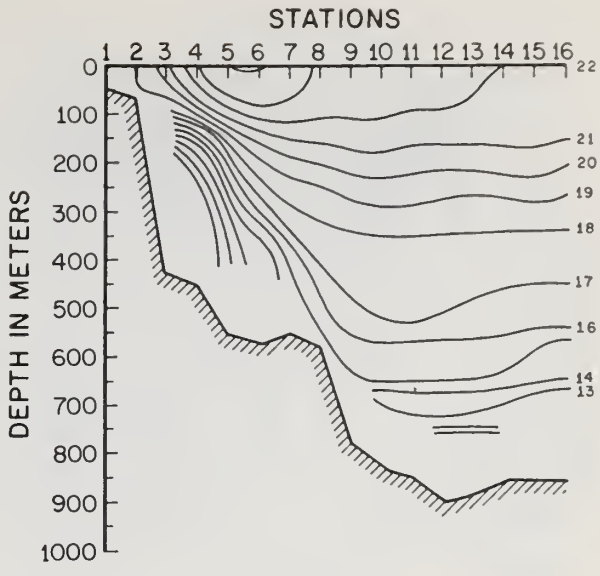

Figure 6. Mean of winter cruises water temperature (°C) cross-section.

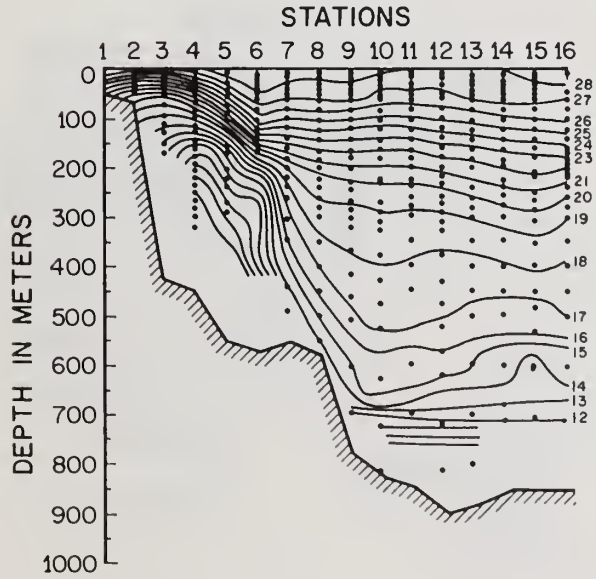

Figure 7. Cruise-1 water temperature (°C) cross-section.

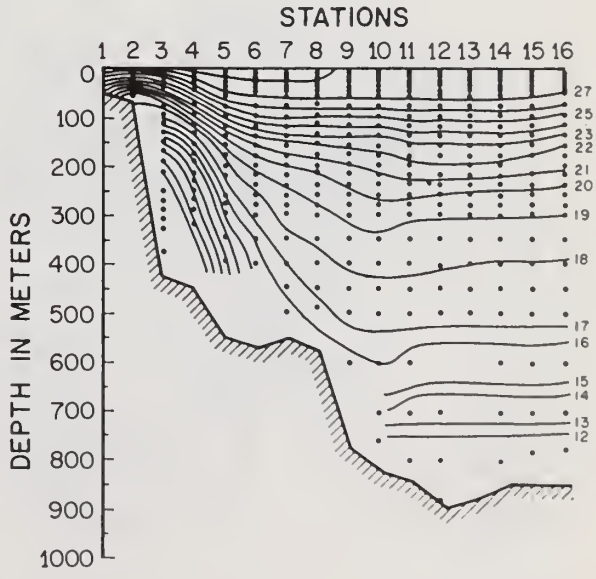

Figure 8. Cruise-2 water temperature (°C) cross-section.

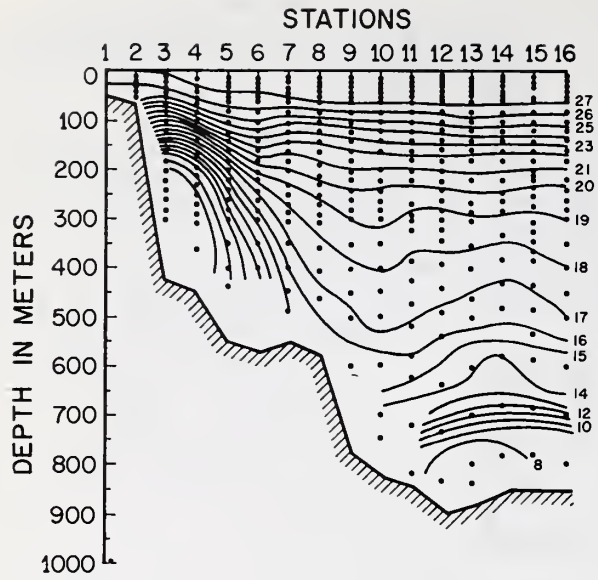

Figure 9. Cruise-4 water temperature (°C) cross-section.

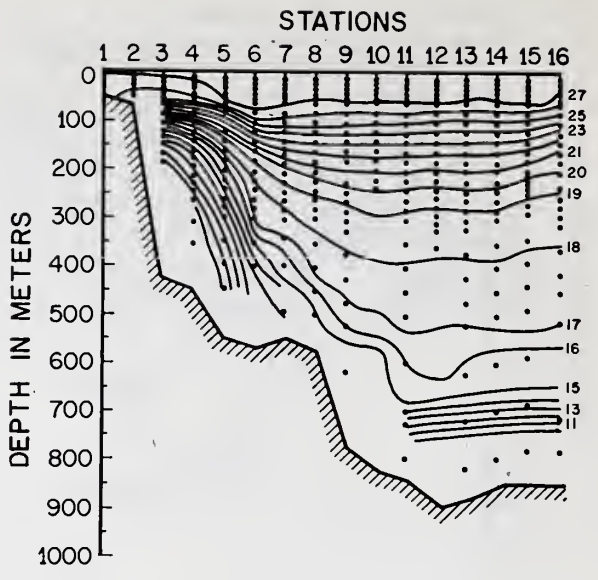

Figure 10. Cruise-5 water temperature (°C) cross-section.

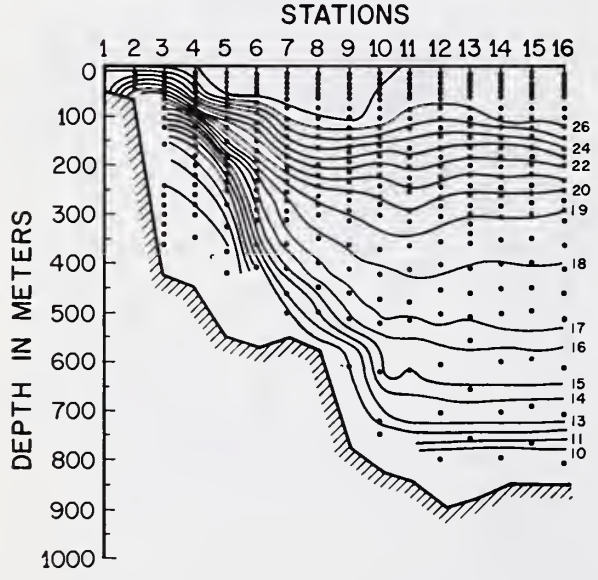

Figure 11. Cruise-6 water temperature (°C) cross-section.

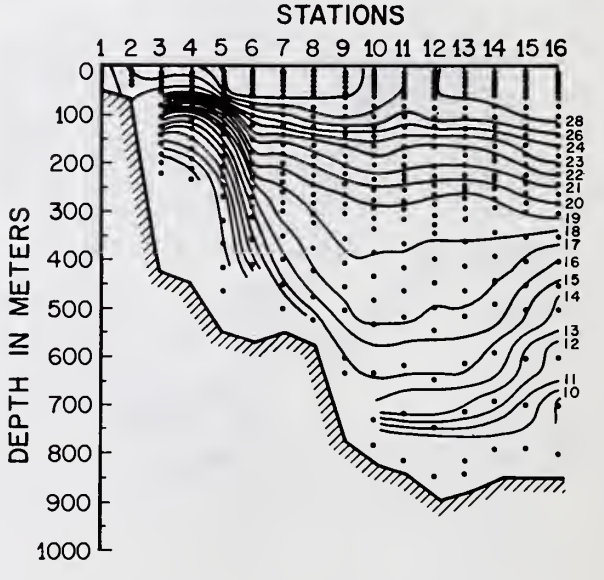

Figure 12. Cruise-7 water temperature (°C) cross-section.

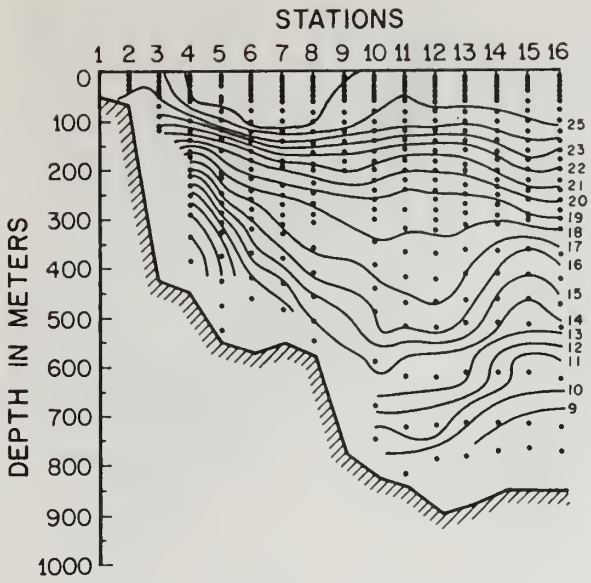

Figure 13. Cruise-8 water temperature (°C) cross-section.

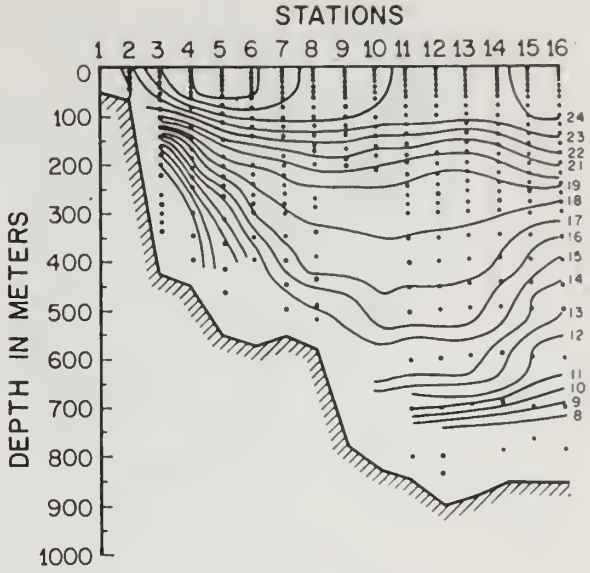

Figure 14. Cruise-9 water temperature (°C) cross-section.

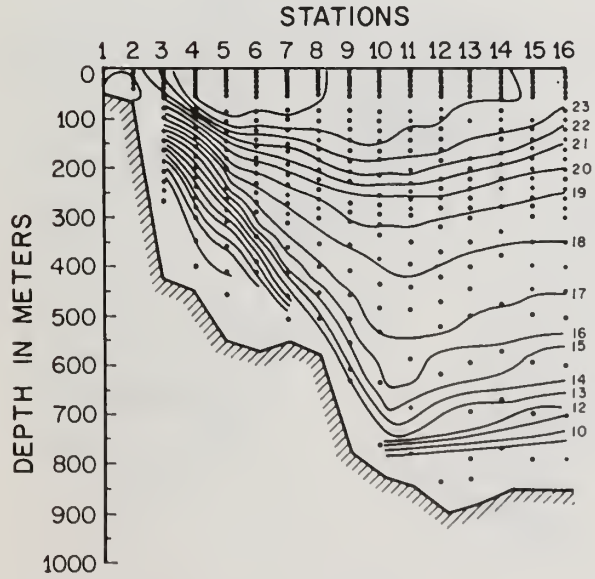

Figure 15. Cruise-10 water temperature (°C) cross-section.

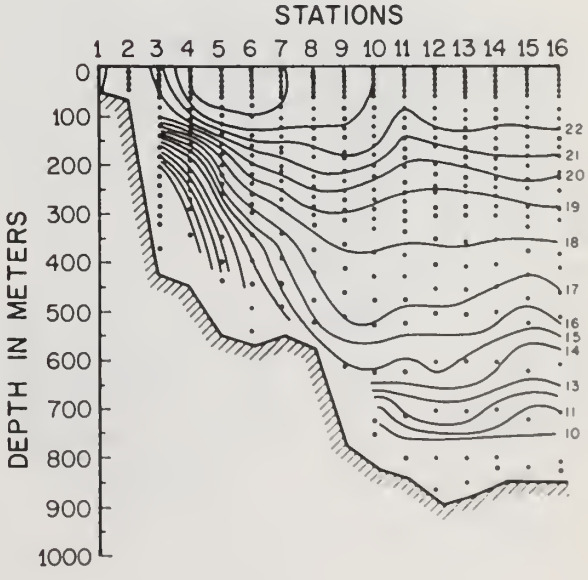

Figure 16. Cruise-12 water temperature (°C) cross-section.

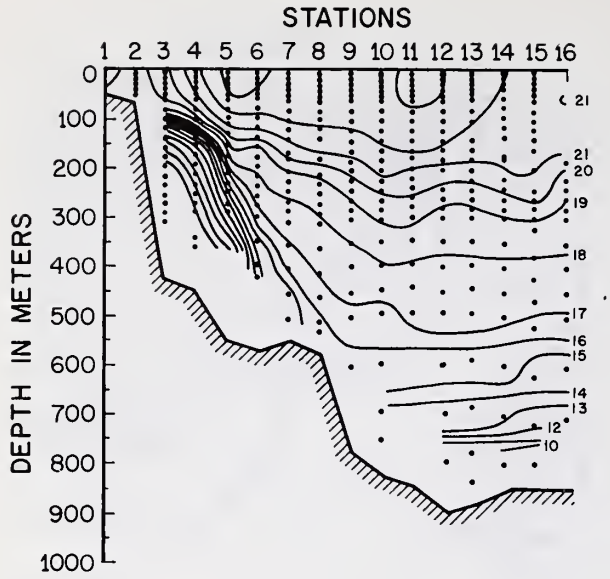

Figure 17. Cruise-14 water temperature (°C) cross-section.

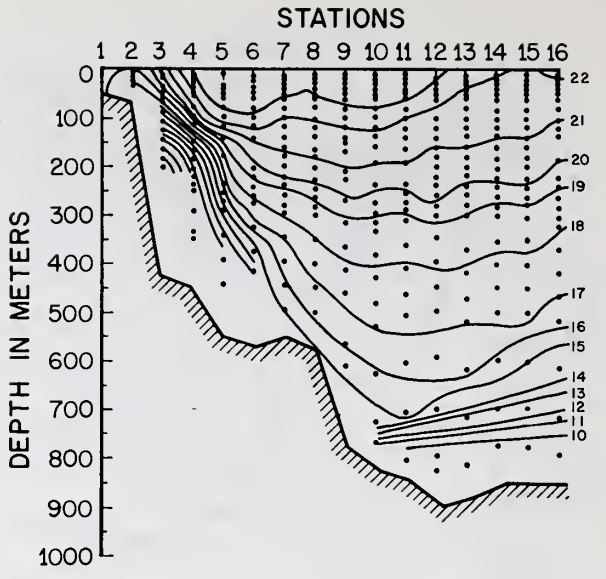

Figure 18. Cruise-15 water temperature (°C) cross-section.

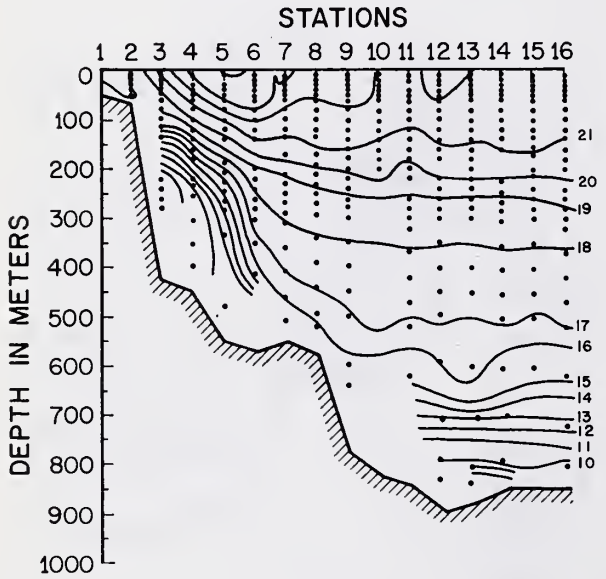

Figure 19. Cruise-16 water temperature (°C) cross-section.

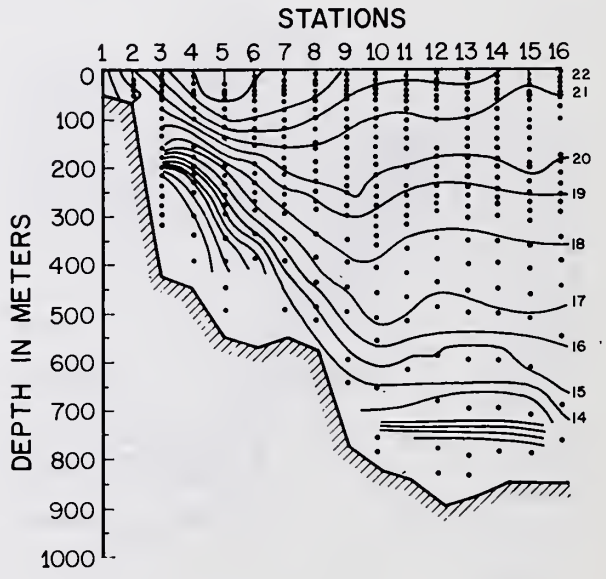

Figure 20. Cruise-18 water temperature (°C) cross-section.

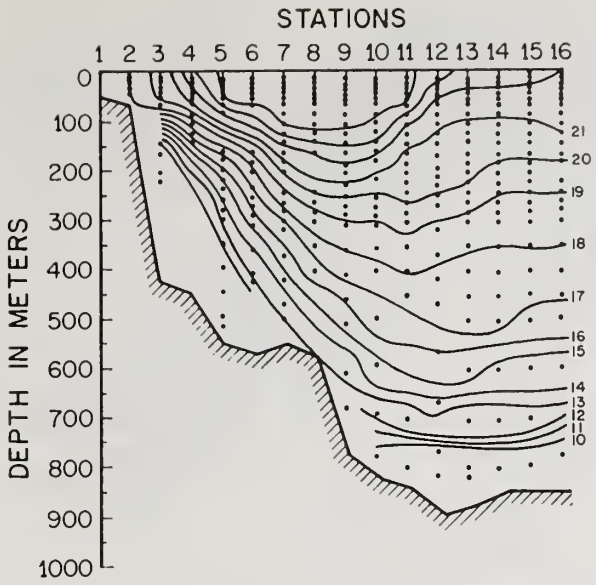

Figure 21. Cruise-19 water temperature (°C) cross-section.

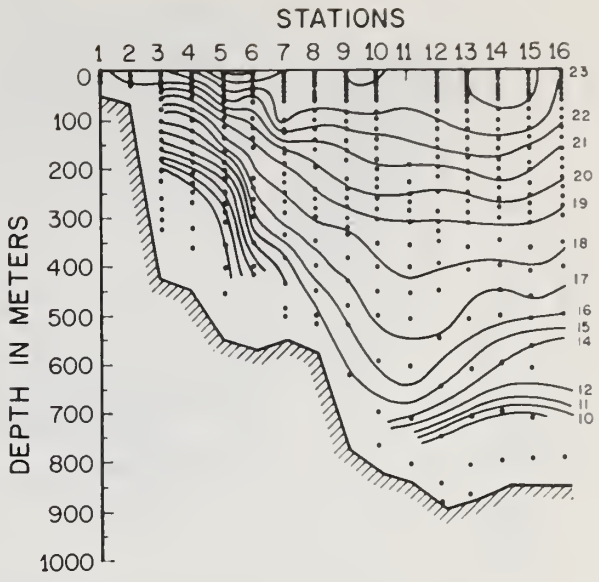

Figure 22. Cruise-20 water temperature (°C) cross-section.

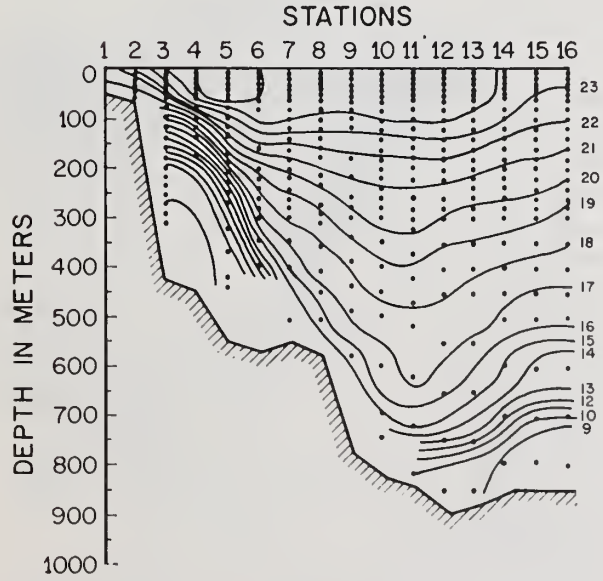

Figure 23. Cruise-21 water temperature (°C) cross-section.

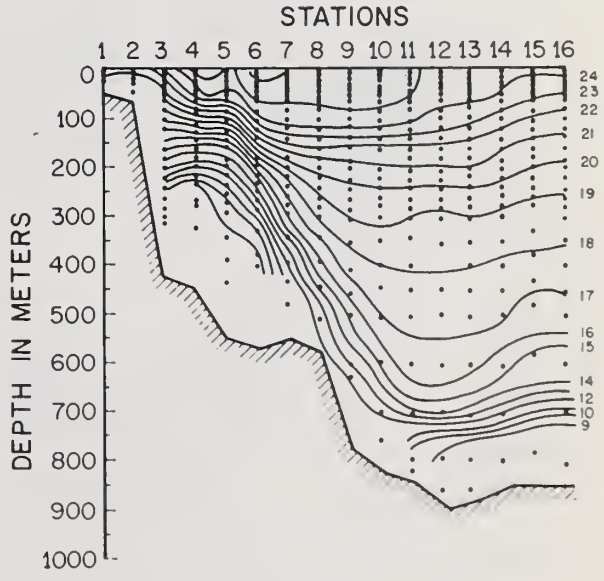

Figure 24. Cruise-22 water temperature (°C) cross-section.

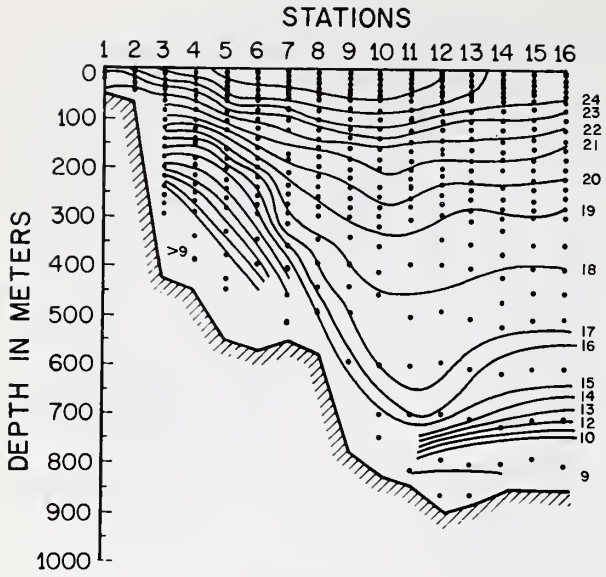

Figure 25. Cruise-23 water temperature (°C) cross-section.

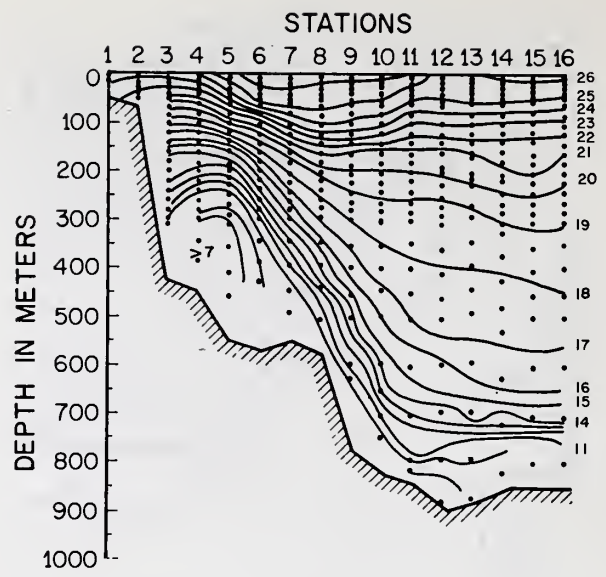

Figure 26. Cruise-24 water temperature (°C) cross-section.

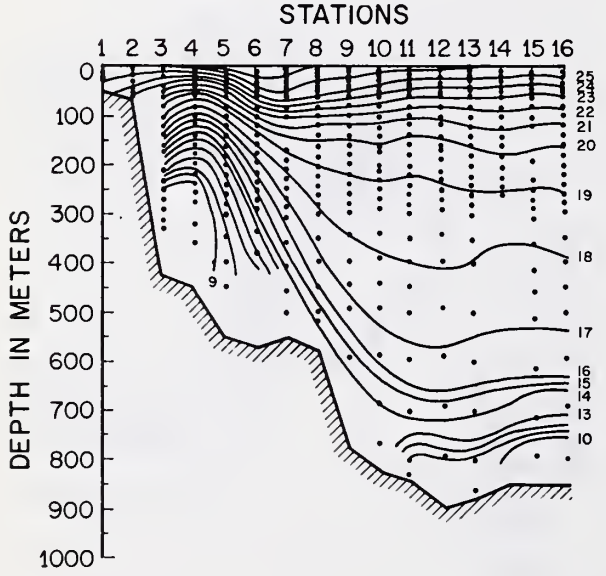

Figure 27. Cruise-25 water temperature (°C) cross-section.

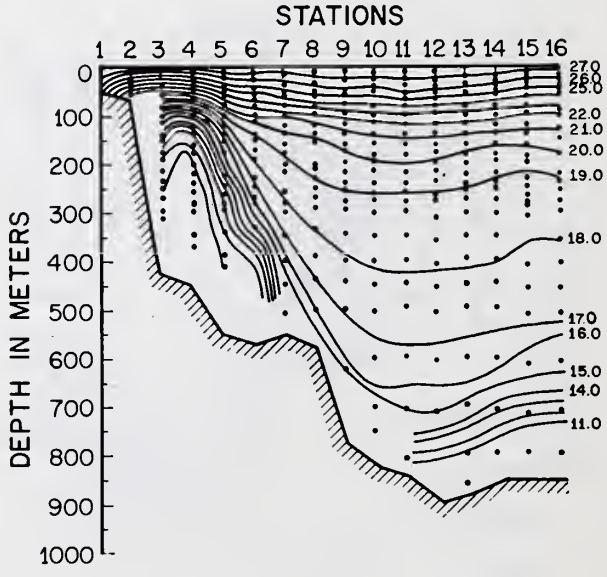

Figure 28. Cruise-26 water temperature (°C) cross-section.

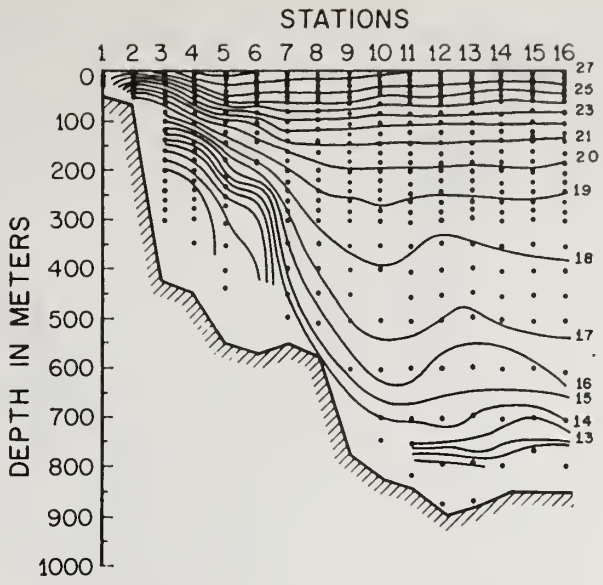

Figure 29. Cruise-27 water temperature (°C) cross-section.

The various physical phenomena that contribute to temperature variation vary in relative importance with depth. From the surface down to about 180-200 m, atmospheric and solar variations are of major importance. Near the bottom, temperature fluctuations are related to water mass movement. Thus the largest fluctuations, having a range of 5° to 10°C, occur at or near the surface over a six-month period. At the bottom, the yearly fluctuations are smaller but significant, varying between 3° and 7°C. Conversely the short term fluctuations at depth are considerably larger than those at the surface. Fluctuations at the bottom as large as 5.5°C occur within two-week periods, and 3° to 4°C variations occur quite frequently. At the surface, cruise-to-cruise temperature variations are usually less than 1°C and seldom exceed 2°C. The large short period bottom fluctuations are definitely geographically oriented. The 3° to 5.5°C variations occur only in the vicinity of stations 3 to 6. At stations 12 to 16 the bottom fluctuations are seldom greater than 2.5°C. Also it is significant that from stations 6 to 16 a large volume of water is found in the vicinity of the 18° isotherm (Worthington, 1959).

Temperature variations related to water mass movement generally are considered to decrease with increasing depth. To some extent this did occur. Seasonal and total means and standard deviations were computed at each standard depth for each station. The standard deviations of all temperature data are graphically presented as Figure 30. This figure indicated that, except for nearshore stations, temperature

variations decrease with increasing depth until a minimum is reached at about mid-depth of 250 to 400 m. Below that depth, temperature variations increased down to 700 m where a secondary maximum is reached. The most unusual temperature variation occurred at station 6 where the maximum standard deviation was recorded at the bottom.

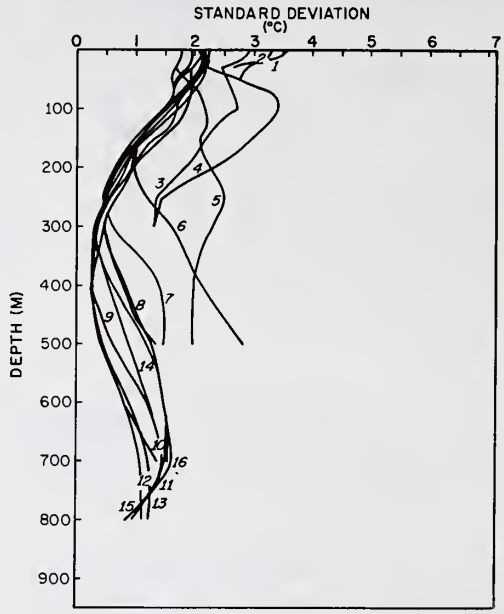

Figure 30. Standard deviations by station obtained by using all temperature data.

The standard deviations for the seasons are graphically presented as Figures 31, 32, 33, and 34. Down to a depth of about 180 to 200 m the standard deviations appear to reflect climatological variations. During summer and winter, surface water variations are low. The surface standard deviations are somewhat larger during spring and fall, indicative of transition periods.

During summer, variations increase with depth to a maximum at about 75 to 100 m, indicative of a shallow mixed layer varying in depth with a strong thermocline below. During winter relatively low standard deviations are recorded from the surface down to about 250 m. These curves indicate a deep mixed layer having relatively little variation with time.

The region of largest standard deviations is found at stations 3, 4, 5, and 6 varying in depth between 50 and 150 m. These large temperature fluctuations reflect variations related to the thermocline, but more importantly, to varying positions or meanderings of the Gulf Stream. Apparently, the velocity core is usually found in the vicinity of stations 5 or 6, but occasionally touches stations 4 or 7.

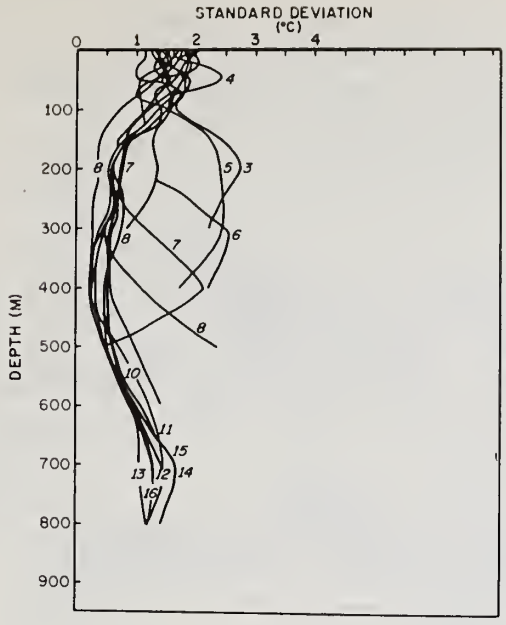

Figure 31. Standard deviations by station, obtained by using spring temperature data.

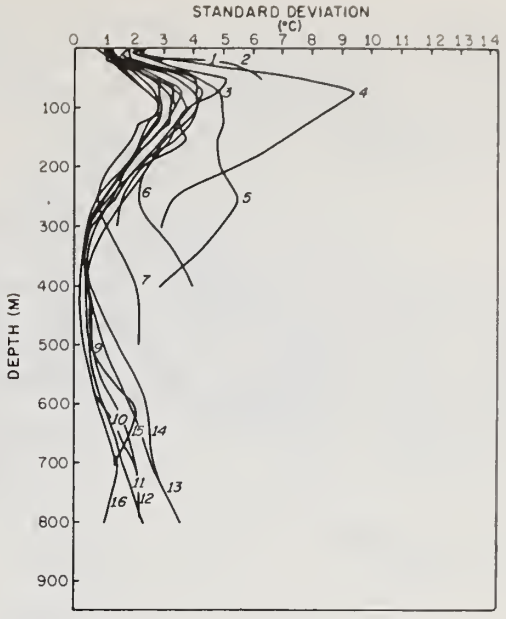

Figure 32. Standard deviations by station, obtained by using summer temperature data.

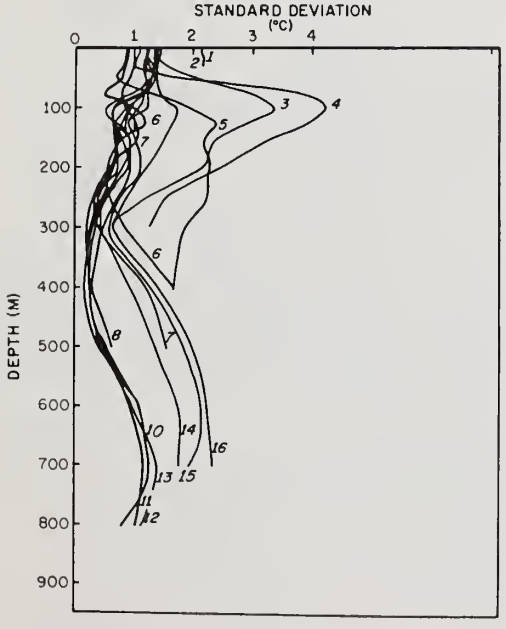

Figure 33. Standard deviations by station, obtained by using fall temperature data.

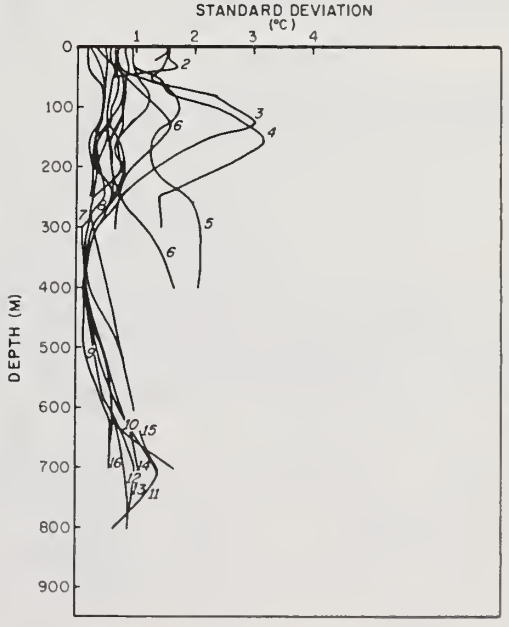

Figure 34. Standard deviations by station, obtained by using winter temperature data.

During the fall, unusually large fluctuations occurred below 300 m at stations 14, 15, and 16. Undoubtedly, they are related to water mass movement, possibly to a counter current at depth (Duing, 1973).

5.2 Salinity

As expected, the mean surface salinity increased with increasing distance from shore. Figure 35 is a cross-section of the mean of all salinity data. A mean value of 36.02°/$_{oo}$ was recorded at station 1, and a mean value of 36.40°/$_{oo}$ was recorded at station 16.

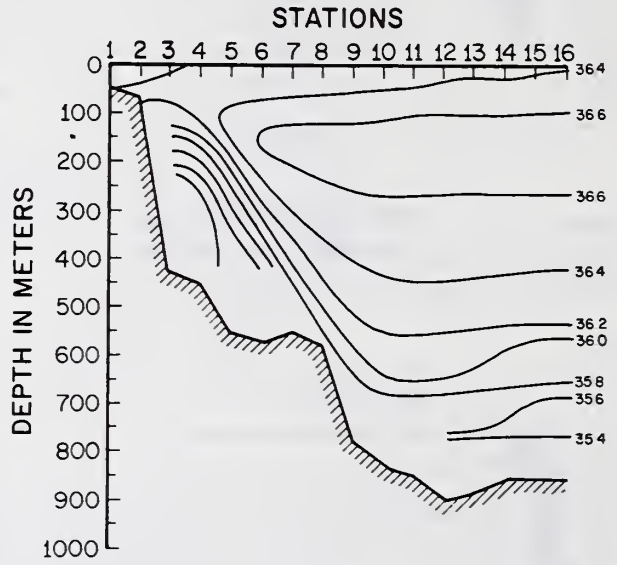

Figure 35. Mean of all cruises salinity cross-section.

Nearshore the maximum salinity of about 36.23°/$_{oo}$ to 36.27°/$_{oo}$ occurs at about 20 to 50 m depth. Below the maximum, the salinity decreases to about 35.12°/$_{oo}$ at the bottom at stations 3, and 4, the lowest value for the entire cross-section.

In the core of the Gulf Stream, the maximum salinity of 36.54°/$_{oo}$ is found at 100 to 125 m. Farther seaward the salinity maximum of about 36.67°/$_{oo}$ to 36.71°/$_{oo}$ is found in a horizontal layer between 100 and 200 m depth. Below the maximum, the salinity gradually decreases to about 35.20°/$_{oo}$ at the bottom.

The surface salinity pattern exhibits considerable seasonal variation. Figures 36, 37, 38, and 39 are the seasonal salinity cross-sections, and figures 40 through 62 are the individual cruise cross-sections. In general, during all seasons the minimum surface values are found at the shoreward end, where a seasonal low of 35.41°/$_{oo}$ occurs during the summer, and the high of 36.34°/$_{oo}$ occurs during the winter.

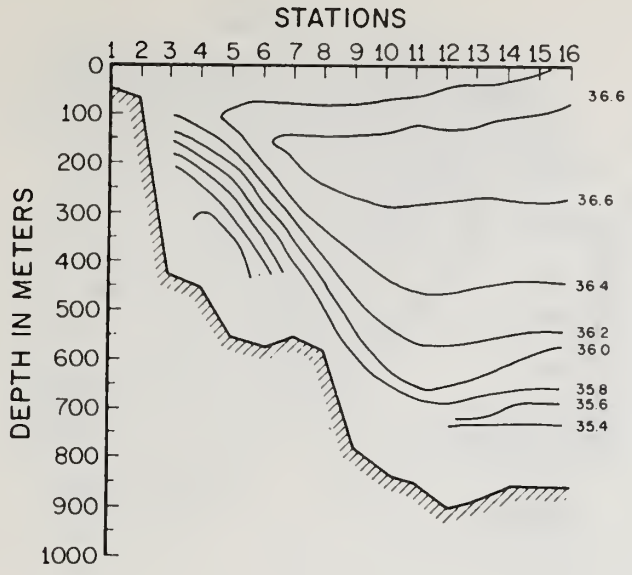

Figure 36. Mean of spring cruises salinity cross-section.

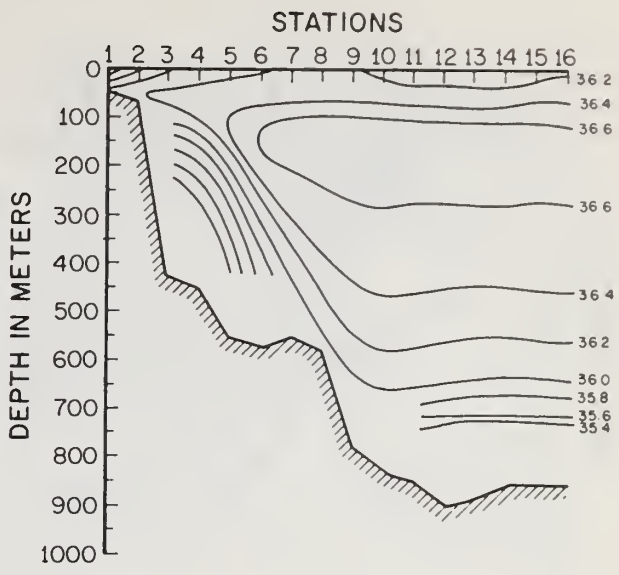

Figure 37. Mean of summer cruises salinity cross-section.

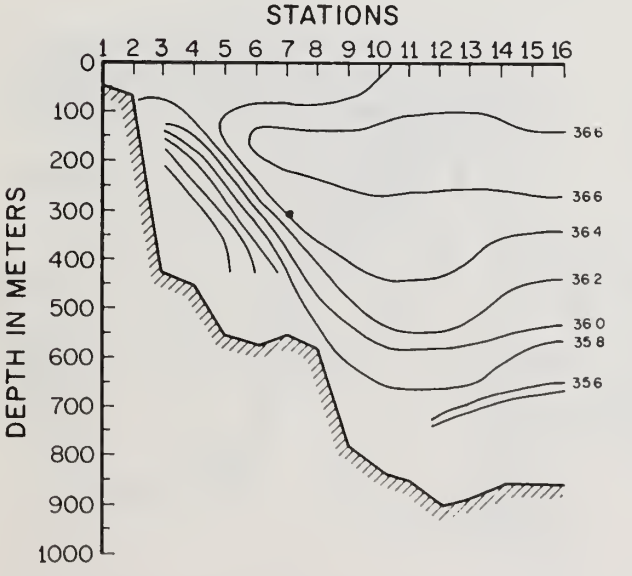

Figure 38. Mean of fall cruises salinity cross-section.

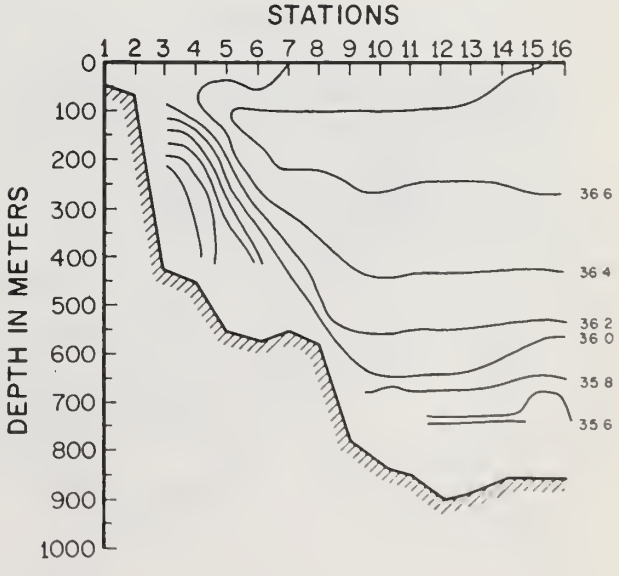

Figure 39. Mean of winter cruises salinity cross-section.

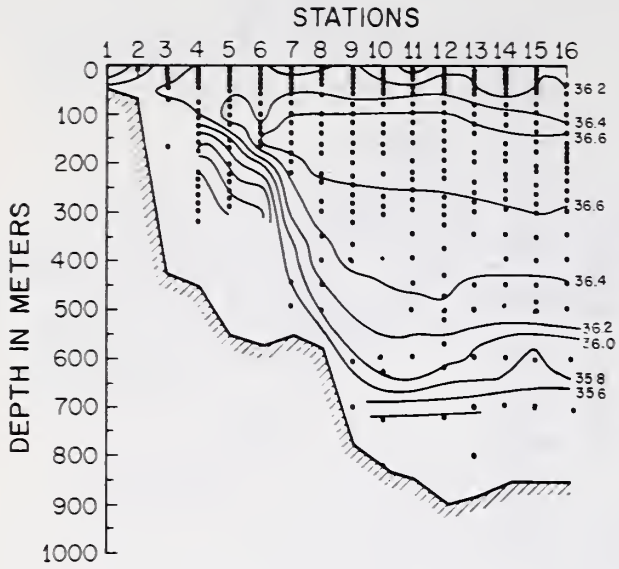

Figure 40. Cruise-1 salinity cross-section.

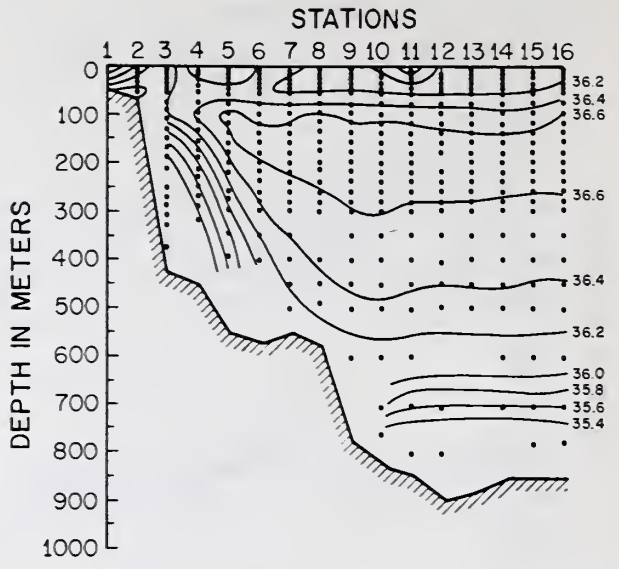

Figure 41. Cruise-2 salinity cross-section.

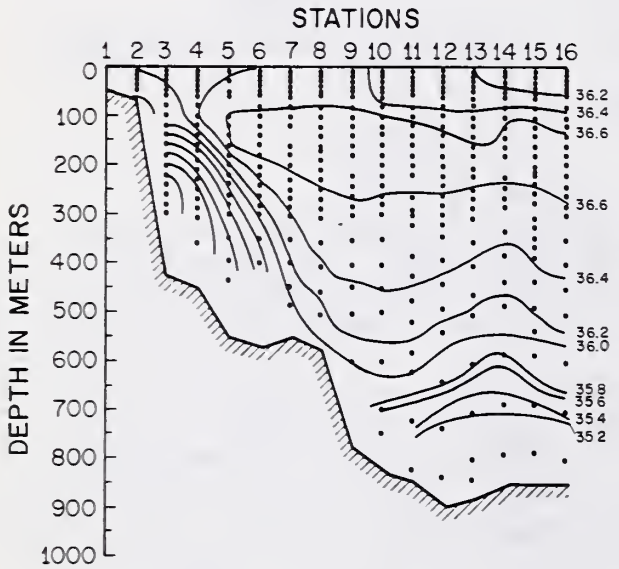

Figure 42. Cruise-4 salinity cross-section.

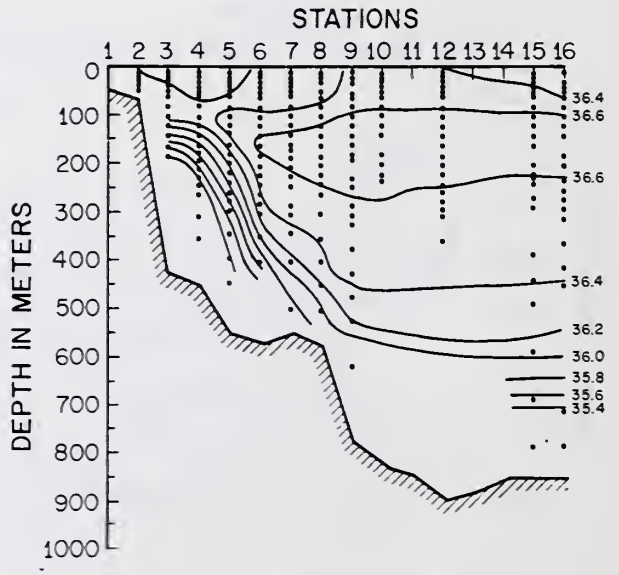

Figure 43. Cruise-5 salinity cross-section.

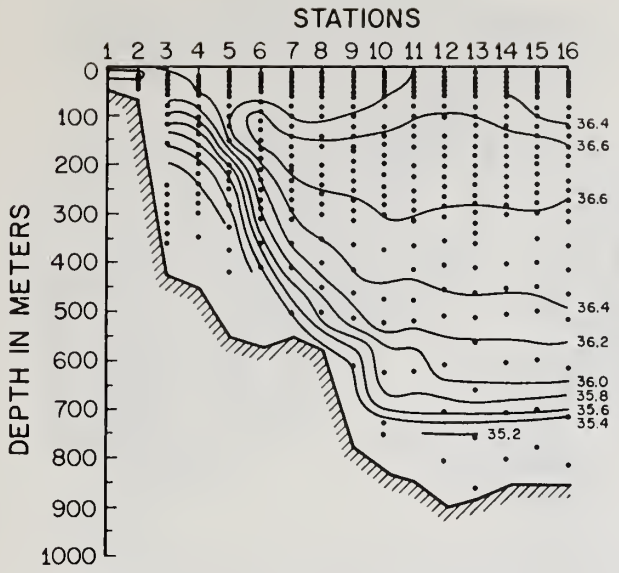

Figure 44. Cruise-6 salinity cross-section.

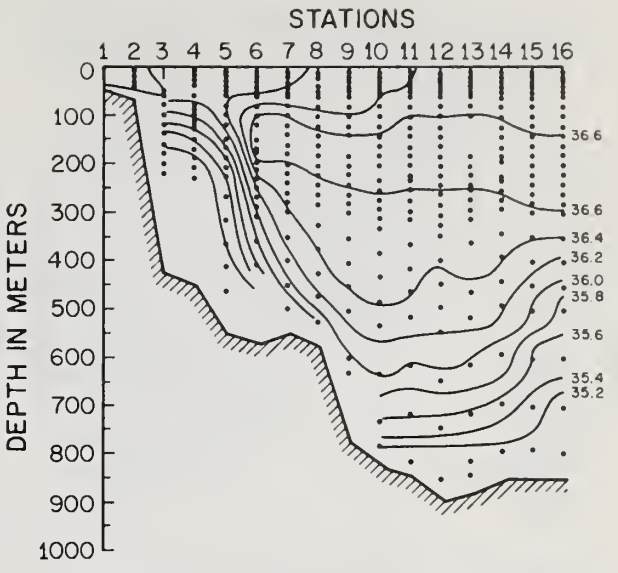

Figure 45. Cruise-7 salinity cross-section.

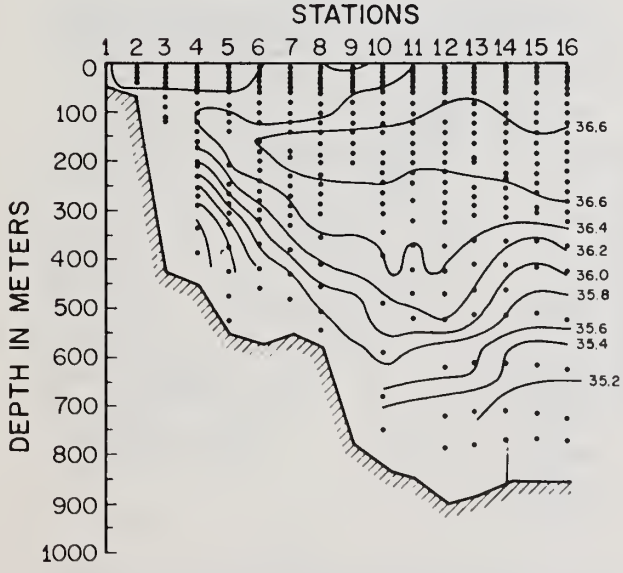

Figure 46. Cruise-8 salinity cross-section.

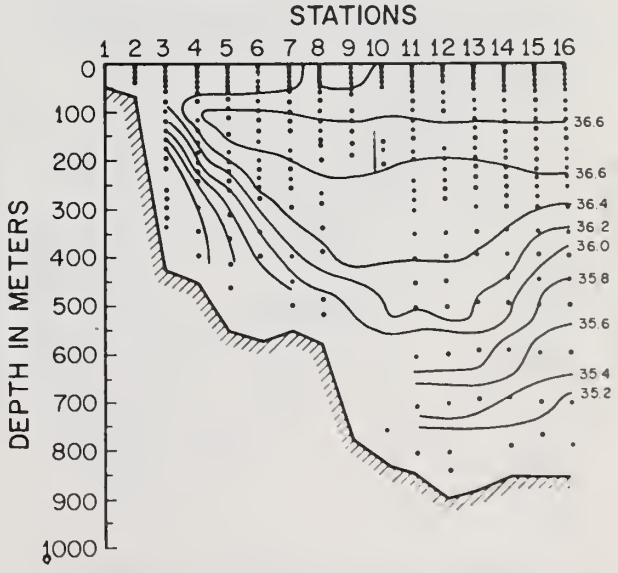

Figure 47. Cruise-9 salinity cross-section.

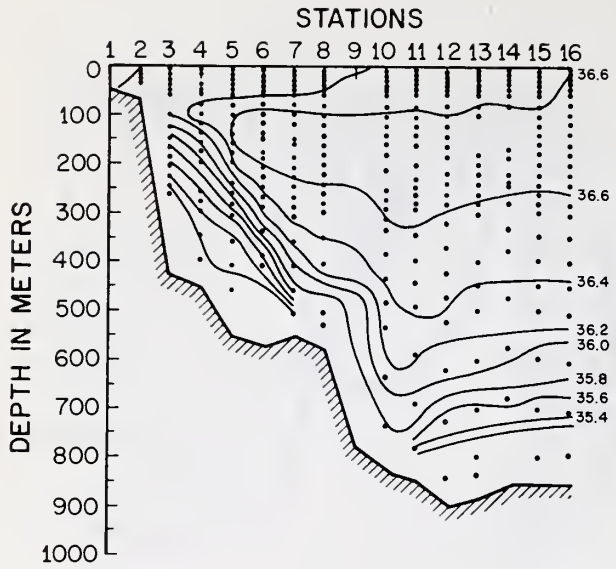

Figure 48. Cruise-10 salinity cross-section.

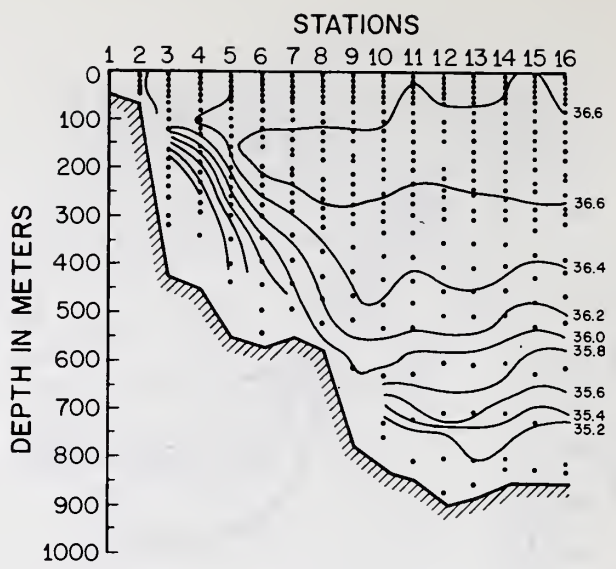

Figure 49. Cruise-12 salinity cross-section.

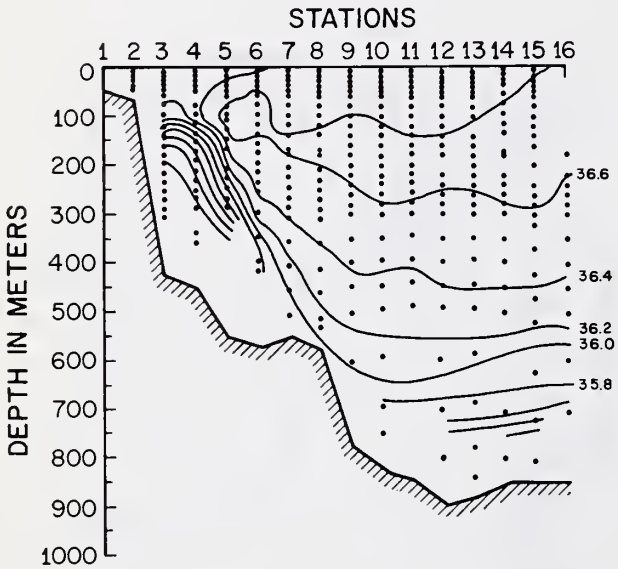

Figure 50. Cruise-14 salinity cross-section.

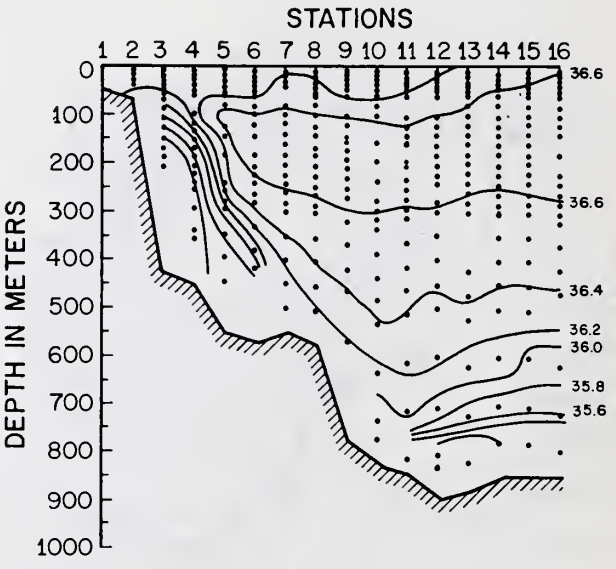

Figure 51. Cruise-15 salinity cross-section.

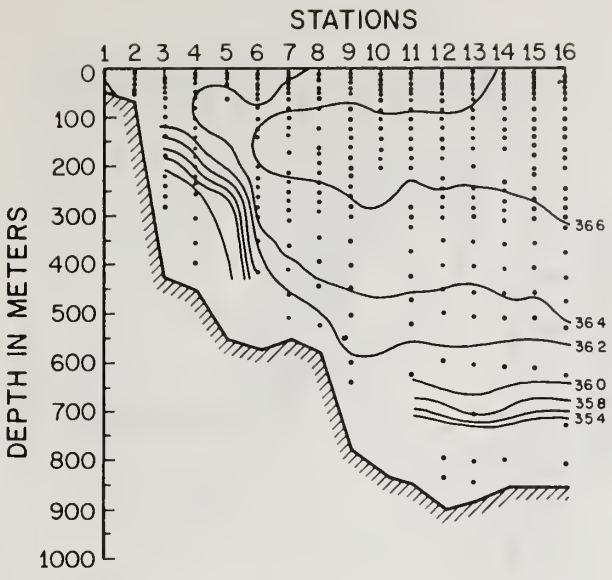

Figure 52. Cruise-16 salinity cross-section.

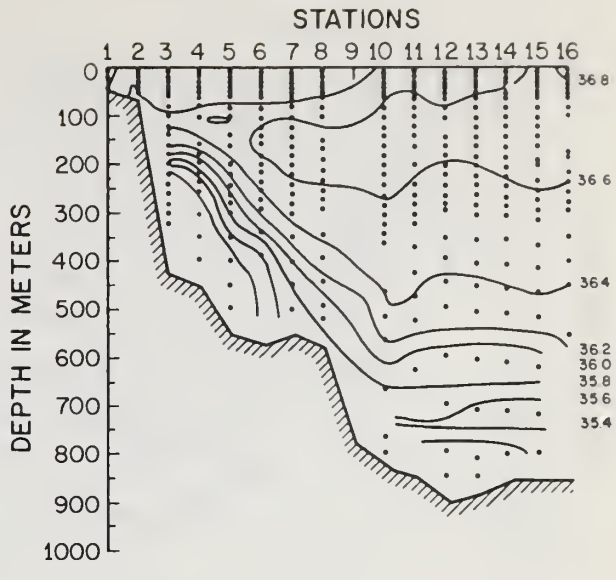

Figure 53. Cruise-18 salinity cross-section.

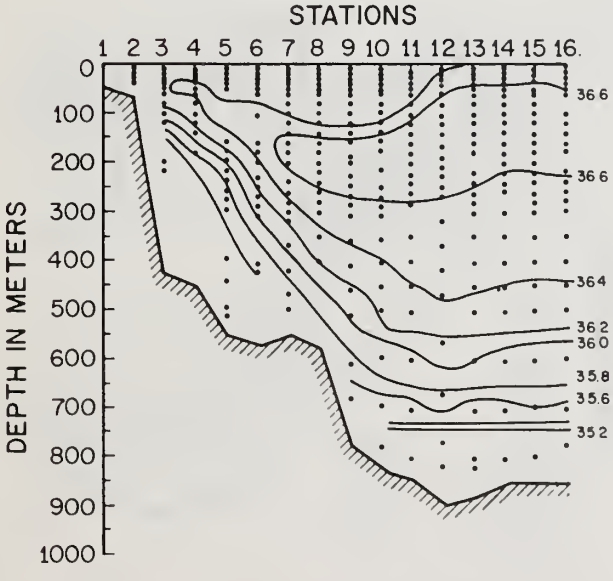

Figure 54. Cruise-19 salinity cross-section.

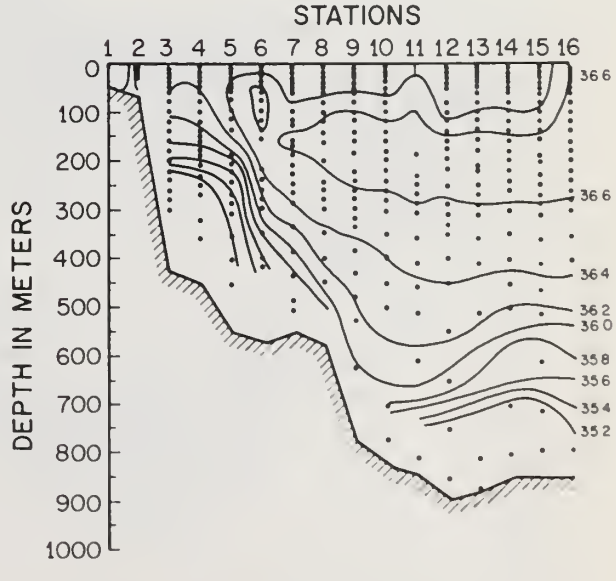

Figure 55. Cruise-20 salinity cross-section.

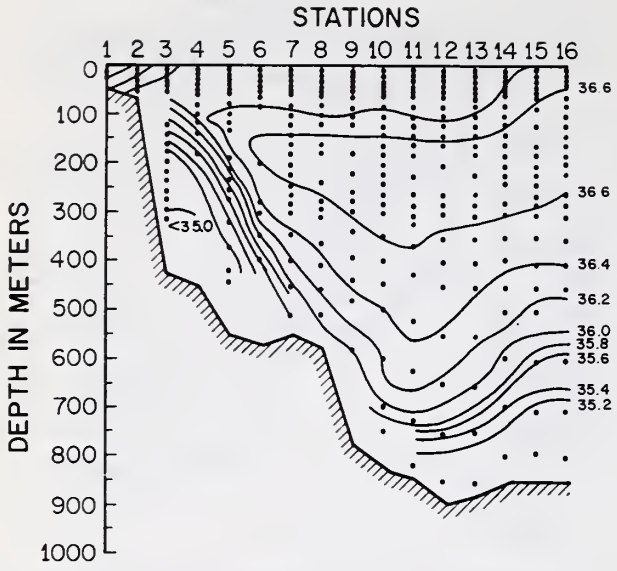

Figure 56. Cruise-21 salinity cross-section.

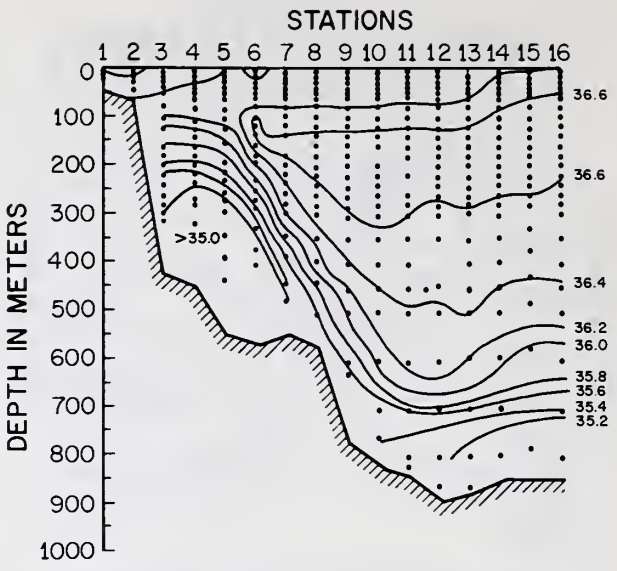

Figure 57. Cruise-22 salinity cross-section.

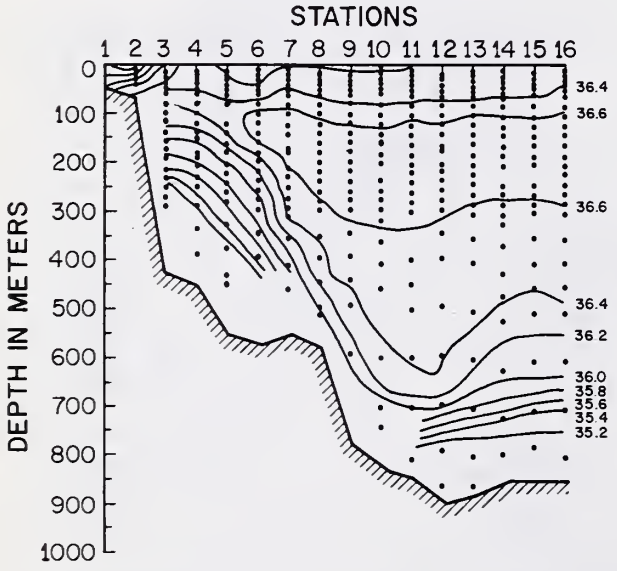

Figure 58. Cruise-23 salinity cross-section.

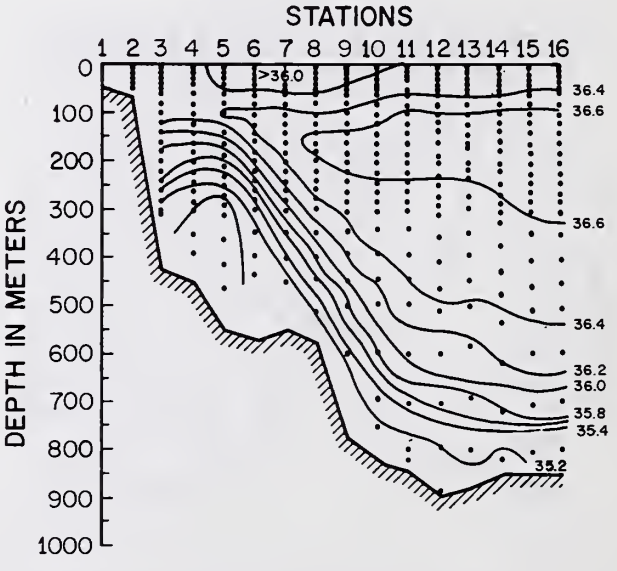

Figure 59. Cruise-24 salinity cross-section.

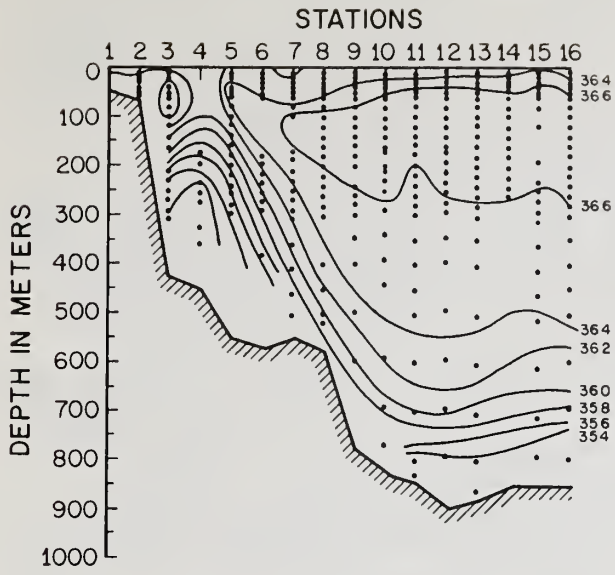

Figure 60. Cruise-25 salinity cross-section.

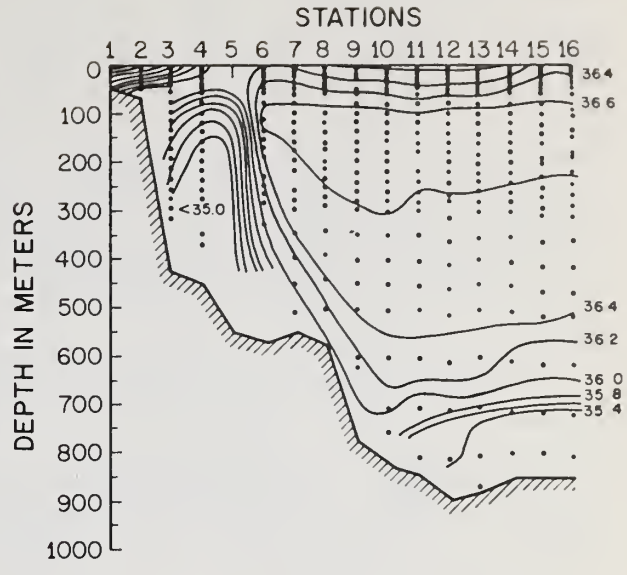

Figure 61. Cruise-26 salinity cross-section.

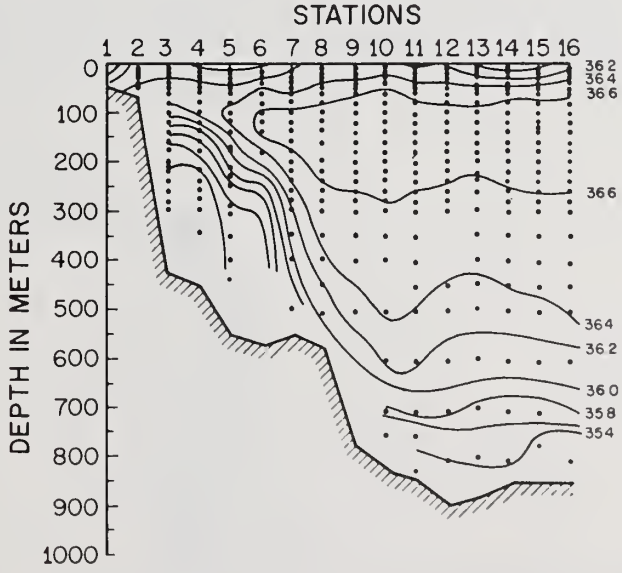

Figure 62. Cruise-27 salinity cross-section.

Coastal water is a mixture of oceanic water and fresh water that has drained from the land. Its salinity depends on the fraction of fresh water and the salinity of the oceanic water. The salinity of offshore surface ocean water is generally greater than 36.00°/₀₀. Surface salinity values less than 36.00°/₀₀ were recorded only during the summer at stations 1, 2, and 3. This indicates that fresh water runoff is most significant during the summer, the period of highest rainfall (Bryson and Hare, 1974). Even at these nearshore stations, the relative high values (all greater than 35.00°/₀₀) indicate that the oceanic water predominates. At all stations the minimum surface salinities occurred during the summer and the maximum during the winter.

The seasonal salinity maximums of 36.71 ± .02°/₀₀ occur in a horizontal lens between 100 and 200 m extending from stations 6 to 16. Minimum salinity for the entire cross-section is found at the bottom in the vicinity of stations 3 and 4. During summer, fall, and winter, the minimum is consistent having a value of 35.02 ± .01°/₀₀. During spring, the minimum rises to 35.17°/₀₀.

Considerable variation was recorded between individual station values at the bottom for stations 8 thru 16 (0.14 to 0.37°/₀₀).

Other than in the near-surface water, the salinity variations are related to dynamic forces. These variations seem to be considerable in some parts of the cross-section and almost non-existent in others. The variations are graphically displayed in Figure 63. For this figure, standard deviations were computed for all cruise data at each station for each standard depth. The resulting curves can be classified into one of three groups, related to water masses and the dynamic forces.

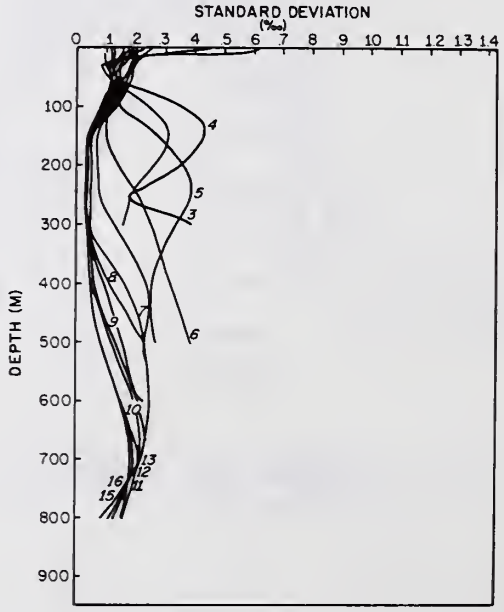

Figure 63. Standard deviations by station obtained by using all salinity data.

The coastal water, stations 1 and 2, exhibit a high salinity variation at the surface that rapidly decreases with depth. Stations 3, 4, and 5 exhibit low surface and near-surface salinity variations that increase with depth until a maximum is reached at about 125 to 250 m. At greater depths, the variation decreases, but it remains greater at the bottom than in the near-surface water.

Stations 8 through 16 exhibit similar salinity variation patterns. The standard deviations from the surface to 100 m are between 0.1 and 0.2. Below 100 m the standard deviations decrease to a minimum of about 0.03 to 0.04 between 150 and 400 m. At greater depths the standard deviations increase to a maximum of about 0.2 at 700 m.

Stations 6 and 7 exhibit a variation pattern that is transitional between 4 and 5 on the one hand and 8 thru 16 on the other.

Of considerable interest are the absolute salinity values at 300 m at stations 3 and 4. At station 3, 38% of the salinity observations are less than 35.00°/$_{oo}$, yet the highest recorded value was 35.66°/$_{oo}$. The standard deviation was an unusually large 0.39°/$_{oo}$. At station 4, 25% of the salinity observations were below 35.00°/$_{oo}$, and the highest recorded was 35.57°/$_{oo}$. This will be discussed further under water masses.

5.3 Dissolved Oxygen

The cross-section mean of all the dissolved oxygen data exhibits a relatively simple pattern (Fig. 64). The maximum surface value is found at station 1. Surface values decrease seaward to station 4. Seaward of station 4, the surface values vary between 4.65 ml/l and 4.76 ml/l. The maximum value for the entire cross-section of 4.96 ml/l is found at the surface at station 1. The maximum values for each station are found in water varying in depth between 10 and 100 m. The values range between 4.96 and 4.69 ml/l.

Below the maximum, oxygen values decrease with increasing depth. The sharpest gradient is found at station 3 where a minimum of 3.24 ml/l is found at 300 m. Similar low values of 3.23 and 3.28 ml/l are found in 800 m at stations 11 and 15. Seaward of station 6, the oxygen gradient between the surface and 600 m is only about 0.05 ml/l per 100 m.

The oxygen patterns for each season (Figs. 65-68) are quite similar to the mean pattern of all the data. That is to say that maximum values are always found in the nearshore water, and the minimum values are found at the bottom. However, definite seasonal patterns exist at all depths.

At any given point on the cross-section, lowest seasonal values are most likely to occur during summer. The maximum summer value of 4.72 ml/l was found at station 11 at 50 m.

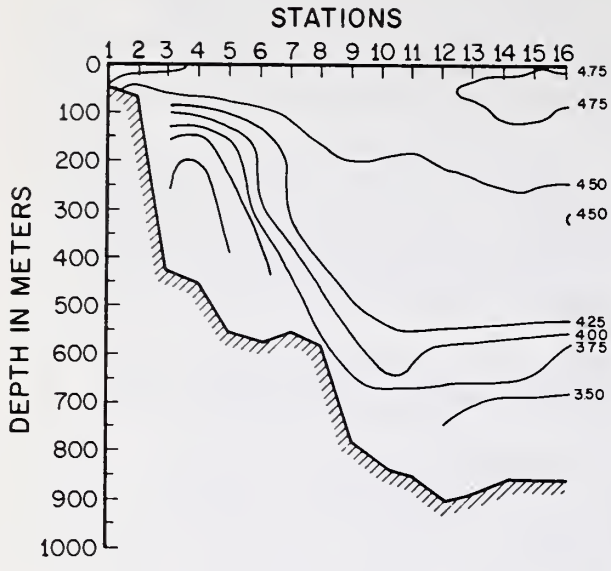

Figure 64. Mean of all cruises oxygen cross-section.

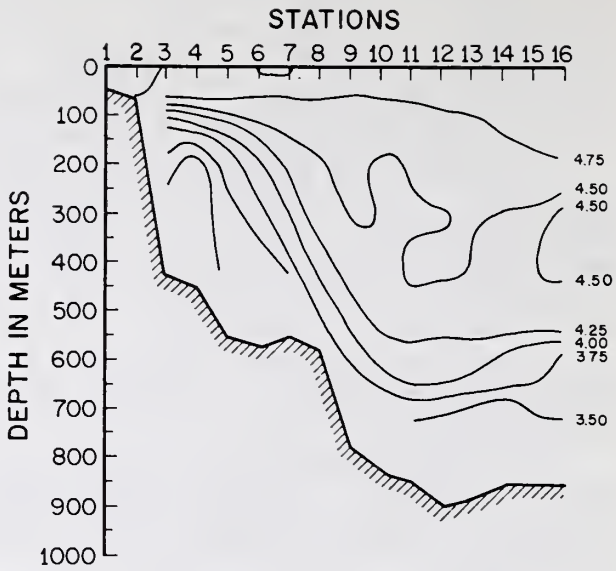

Figure 65. Mean of spring cruises oxygen cross-section.

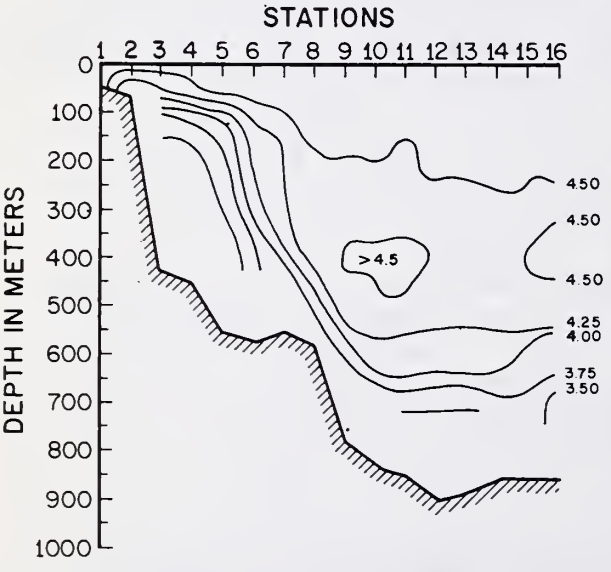

Figure 66. Mean of summer cruises oxygen cross-section.

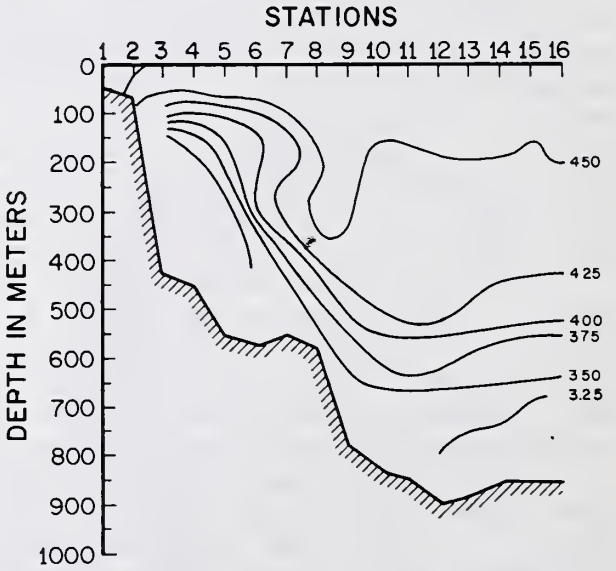

Figure 67. Mean of fall cruises oxygen cross-section.

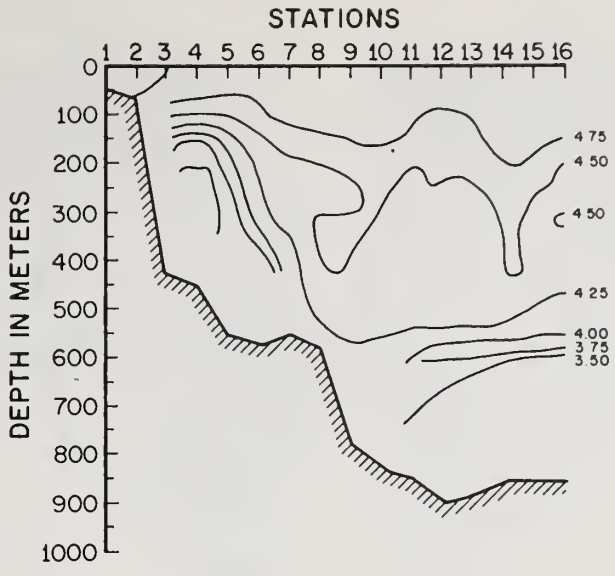

Figure 68. Mean of winter cruises oxygen cross-section.

Values below 3.20 occurred below 150 m at stations 3, 4, and 5 and also below 700 m at station 13. Generally, oxygen values were considerably higher during the winter. The maximum value of 5.38 ml/l was found at station 1 in 20 m of water. Winter minimum values of 3.29 ml/l were recorded at station 4 in 200 m and 3.04 ml/l at station 12 in 800 m of water.

In general, the individual cruise cross-sections are similar to the seasonal ones (Figs. 69-91). One striking feature is masked by the seasonal ones. Generally, the oxygen minimum for a station occurs at the lowest bottle at the station. However, occasionally the minimum observation is reached above the bottom and a slight or sharp increase is recorded at the bottom bottle.

Where the increase in the oxygen value at the bottom is slight, the indication is that the actual oxygen minimum has been reached. This occurs at a sigma-t of 27.12. A sharp increase in the oxygen value at the bottom may indicate a different water mass.

Standard deviations at standard depths for each station using the entire year of data do not form a neat pattern as they do for temperature and salinity (Fig. 92). However, they usually exhibit minimum variation in water less than 100 m. The largest standard deviations are usually recorded at or near the bottom at the seaward end of the line.

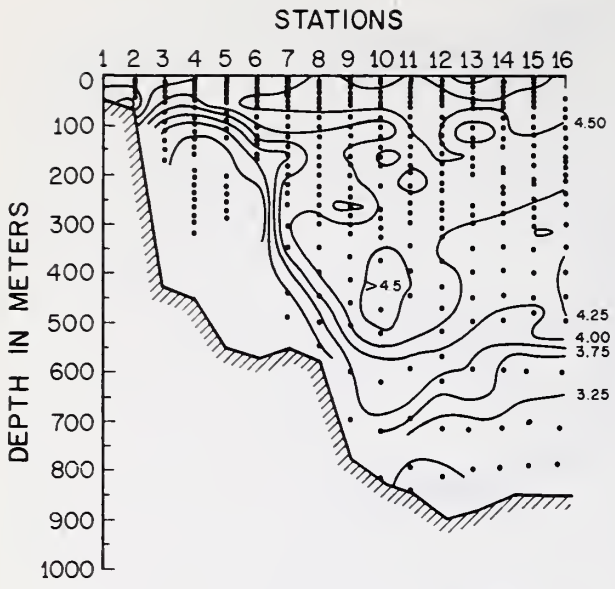

Figure 69. Cruise-1 oxygen cross-section.

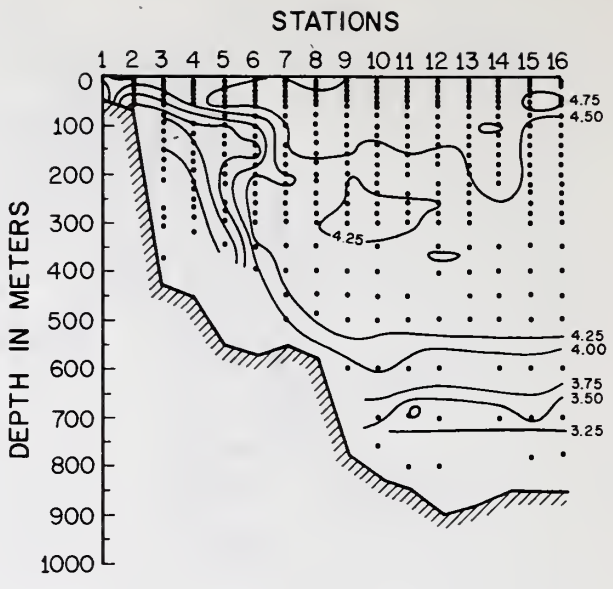

Figure 70. Cruise-2 oxygen cross-section.

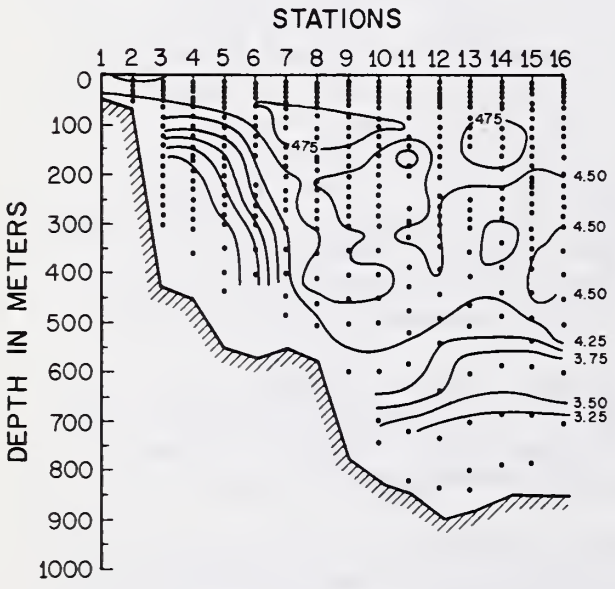

Figure 71. Cruise-4 oxygen cross-section.

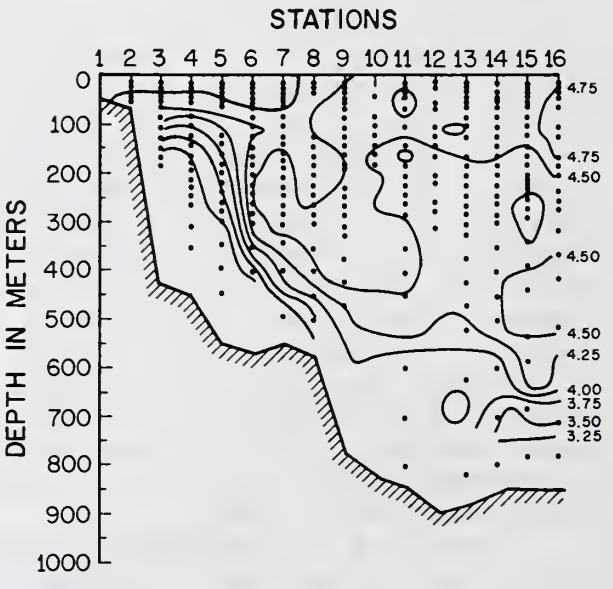

Figure 72. Cruise-5 oxygen cross-section.

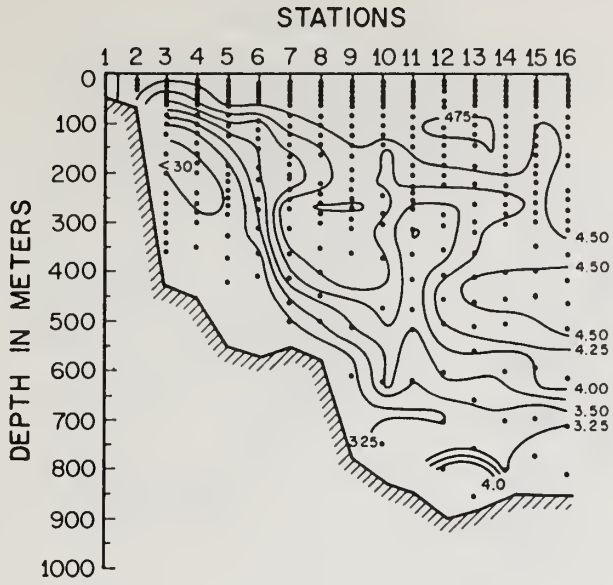

Figure 73. Cruise-6 oxygen cross-section.

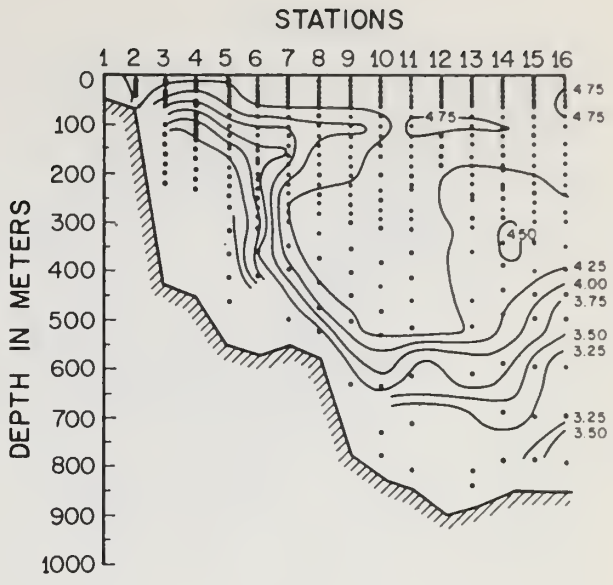

Figure 74. Cruise-7 oxygen cross-section.

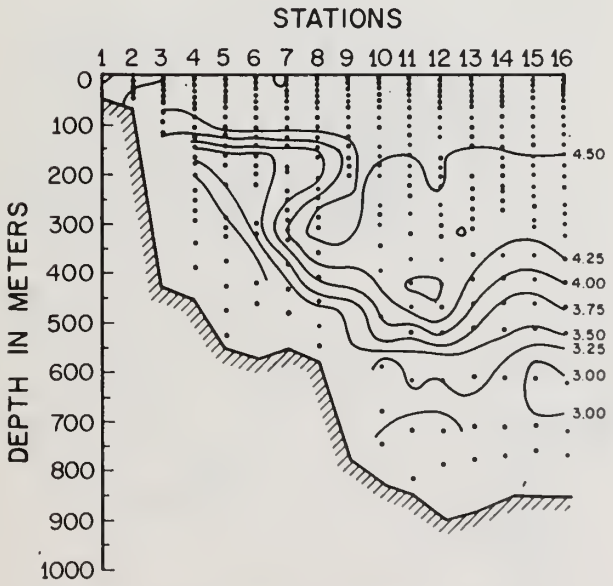

Figure 75. Cruise 8 oxygen cross-section.

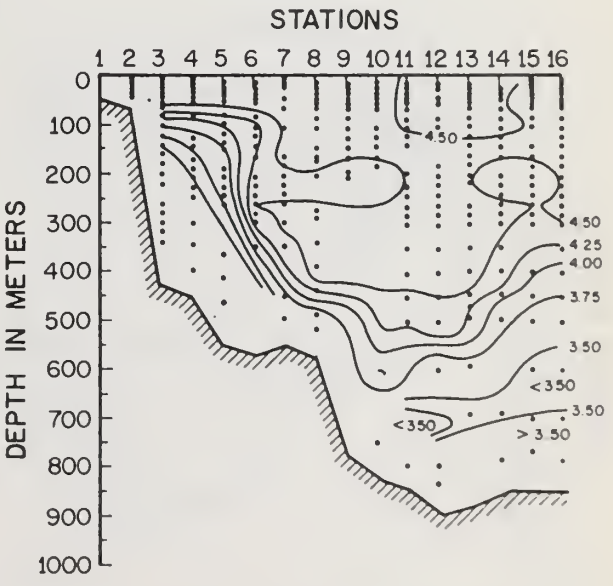

Figure 76. Cruise 9 oxygen cross-section.

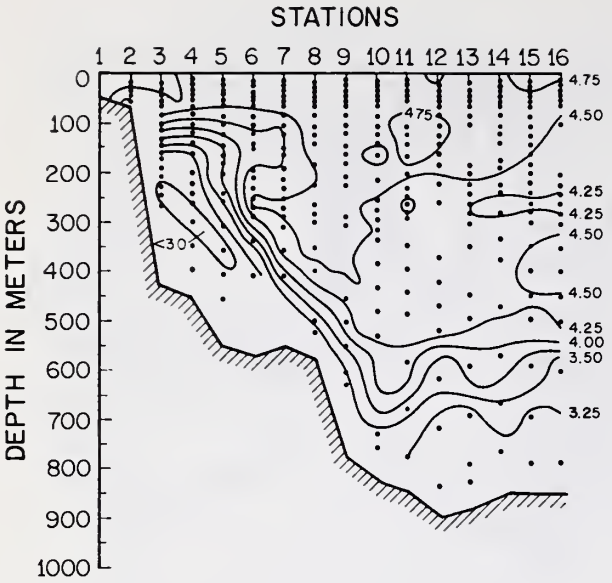

Figure 77. Cruise-10 oxygen cross-section.

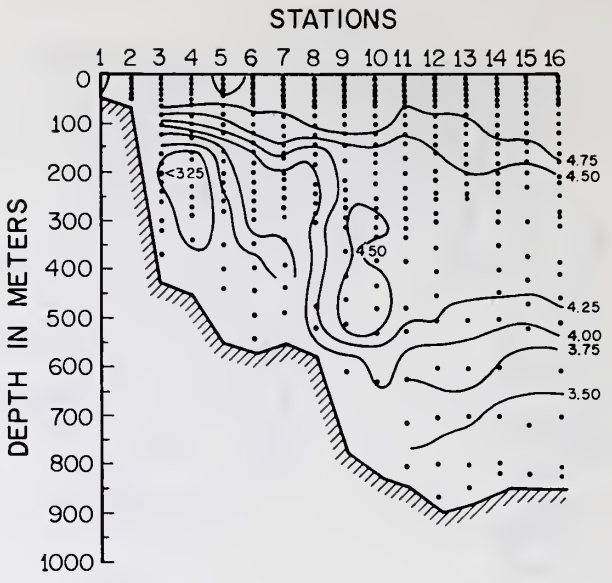

Figure 78. Cruise-12 oxygen cross-section.

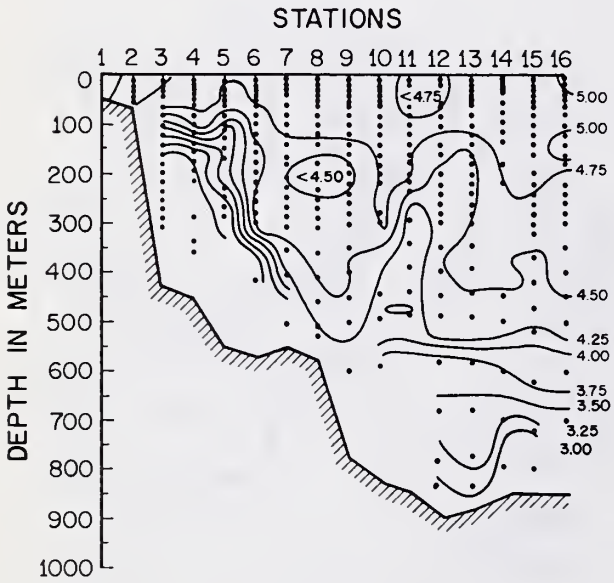

Figure 79. Cruise-14 oxygen cross-section.

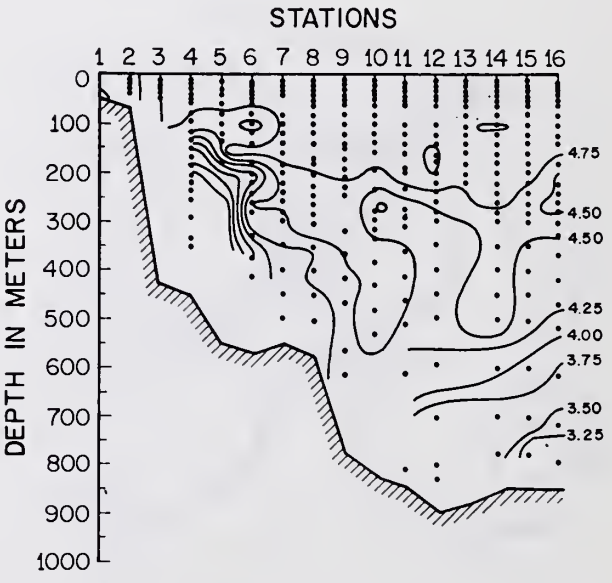

Figure 80. Cruise-15 oxygen cross-section.

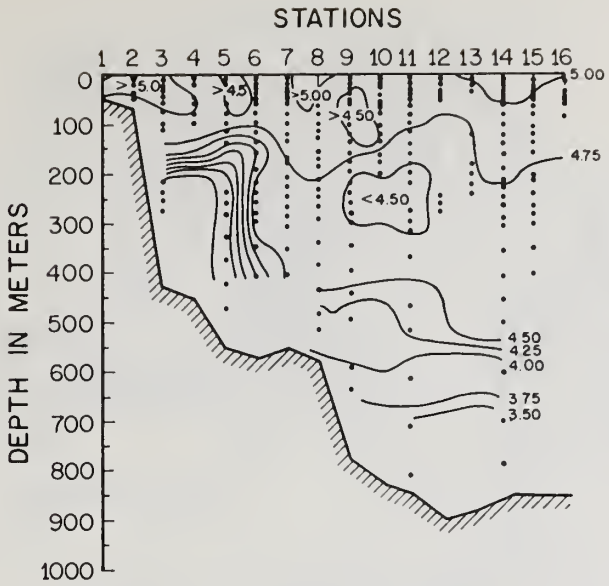

Figure 81. Cruise-16 oxygen cross-section.

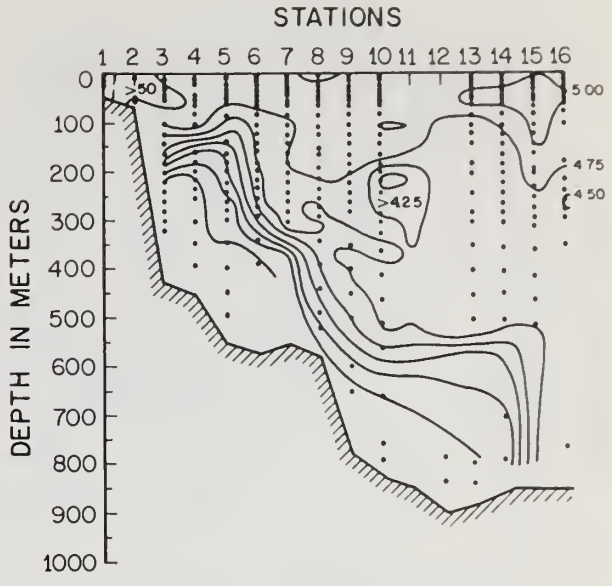

Figure 82. Cruise-18 oxygen cross-section.

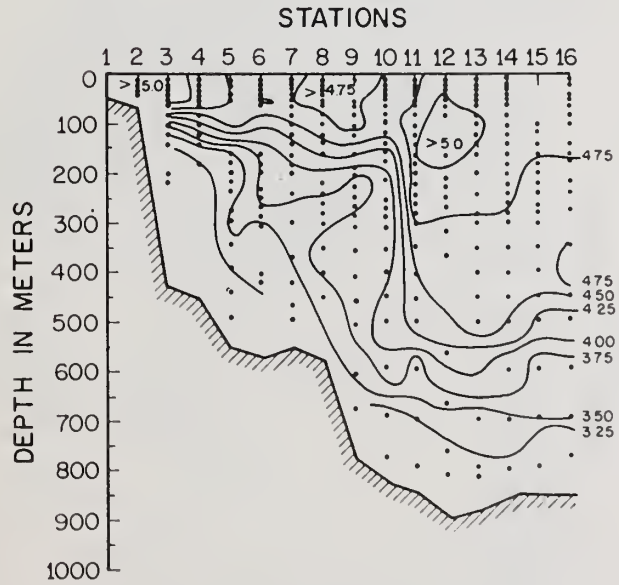

Figure 83. Cruise-19 oxygen cross-section.

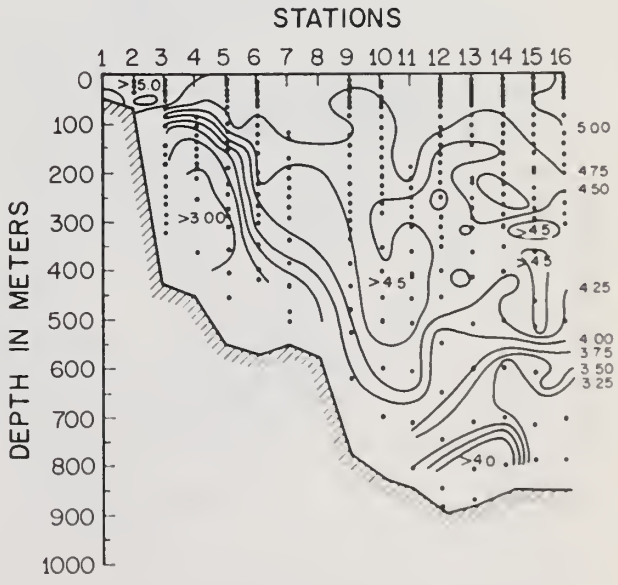

Figure 84. Cruise-20 oxygen cross-section.

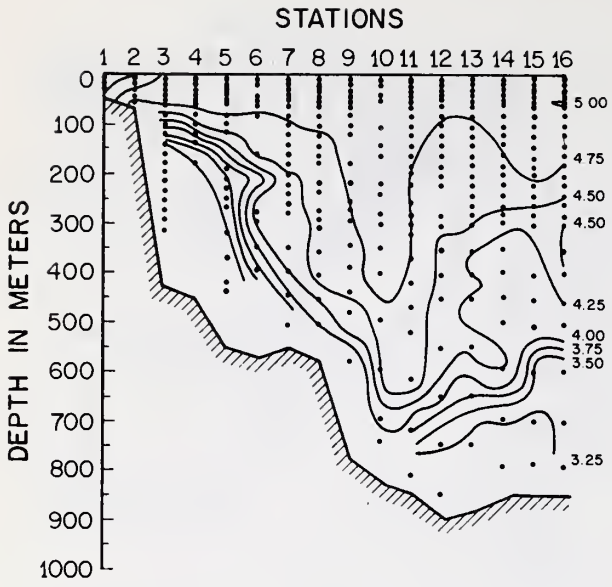

Figure 85. Cruise-21 oxygen cross-section.

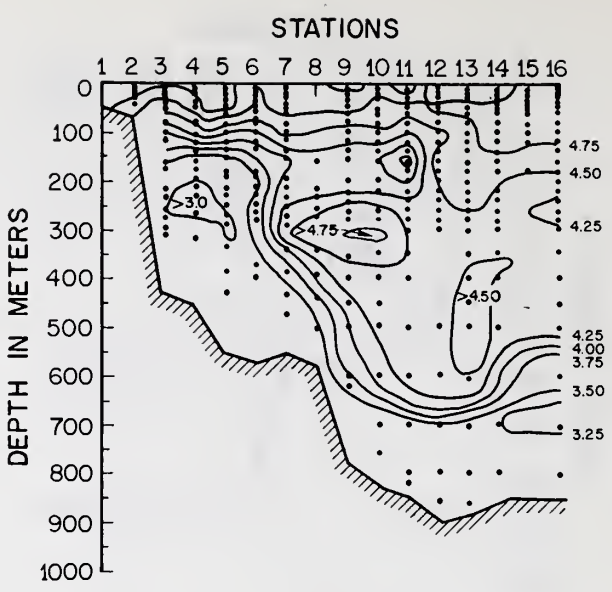

Figure 86. Cruise-22 oxygen cross-section.

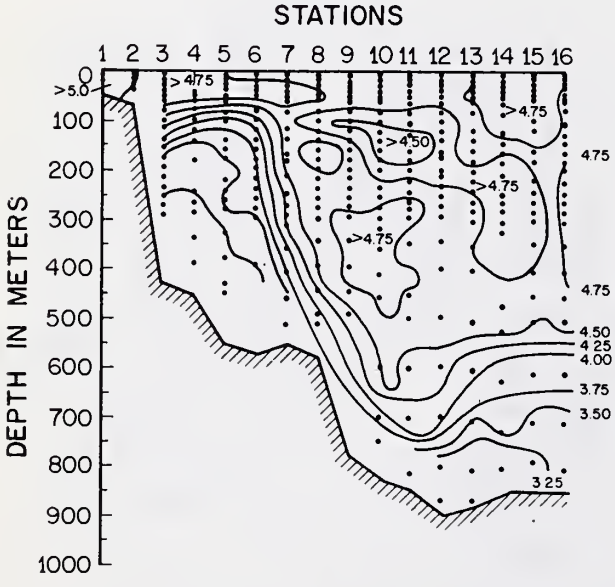

Figure 87. Cruise-23 oxygen cross-section.

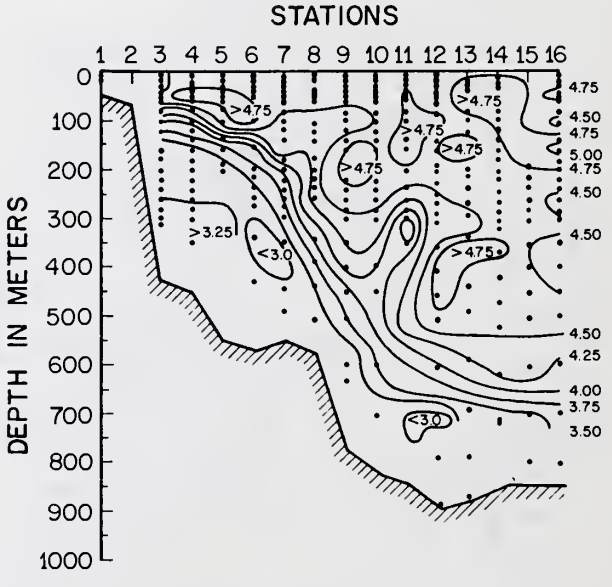

Figure 88. Cruise-24 oxygen cross-section.

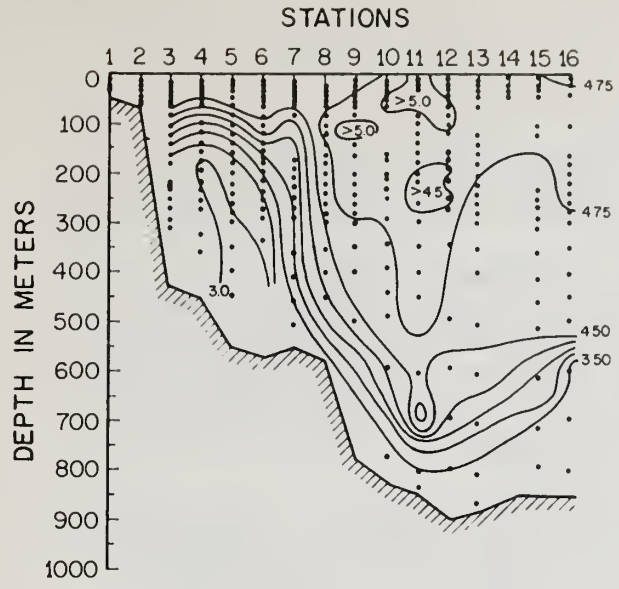

Figure 89. Cruise-25 oxygen cross-section.

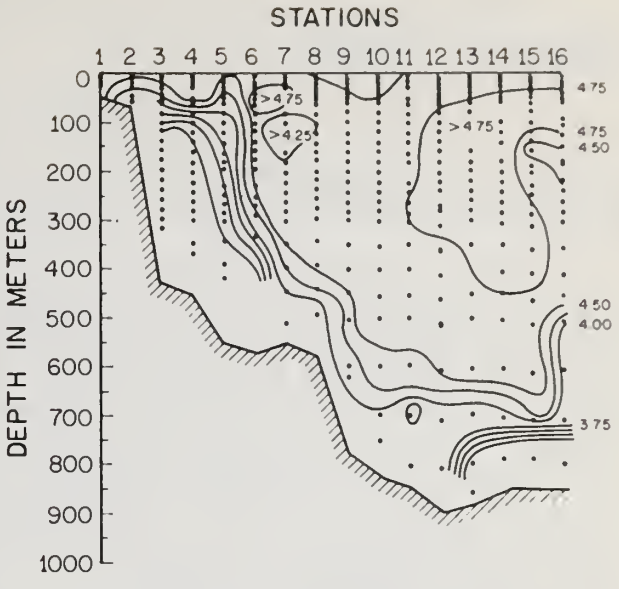

Figure 90. Cruise-26 oxygen cross-section.

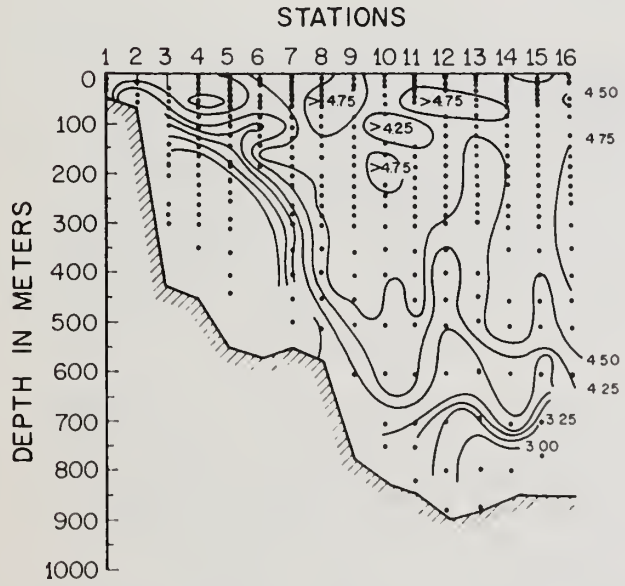

Figure 91. Cruise-27 oxygen cross-section.

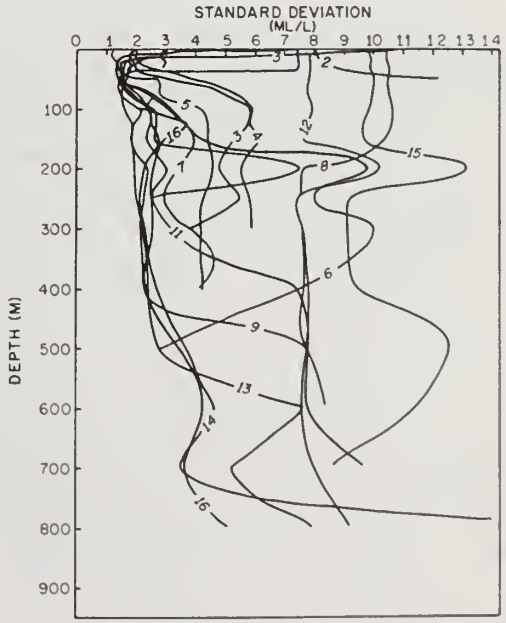

Figure 92. Standard deviation by station, obtained by using all oxygen data.

"Percentage saturation" of oxygen is frequently computed using the formula

$$O_2/O_2' \times 100 = O_2\%$$

where O_2 is the observed oxygen content, O_2' is"100% saturation", 100% saturation is computed from tables derived by Weiss (1970).

The percentage saturation for the near-surface water for all the cruises was close to 100% when computed by seasons. All stations exhibited a percentage saturation between 100% and 104% from the surface to 50 m. Winter was an exception. During winter, nearshore stations did not exhibit 100% saturation, and the rest of the stations exhibited 100% saturation only down to an average depth of 24 m.

The depth of 90% saturation was also computed for each station for each season. All curves were similar. Nearshore 90% of saturation was in 30 to 40 m. Depths increased with increasing distance from shore. The lowest depths were recorded during winter and the highest during the fall. The curves are given as Figures 93-96.

5.4 Sigma-t

The mean cross-section of the entire year of data relates a simple pattern (Fig. 97). The 24.00 isopycnic is found only at stations 5 and 6. This isopycnic line outlines the core of the Gulf Stream in the near-surface water. The 24.20 to 25.20 isopycnic lines slope gently downward from station 1 to station 7 then are generally horizontal out to station 16.

The maximum sigma-t of 27.33, a reflection of the minimum water temperature, is found at station 3 in 300 m. All isopycnic lines from 25.40 to 27.20 slope downward from station 3 to about 8 or 9. Further seaward the isopycnic lines are approximately horizontal.

The seasonal cross sections (figs. 98-101) exhibit patterns similar to the mean cross section of the entire year's data. The maximum sigma-t is always found at the bottom at station 3. No seasonal sigma-t variation is noted at this point, as the values vary only from 27.30 to 27.35. No seasonal variation occurs at the bottom seaward of station 3.

The minimum seasonal isopycnic line is always found including stations 5, 6, and 7. This line varies with the seasonal temperature change from a low of 23.20 during summer to a high 24.80 during winter. As there is almost no variation at the bottom at station 3, the gradient of the isopycnic lines between these areas varies considerably with the season. During summer,

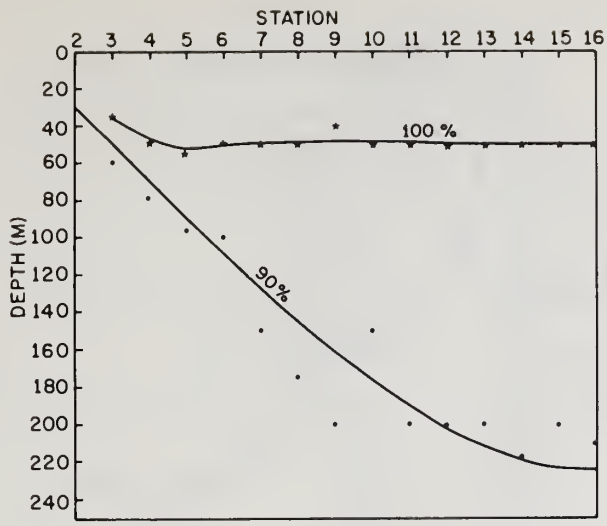

Figure 93. Depth of 100% and 90% oxygen saturation (spring).

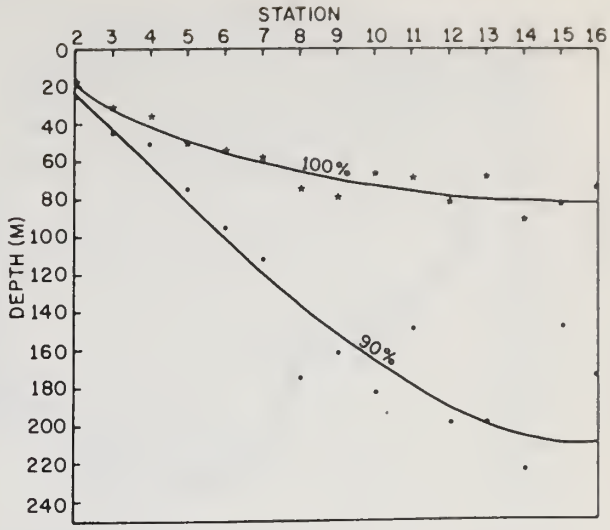

Figure 94. Depth of 100% and 90% oxygen saturation (summer).

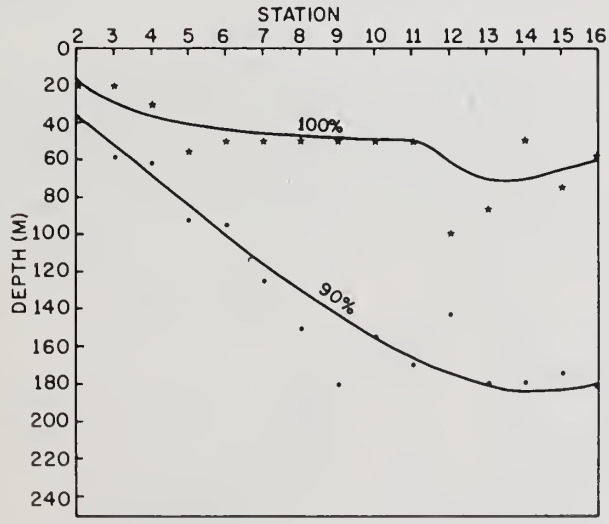

Figure 95. Depth of 100% and 90% oxygen saturation (fall).

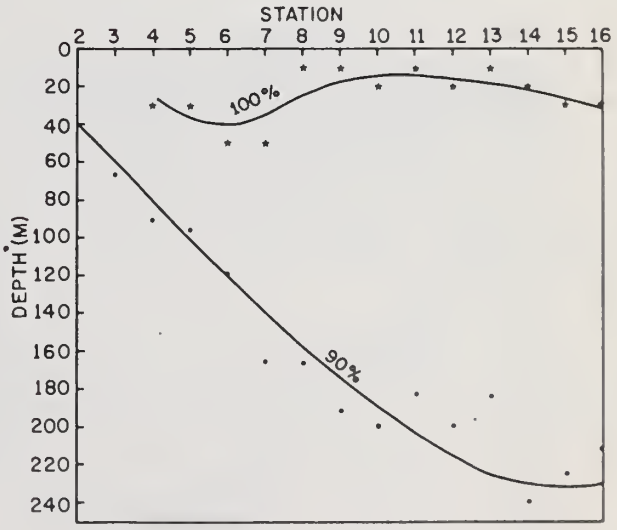

Figure 96. Depth of 100% and 90% oxygen saturation (winter).

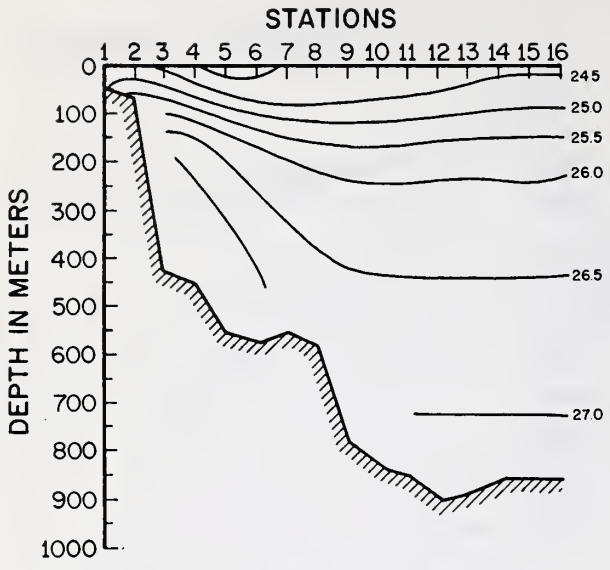

Figure 97. Mean of all cruises sigma-t cross-section.

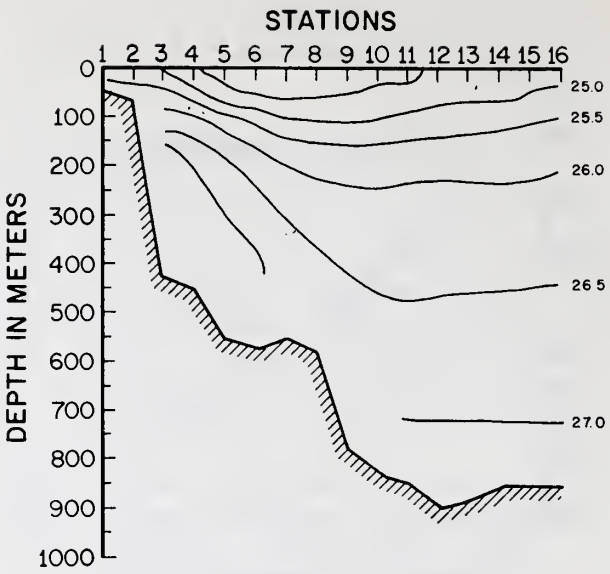

Figure 98. Mean of spring cruises sigma-t cross-section.

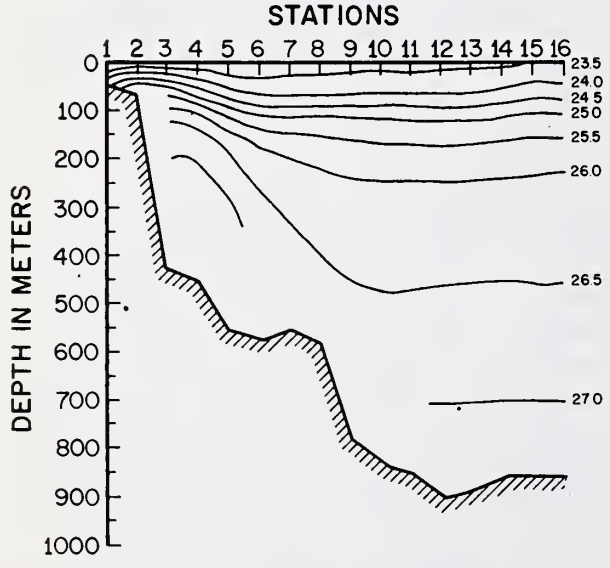

Figure 99. Mean of summer cruises sigma-t cross-section.

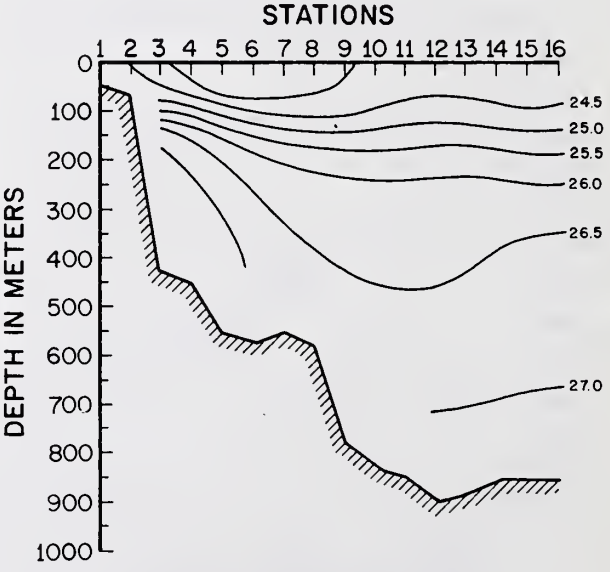

Figure 100. Mean of fall cruises sigma-t cross-section.

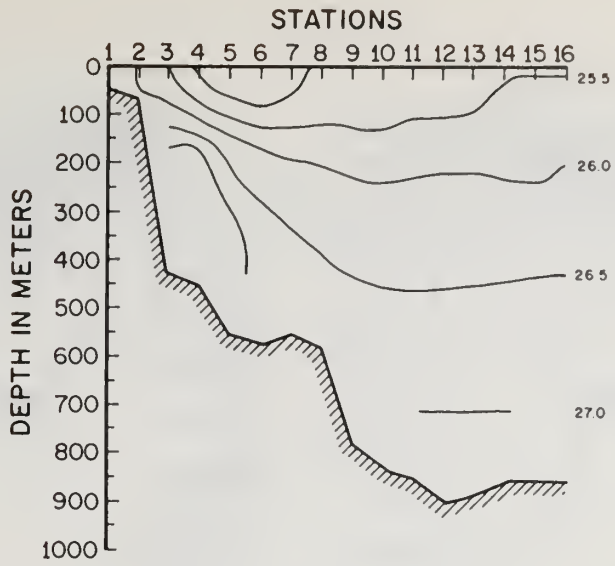

Figure 101. Mean of winter cruises sigma-t cross-section.

a strong seasonal thermocline is very apparent in the upper 200 m, where a gradient of 1.25 per 100 m occurs. In the winter, almost no gradient exists.

In general, the individual cruise sigma-t cross-sections were similar to the seasonal means in their main features (Figs. 102-124). However, seasonal means did mask shorter-term variations that occurred. Figure 125 shows the standard deviations at standard depths for each station, computed using the entire year's data. The largest variation occurred at the surface at station 1. In fact, the largest variations occurred at the nearshore stations reflecting the coastal influence upon these stations.

Away from the nearshore stations, the largest variations occurred at the surface. Exceptions were stations 4 and 5, where in the core of the Gulf Stream the maximum station standard deviations were recorded at about 75 m in depth. Below 200 m standard deviations were quite small, usually less than 0.2.

Variations that were noted occurred in three areas. Usually the lowest density water for a cross-section was found at the surface at stations 5 and 6. However, the lowest density water (20.77) for the entire year's data was found during the summer at station 1. This low density was a reflection of warm land air warming the nearshore water. The nearshore water also had low salinity reflecting the summer rainy season and land runoff.

As previously mentioned, lowest density water was usually found at stations 5 and 6. However, this low density near-

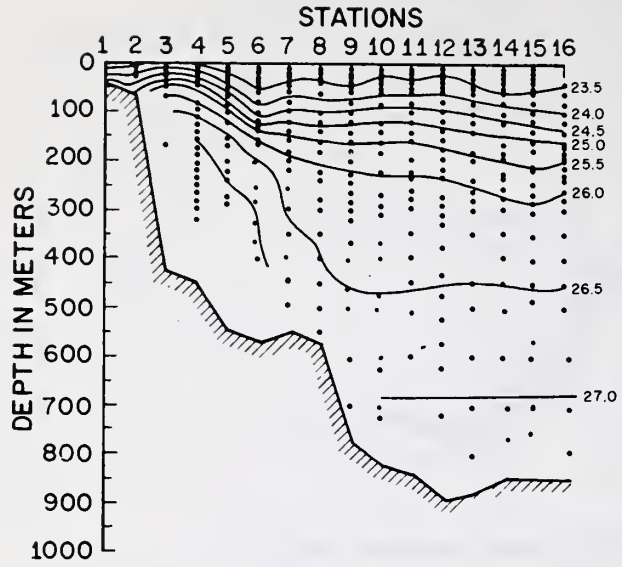

Figure 102. Cruise-1 sigma-t cross-section.

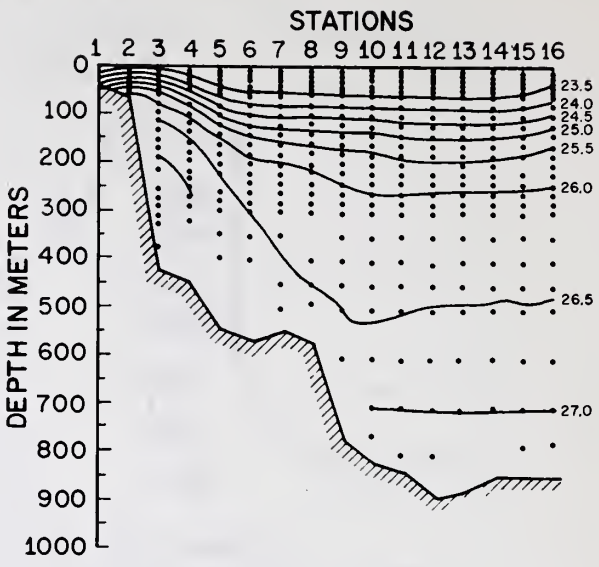

Figure 103. Cruise-2 sigma-t cross-section.

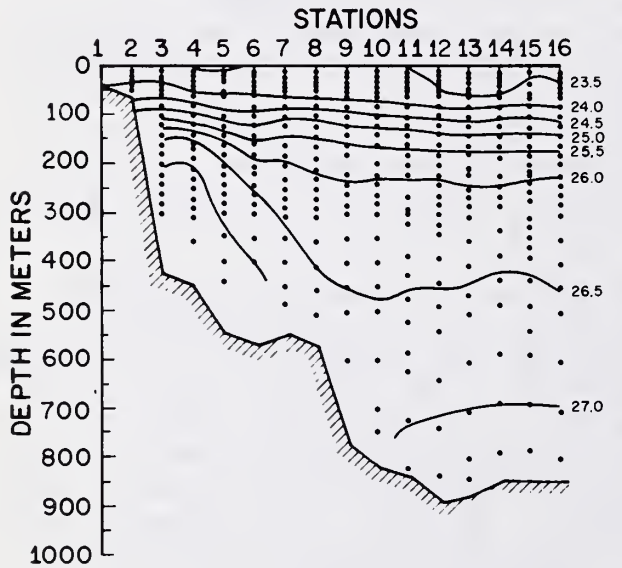

Figure 104. Cruise-4 sigma-t cross-section

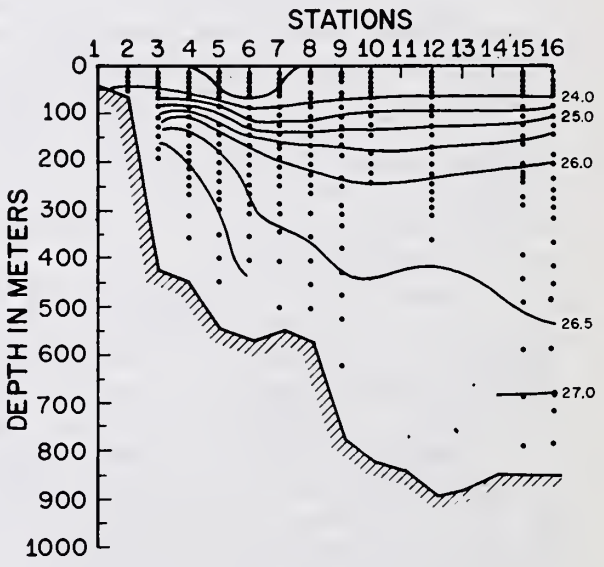

Figure 105. Cruise-5 sigma-t cross-section.

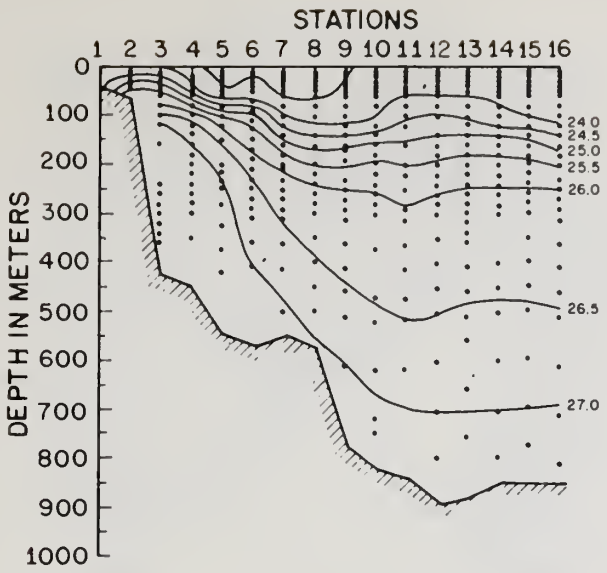

Figure 106. Cruise-6 sigma-t cross-section.

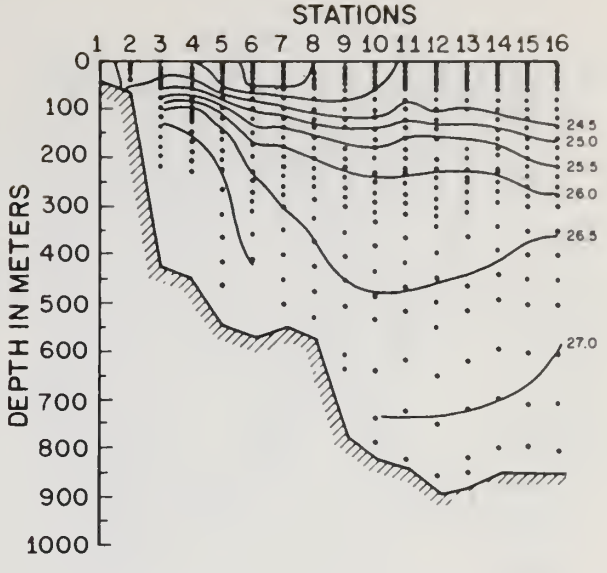

Figure 107. Cruise-7 sigma-t cross-section.

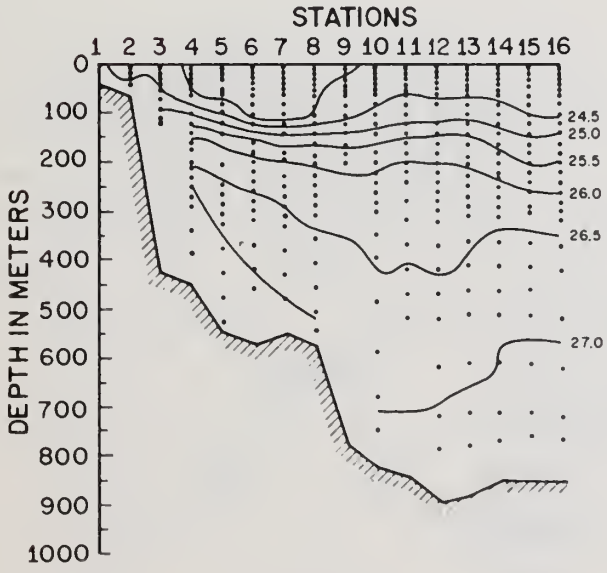

Figure 108. Cruise-8 sigma-t cross-section.

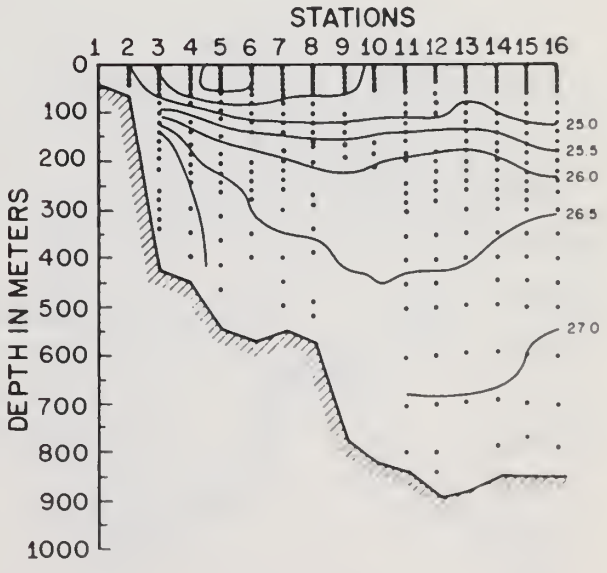

Figure 109. Cruise-9 sigma-t cross-section.

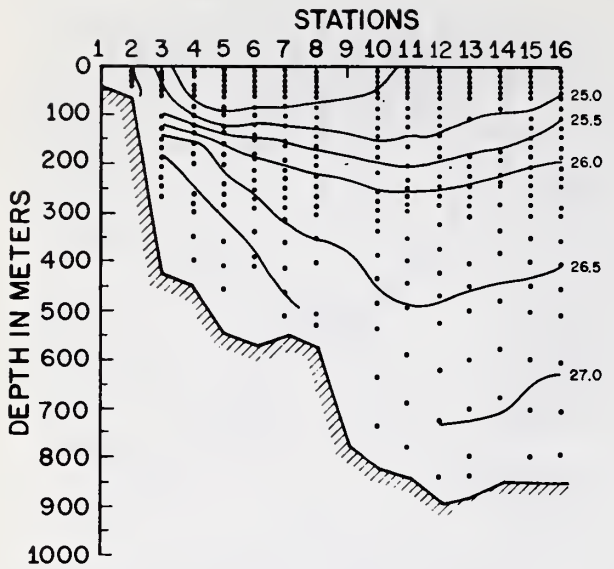

Figure 110. Cruise-10 sigma-t cross-section.

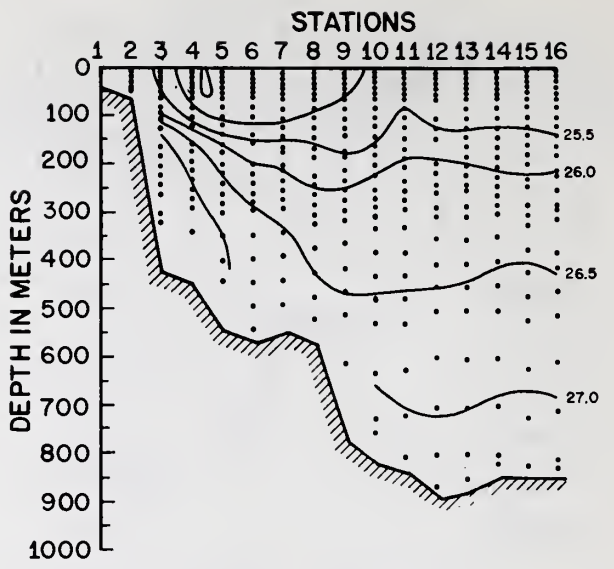

Figure 111. Cruise-12 sigma-t cross-section.

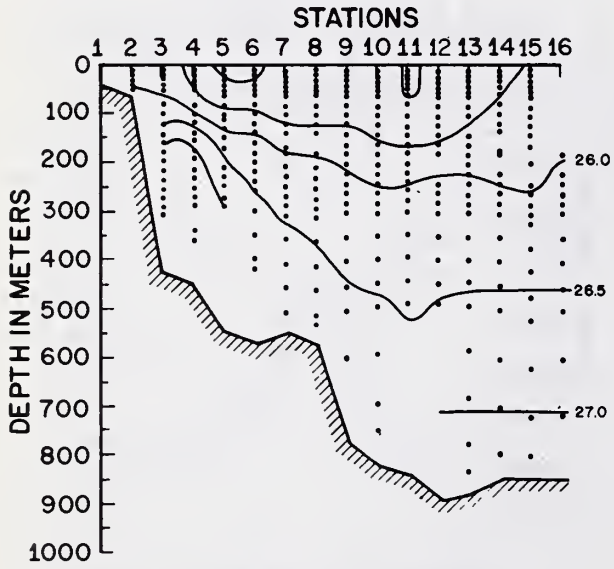

Figure 112. Cruise-14 sigma-t cross-section.

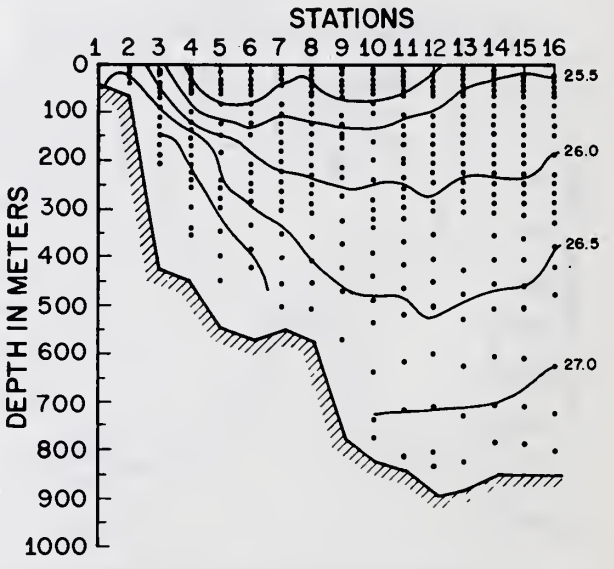

Figure 113. Cruise-15 sigma-t cross-section.

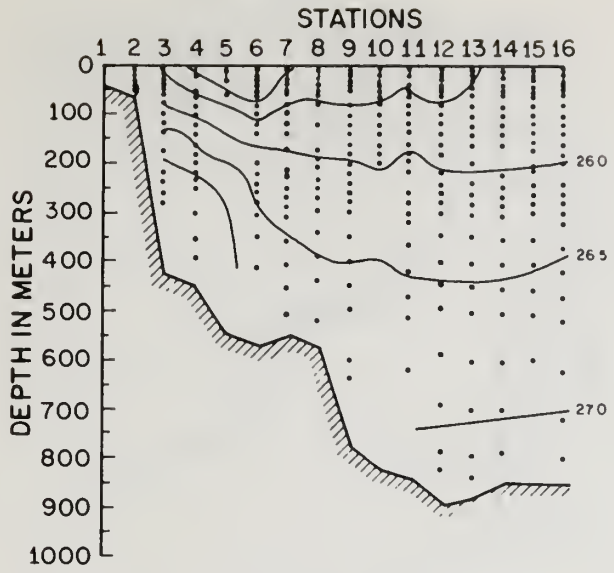

Figure 114. Cruise-16 sigma-t cross-section.

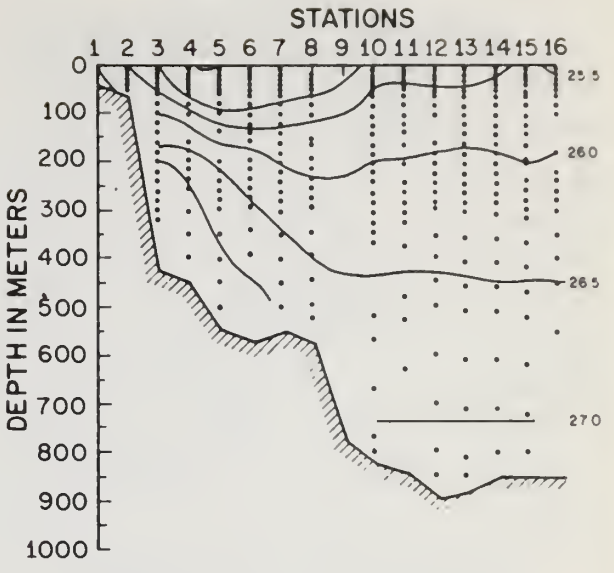

Figure 115. Cruise-18 sigma-t cross-section.

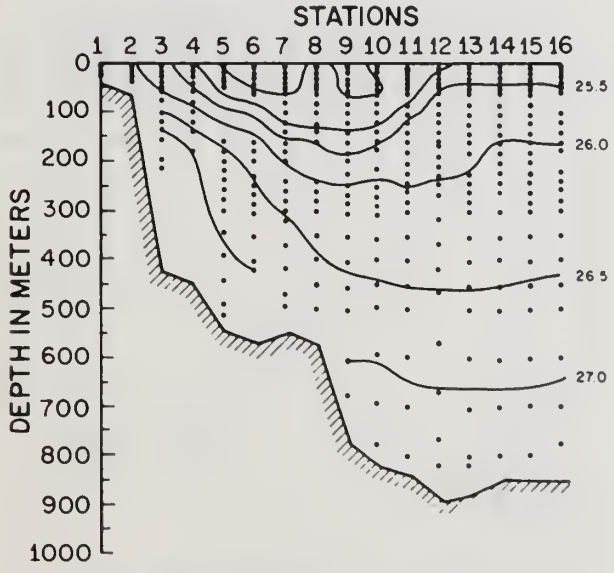

Figure 116. Cruise-19 sigma-t cross-section.

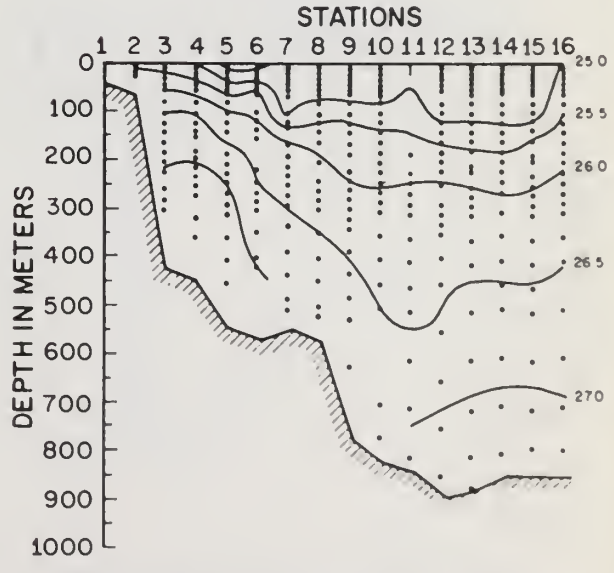

Figure 117. Cruise-20 sigma-t cross-section.

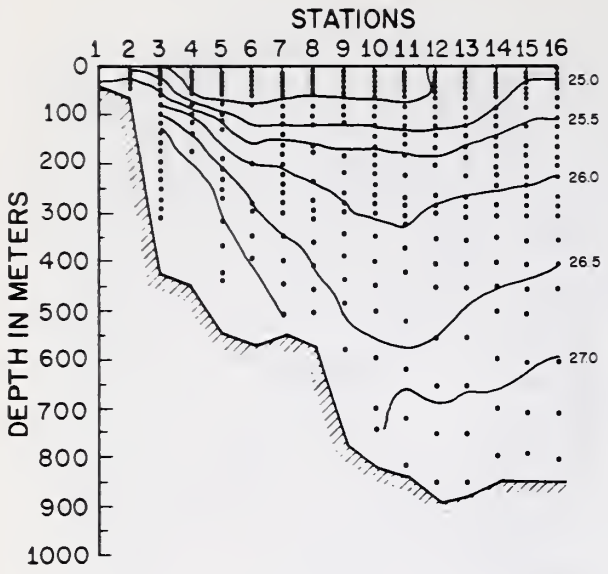

Figure 118. Cruise-21 sigma-t cross-section.

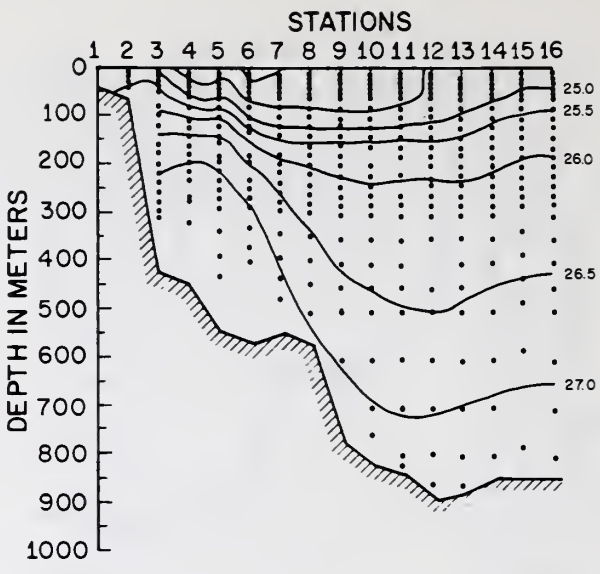

Figure 119. Cruise-22 sigma-t cross-section.

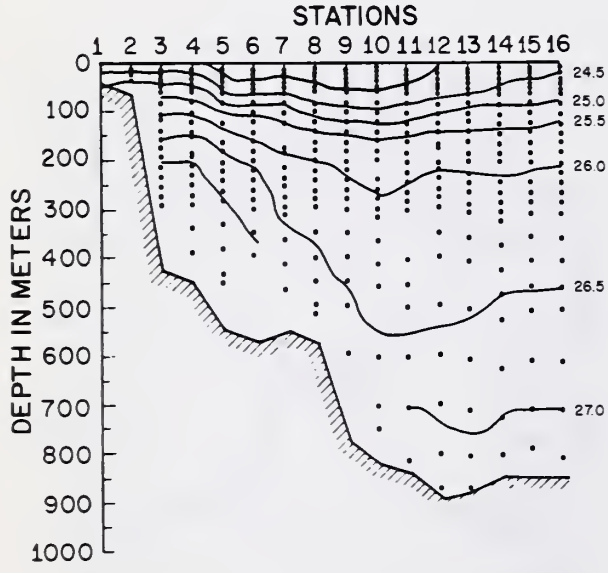

Figure 120. Cruise-23 sigma-t cross-section.

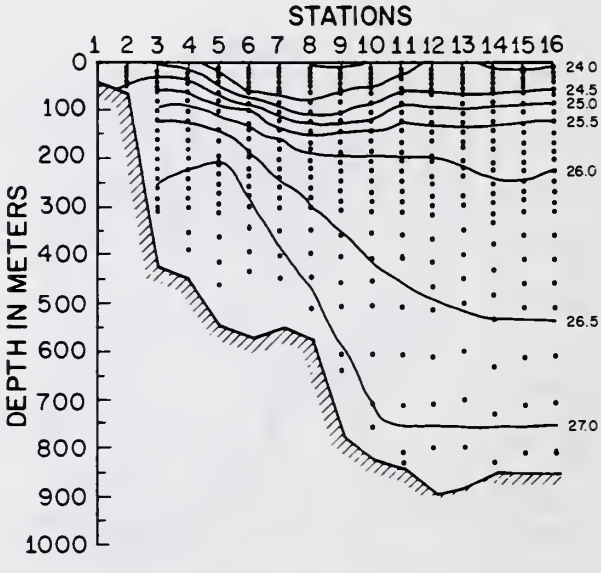

Figure 121. Cruise-24 sigma-t cross-section.

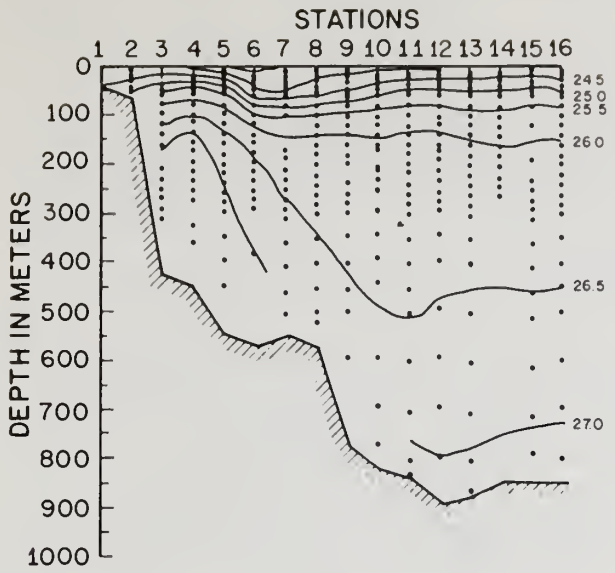

Figure 122. Cruise-25 sigma-t cross-section.

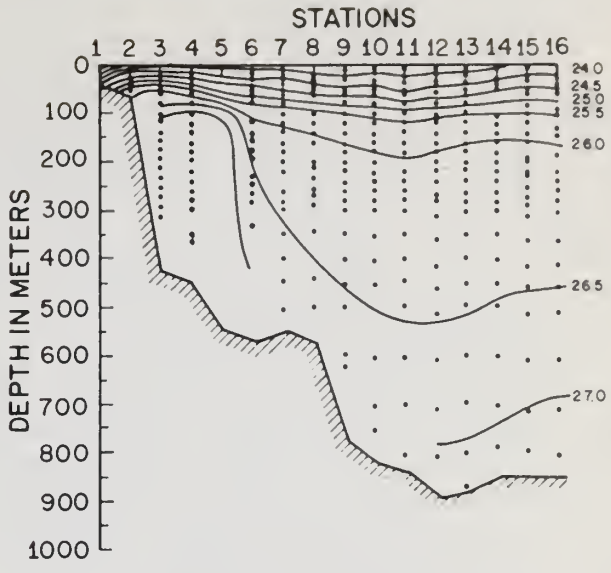

Figure 123. Cruise-26 sigma-t cross-section.

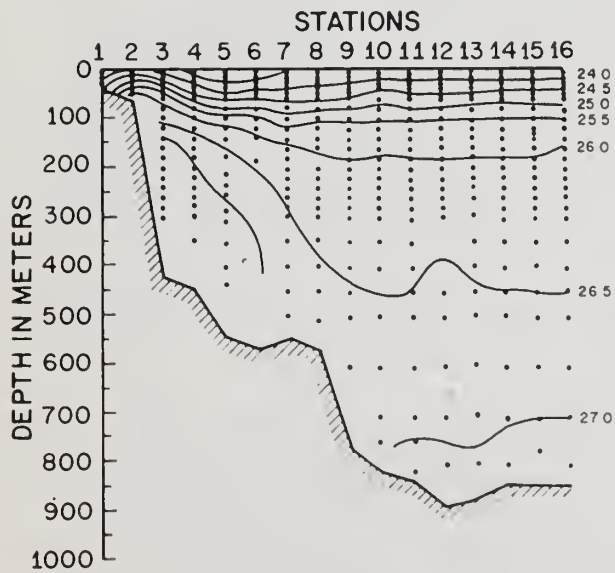

Figure 124. Cruise-27 sigma-t cross-section.

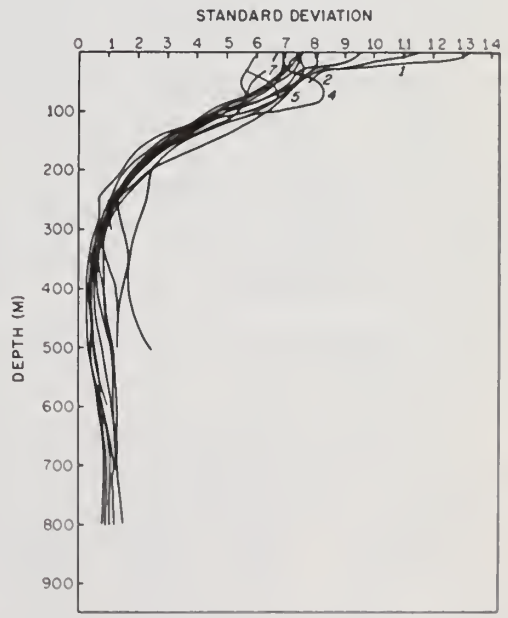

Figure 125. Standard deviations by stations, obtained by using all sigma-t data.

surface water spread from stations 5 through 9 during cruises 19 and 23. Cruise 19 was unique in that the low density water not only spread out horizontally but also extended vertically down to 50 to 100 m.

Cruise 22 also was somewhat unusual. Stations 6 and 10 (Fig. 1) and also their corresponding downstream stations recorded the low surface density water usually associated with this area. Yet a relatively higher density was recorded at station 8, and its corresponding downstream station. This unique water extended to a depth of about 100 m. The higher density resulted from the water temperature at station 8 being about 1.5°C colder than at station 6 and about 2.0°C colder than at station 10.

The third area of unusual variations was located at the bottom at stations 12 and 13. This was the deepest area along the entire cross-section. Usually a sigma-t of about 27.20 to 27.26 was recorded. However, during several cruises, notably 2, 6, 16, and 20, sigma-t's of 27.50 to 27.65 were recorded. Associated with these high densities were unusually low temperatures and high oxygens. Obviously, another water mass had entered the area.

6. GEOSTROPHIC CURRENTS AND VOLUME TRANSPORT

It is standard oceanographic practice to compute space variations in the dynamic height of the sea surface from the observed sub-surface density distribution assuming that a certain deep-level motion may be assumed to be negligible and an isobaric surface essentially level. The dynamic slope of an upper isobaric surface can be found from the variation of specific volume (reciprocal of density) along the isobaric layer. Thus the current at the upper surface relative to any possible current at the lower surface is determined. It is customary in deep water to assume an isobaric surface of 2000 decibars (approximately 2000 m deep) as a so-called layer of no motion.

The Peirce cross-sections were taken crossing the continental shelf and slope. The water depth varied between 30 m and about 900 m.

In similar circumstances, Dietrich (1937) computed the elevations of the sea surface along sections assuming there was a level of no motion in the oxygen minimum layer between 250 and 950 m. Again the Peirce Gulf Stream data were in too shallow water. The oxygen minimum layer was seldom reached. Dietrich, also confronted with this problem, assumed a vanishing horizontal pressure gradient at the bottom. According to Montgomery (1938), this method is very unreliable. Thus, because it appears that no reliable method exists to accurately determine dynamic currents from the early Peirce cruise data, no determinations were made.

Starting with cruise 20, surface drogues were planted in the water at each even (upstream) numbered station and then tracked for 30 minutes to one hour. For purposes of calculating geostrophic currents, the measured currents were assumed to have occurred at both the upstream station and the station directly downstream. The component of the measured current normal to the cross-section was calculated. Geostrophic currents then were computed from the dynamic heights downward from the surface from stations 2 through 10. The method used is described by von Arx (1962).

The surface drogue measurements exhibit a pattern of variability that had already become apparent by the analysis of the temperature-salinity data. The surface drogue measurements indicate that the axis of the Gulf Stream is usually in the vicinity of stations 5 or 6, but on occasion touches stations 4 and 7. The maximum recorded current also varied from cruise to cruise from a low of 141.5 cm/sec during cruise 23 to a high of 218.8 cm/sec during cruise 22. The mean at the core was 178.5 cm/sec. A large variation was recorded at other stations. For example, station 9 varied between a high of 96.6 cm/sec during cruise 20 to a low of 0 during cruise 25.

The current between stations 2 and 3 flowed as part of the Gulf Stream during cruises 21, 22, 26, and 27. During cruises 23, 24, and 25, the current flowed in the reverse direction. Although the water depth in this area varied between 60 and 300 m, the geostrophic current data extended down only to 30 m. The reverse current varied in velocity between 10 and 40 cm/sec. This confirms Bumpus'(1955) report that south of Cape Hatteras a southerly-flowing coastal current was a transient affair.

Generally, the current of the Gulf Stream decreases outward from the core and downward from the surface. However, an increase in velocity with depth does occur locally. For example, during cruise 20, stations 5 to 6 recorded a maximum velocity of 206.8 cm/sec at 75 m. Several other examples were recorded where the maximum station velocity was between 75 and 250 m. Figures 126 to 133 give the current variation across the section at the surface and 100 m. Several examples were noted where the current at 100 m was greater than at the surface.

In this area, the Gulf Stream sometimes extends beyond the entire cross-section, a distance of 90 nautical miles. Station 10, the farthest seaward station that current measurements were made, recorded a mean velocity of 48.0 cm/sec. The velocity cross-section for cruises 20 through 27 are given as Figures 134 through 141. It is to be noted that the axis of the stream is not vertical, but rather exhibits a seaward tilt on nearly every cross-section.

If the geostrophic velocity is computed for each successive layer, the volume transport normal to the lines joining each pair of stations can be computed by summing the products of cross-sectional area and mean velocity for each depth interval. This was done for each Peirce cross-section from cruises 20 to 27. The computational methods for applying the geostrophic

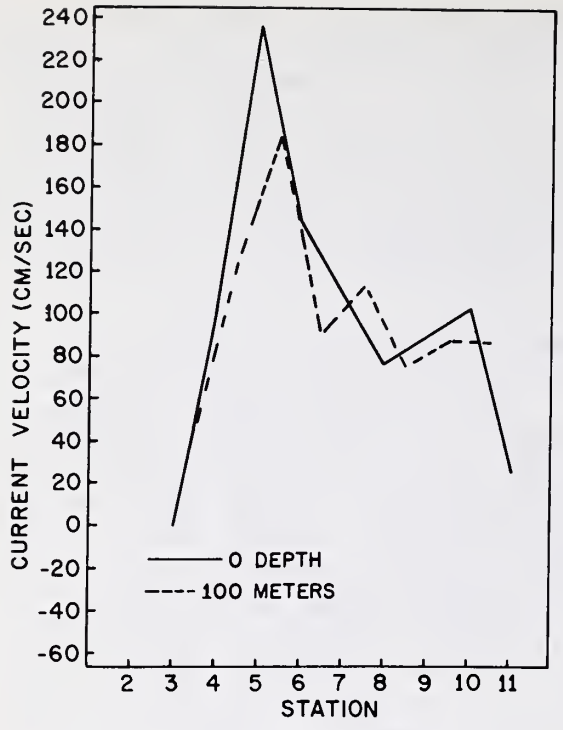

Figure 126. Current velocity at 0 and 100 m for cruise 20.

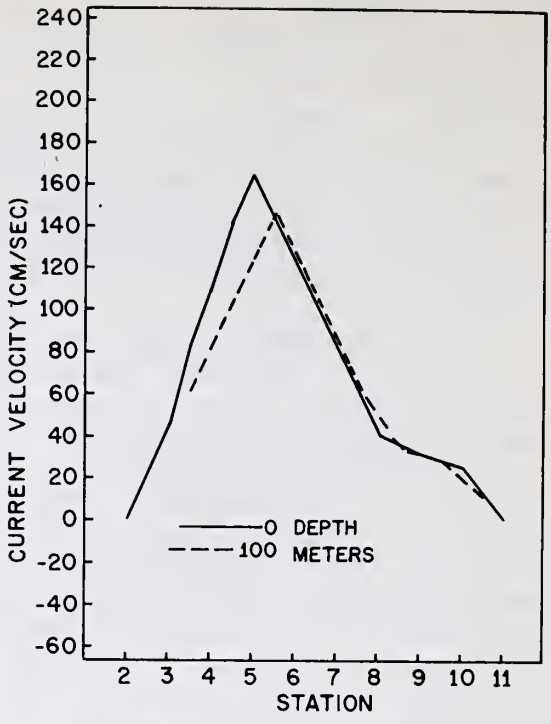

Figure 127. Current velocity at 0 and 100 m for cruise 21.

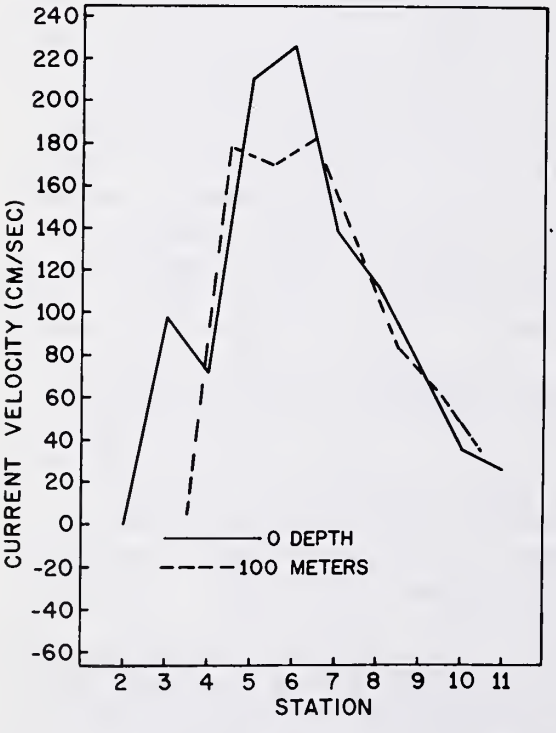

Figure 128. Current velocity at 0 and 100 m for cruise 22.

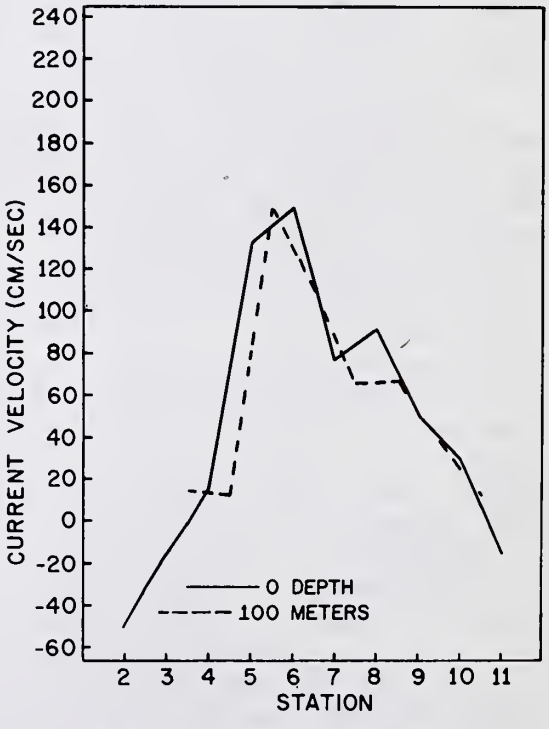

Figure 129. Current velocity at 0 and 100 m for cruise 23.

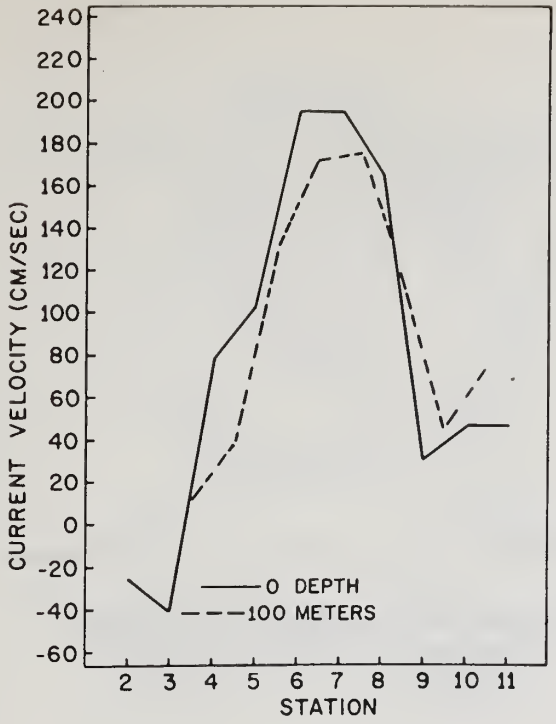

Figure 130. Current velocity at 0 and 100 m for cruise 24.

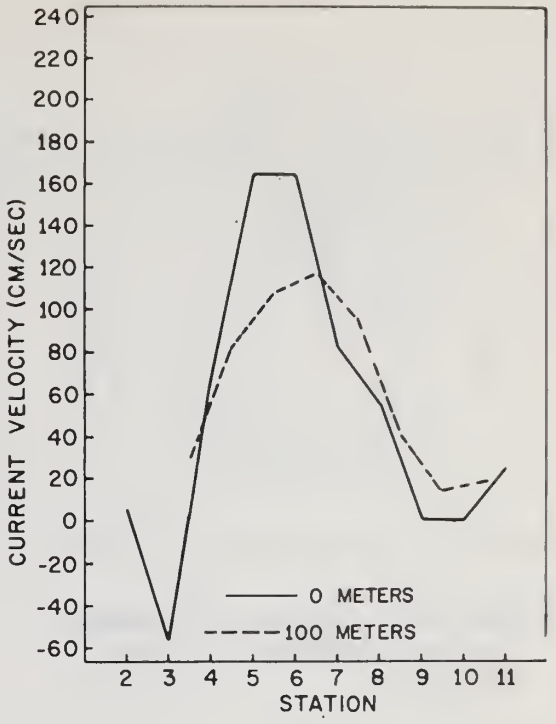

Figure 131. Current velocity at 0 and 100 m for cruise 25.

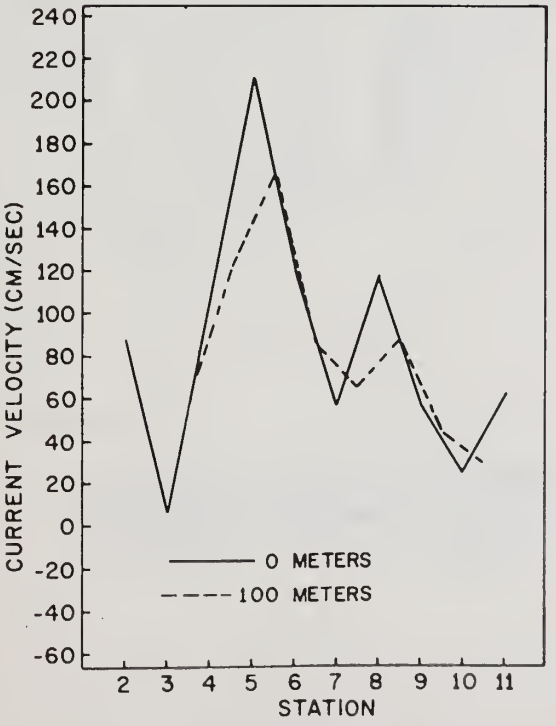

Figure 132. Current velocity at 0 and 100 m for cruise 26.

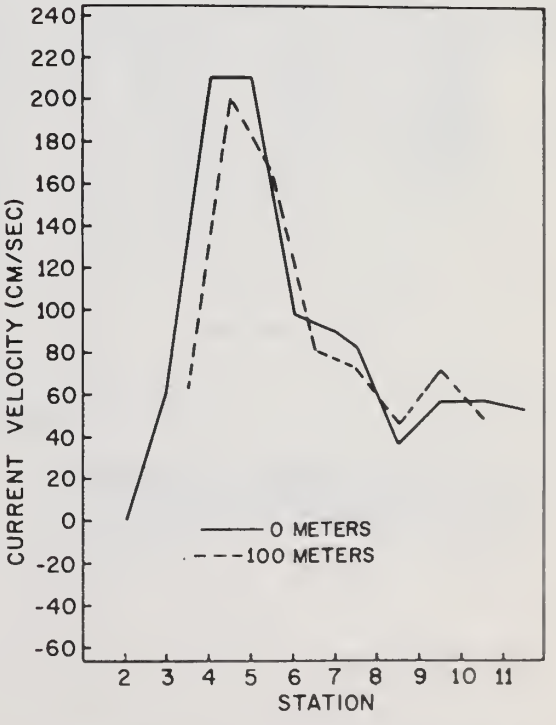

Figure 133. Current velocity at 0 and 100 m for cruise 27.

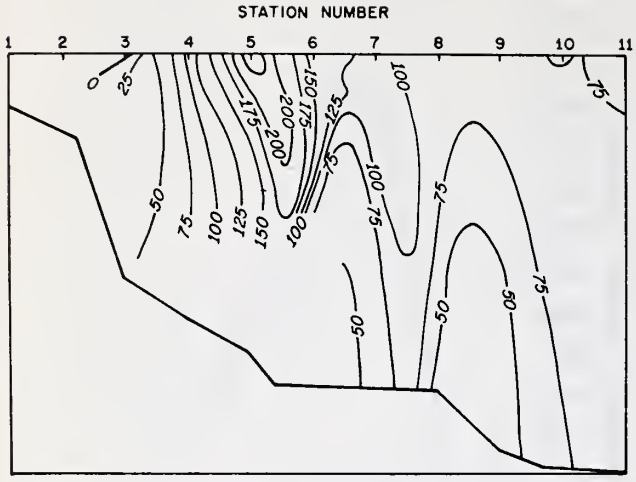

Figure 134. Cruise-20 northern line geostrophic currents (cm/sec).

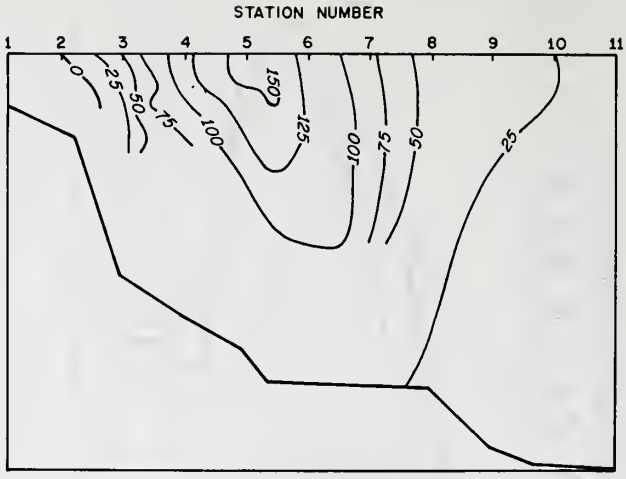

Figure 135. Cruise-21 northern line geostrophic currents (cm/sec).

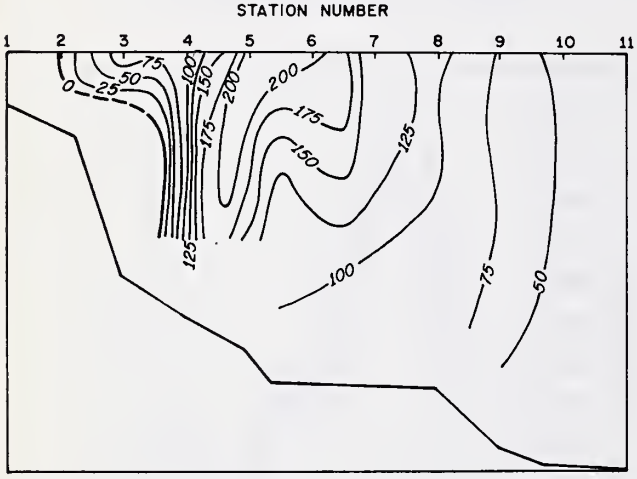

Figure 136. Cruise-22 northern line geostrophic currents (cm/sec).

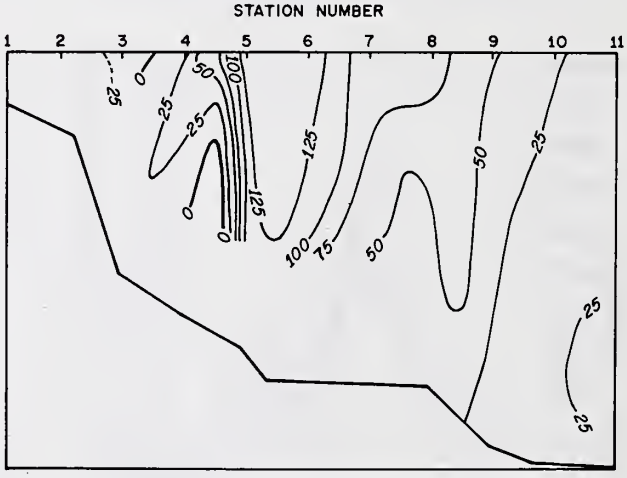

Figure 137. Cruise-23 northern line geostrophic currents (cm/sec).

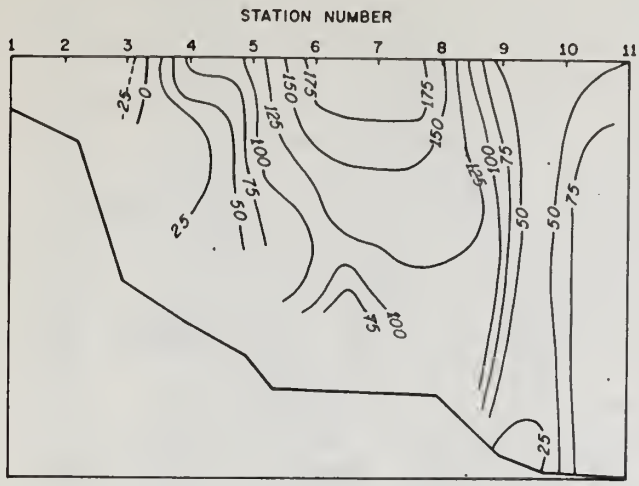

Figure 138. Cruise-24 northern line geostrophic currents (cm/sec).

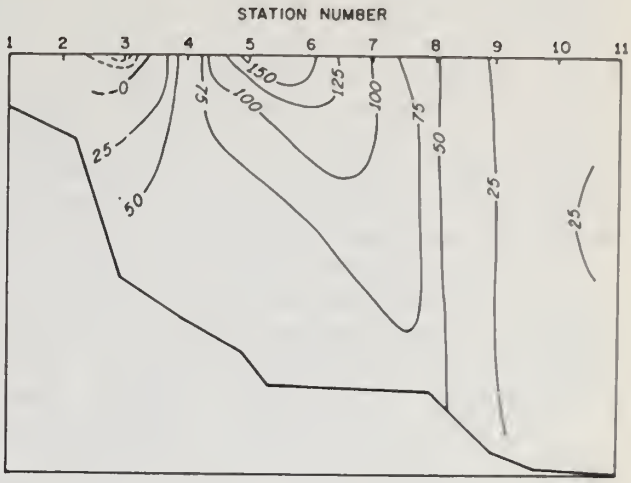

Figure 139. Cruise-25 northern line geostrophic currents (cm/sec).

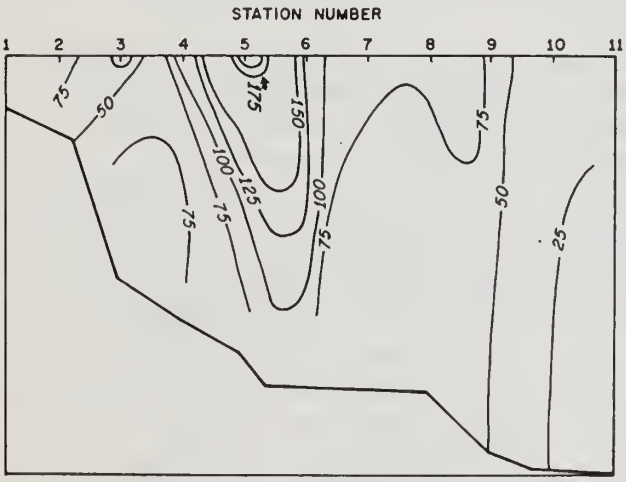

Figure 140. Cruise-26 northern line geostrophic currents (cm/sec).

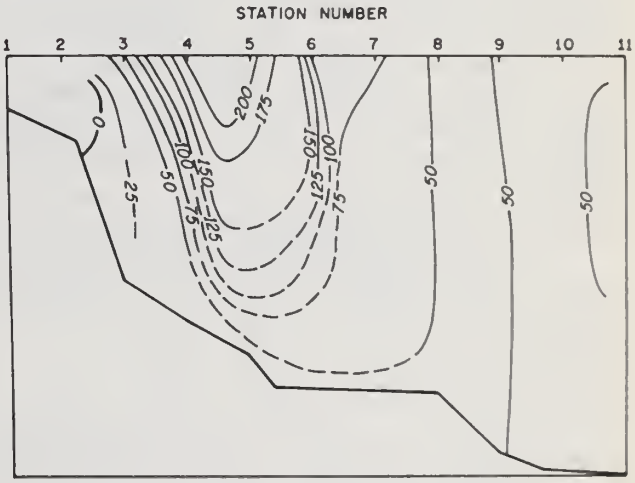

Figure 141. Cruise-27 northern line geostrophic currents (cm/sec).

method are given in H. O. pub 614 (U.S. Navy Hydrographic Office, 1951). Also von Arx (1962) gives a good summary.

These calculations will not accurately reflect the total Gulf Stream volume transport, as several sources of error exist. The surface drogue measurements did not extend completely across the Gulf Stream. As no drogue measurements were made at the seaward end of the line, no volume transport calculations could be made. Additional volume was missed, as the data did not always extend to the bottom.

The accuracy of the volume transport calculations is closely correlated with the accuracy of the surface drogue current measurements. The ship's navigation for the drogue current measurements was by HIFIX. However, the ship's navigation procedure allows its accuracy to be questioned.

Also occupation of oceanographic stations in a current demand a high degree of skill. The ship must maneuver to hold position and also keep a small wire angle to allow the messenger to slide freely and trip the Nansen bottles. But the maneuvering plus drifting in the wind and current may move the ship as much as a mile between the deep and shallow casts in what is nominally the same oceanographic station. During processing of the station data, adjustments were made to give a mean position. Also smoothing of the temperature and salinity data were carried out in the area of overlap between the deep and shallow casts.

Iselin (1940) also was concerned about the various sources of errors inherent in transport calculations. He used tide gage records to prove that his transport values were surprisingly accurate. He concluded that a calculated transport value could be in error by more than 10%, but that the average error of the values was much less.

The individual cruise transport values fluctuate from a low of 25.6×10^6 m^3/sec on cruises 21 and 23 to a high of 65.5×10^6 m^3/sec (Fig. 142). The mean values for the eight cruises are 46.2×10^6 m^3/sec for the north line and 45.3×10^6 m^3/sec for the south line. The mean values appear to be quite reasonable. Schmitz and Richardson (1968) reported the volume transport between Miami and Bimini to be $32 \pm 3 \times 10^6$ m^3/sec, and Iselin (1940) reported various values between 76.4 and 93.5×10^6 m^3/sec for the transport across the Gulf Stream between Montauk Pt., New Jersey, and Bermuda. Iselin noted that his data indicated seasonal periodicity, but thought it did not indicate short period variations. However, he conceded that his computational methods tended to minimuze short-period changes.

Conversely, Von Arx (1962) mentions several reports of diurnal fluctuations in the flow of the Florida Current and Gulf Stream by direct measurements. Von Arx reports "in addition to the tidal variations in the Florida Current, there is an irregular variation of transport based on 24-hour averages taken so as to eliminate the tidal influences. These irregularities show a wide range of variation (by a factor of two) in

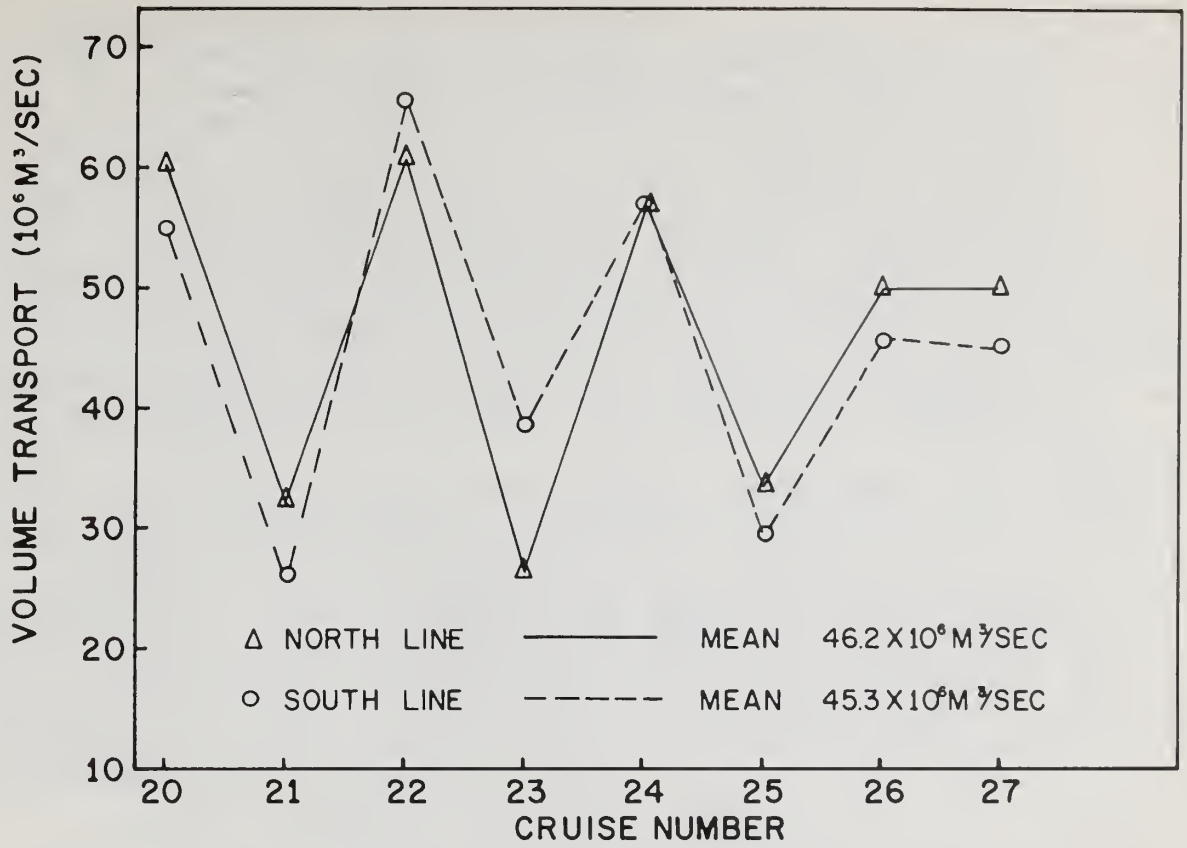

Figure 142. Volume transport across the Gulf Stream for cruises 20-27.

the course of a month and other oscillations having a similar slope but less amplitude." Thus it appears that these transport values are acceptable, having a maximum error of 10 percent.

7. WATER MASS ANALYSIS

It is well established that, as the Gulf Stream flows northward off the east coast of the U.S., its volume of water increases. However, the source of this water has not been well established. It is possible that water mass analysis might indicate the sources of this additional water.

The most widely used method of defining the characteristics of various water masses and of studying their origins and relationships is by the temperature-salinity correlation method first introduced by Helland-Hansen (1918). Since then, the nomenclature of the water masses in the North-Atlantic Ocean has become quite confused, although apparently the water masses themselves have remained essentially the same.

Wright and Worthington (1970) have made a comprehensive report on the nomenclature as used by various authors. Thus a nomenclature discussion here will be limited to that necessary to understand the water masses that occur in the area of interest.

According to Nowlin (1971), the water beneath the surface mixed layer but above the 17°C water is the only distinct water mass formed in the Gulf of Mexico. This water mass, referred to as Continental Edge Water by Wennekins (1959), is characterized by an increase in salinity from about 36.00°/oo to 36.45°/oo between about 25°C and 18°C. Thus the salinity is considerably less for a given temperature than is the water referred to as Yucatan Straits Water by Wennekins.

The water that passes through the Yucatan Straits either passes around the western end of Cuba and directly into the Florida Straits as the Florida Current or flows as the Loop Current in a clockwise direction in the eastern Gulf of Mexico before joining the Florida Current. According to Wust (1964) as well as Nowlin (1971), the water flowing through the Yucatan Straits is made up of the Subtropical Underwater, characterized by an intermediate salinity maximum (36.60 - 36.80°/oo) in depths between 50 and 200 m. Below this is water characterized by an intermediate oxygen minimum in about 400 to 600 m depth, and beneath these is found a remnant of Sub Antarctic Intermediate Water identified by an intermediate salinity minimum in various depths between 700 and 850 m in the Caribbean Sea. Nowlin indicates the depth of this layer varies between 900 and 1100 m in the Gulf of Mexico.

These water masses can be considered the source waters of the Florida Current. Starr (1970) found evidence that some water was added through the Santaren Channel in the central Florida Straits. Farther north, Richardson and Finlen (1967) found indications of water addition to the Florida Current through the Northwest Providence Channel.

Jacobsen (1929) explained all the water in the North Atlantic as combinations of six basic water types; among them was the Antilles Current Water. Iselin (1936) describes the Antilles Current as flowing northwestward along the line of the Bahama Islands and joining the Florida Current north of Little Bahama Bank. Wust (1924) calculated that it supplied the Gulf Stream with about half as much water as does the outflow from the Straits of Florida. The Atlantis took hydrographic stations in this area in February 1932 and April 1933. Iselin (1940) concluded that there was no evidence of a powerful Antilles Current. However, he suggested that, because it is primarily a wind-driven current, as the trades move north-ward in summer the resulting flow might be broader and swifter. He further stated "that on the basis of the present data, the term Antilles Current had best be reserved for the shallow and weak stream of

equatorial water near the islands."

The water found in the Sargasso Sea probably has had more names than any other water mass found in the North Atlantic. Iselin (1936) called it Central Atlantic Water. Its descriptive T-S curve varies from a high of 18°C with a salinity of ·36.5°/oo to a low of 4°C with a salinity of 35.00°/oo . This water is roughly equivalent to the North Atlantic Central Water described by Sverdrup, et al.(1946). Wright and Worthington (1970) call this water the Western North Atlantic Water. According to Worthington (1959), a considerable part of this water, referred to as 18° water, is formed in the northern part of the Sargasso Sea during the winter. It has a characteristic inflection point close to 300-m depth where the temperature is 17.9 ± 0.3°C and the salinity is 36.50 ± 0.10 °/oo. It is hypothesized that these water masses must be the source water for the Gulf Stream in the vicinity of the Peirce cruises.

To define the T-S relationships of the various water masses found in the vicinity of the Peirce cruises, station data from the various source areas were plotted and compared. Figure 143 shows the T-S curve of Continental Edge Water as reported by Wennekens (1959). Also shown are the T-S curves reported by Wennekens (1959) and Iselin (1936) of water in the vicinity of the Yucatan Straits.

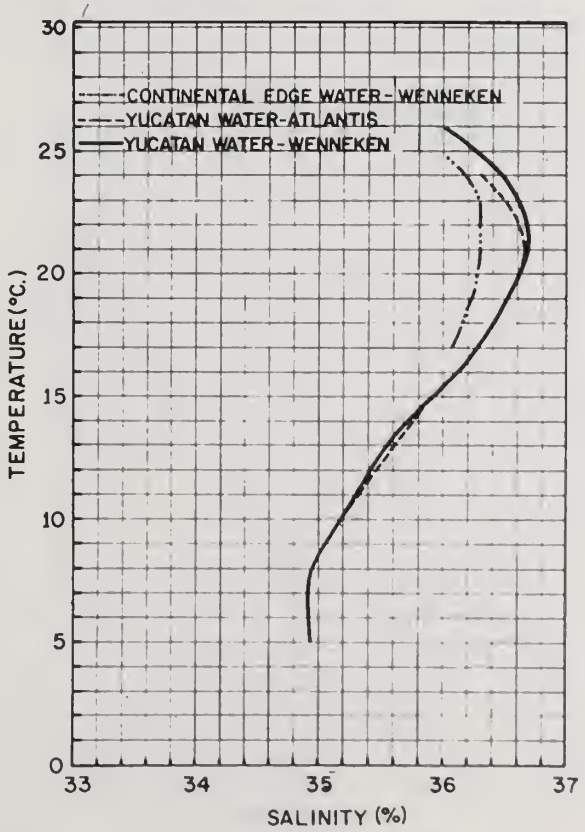

Figure 143. Comparison T/S curves-Continental Edge Water and Yucatan Strait Water.

Comparison curves also were drawn for the water in the vicinity of the Antilles Current. Data were used from the Atlantis cruises of April 1932, and February 1933, the cruise of the Requisite of March 1962, and cruises of the Explorer of April and May 1962 and May 1964. The Explorer and Requisite data are in good agreement below 19°C. As a matter of fact, between 19°C and 11°C and below 6°C, the three curves agree very well. However, between 11°C and 6°C the Requisite and Explorer data exhibit lower salinity values indicating that the Antarctic Intermediate salinity minimum is more prominent than in the Atlantis data. Figure 144 shows these curves.

The Requisite and Explorer also recorded salinity values in the upper 200 m between 36.70°/oo and 37.00°/oo. These values are considerably higher than those recorded by the Atlantis. This great variation in salinity between cruise data is not surprising. Deductions from observations from cruises widely spaced in time may be untrustworthy. This would be especially true in this area, as the Antilles current, according to Iselin (1936), is primarily wind-driven and related to the trades. Defant (1936) indicates that the water in the vicinity of the salinity maximum is a mixture of waters from the southeast and northeast.

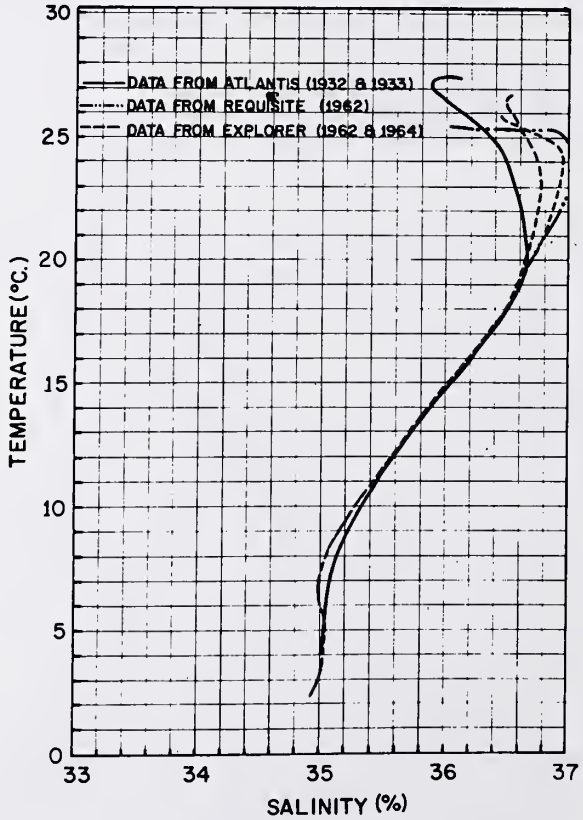

Figure 144. Comparison T/S curves Antilles Current Water.

T-S comparison curves for the water in the Sargasso Sea were drawn using Atlantis data between Chesapeake Bay and Bermuda and Explorer data taken north of the Antilles Current. Between 18°C and 4°C, the limits of the Atlantis data, the two curves are in excellent agreement (Fig. 145). It is not possible to differentiate between water passing through the Yucatan Straits, the Antilles Current, and the water from the Sargasso Sea between 18°C and 22°C. Also Antilles Current Water cannot be differentiated from Sargasso Sea Water between 18°C and 11°C.

Station mean T-S curves for the entire year of data were computed and drawn and are presented as Figure 146. As stations 6 through 16 are very similar, only stations 6, 11, and 16 are shown as examples.

Both surface and maximum salinity values increase with distance from shore, indicating several water masses are crossed. Stations 1 and 2 exhibit a nearshore or coastal water type of local origin. At station 2 Continental Edge Water appears at 30 to 50 m depth. Stations 4 and 5 contain a mixture of Continental Edge Water and water that has passed through the Yucatan Straits (Florida Current Water), the later water type predominating.

Seaward of station 6, water from the Sargasso Sea or Antilles Current predominates.

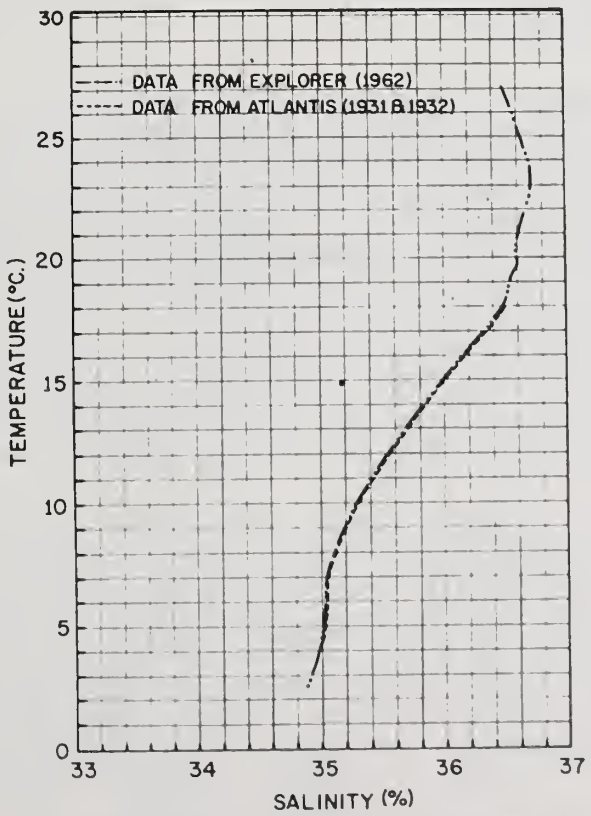

Figure 145. Comparison T/S curves for Sargasso Sea Water.

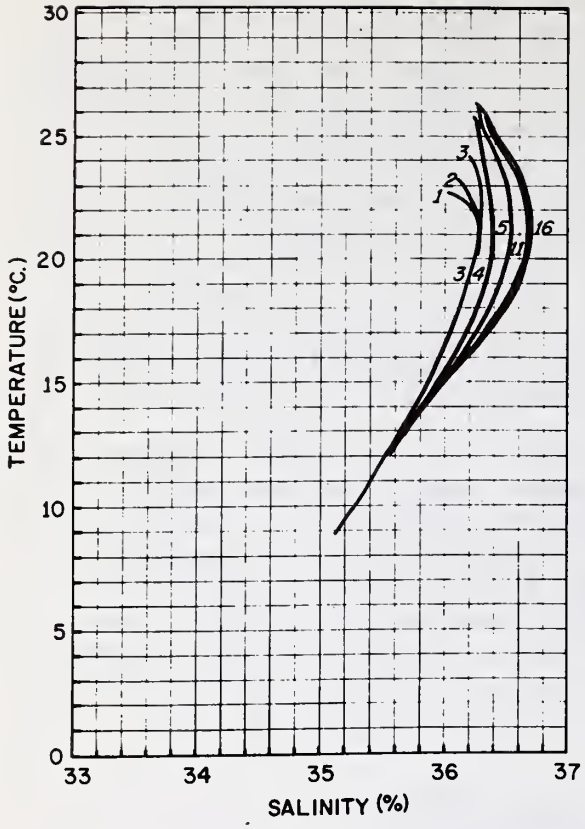

Figure 146. Mean station T/S curves obtained by using all data.

Seasonal mean station T-S curves were computed and given as Figures 147-150. These seasonal T-S curves exhibit patterns similar to the total of all data T-S curves. The same seasonal transition from coastal water to Continental Edge Water to Yucatan Straits Water to Antilles Current Water or Sargasso Sea Water exists. Considerable variation in maximum salinity from season to season was recorded at stations 1 through 6. This indicates considerable variation in the percentage of each water mass in the core of the Gulf Stream. The dominant forces that control the cross-stream mixing must vary with time in a way that is not clear from the mean T-S curves. The T-S curves for stations 7 through 16 coincide during each season.

Seasonal composite station T-S curves were drawn. Figures 151-155 are examples of these curves. Figure 151 shows the composite curves for the spring at station 4. The velocity core of the stream is usually seaward of this station. Identifiable are Continental Edge Water, Yucatan Straits Water, and water that is a mixture of the two. By station 5 (Fig. 152) Yucatan Straits Water predominates; a small amount of water from the Antilles Current can be identified at about 21-23°C during four of the six summer cruises. Station 6 (Fig. 153) still has Yucatan Straits Water predominating. Continental Edge Water no longer is evident. The envelop of T-S curves is relatively wide indicating that during some cruises Antilles Current Water or possibly Sargasso Sea Water has come into the area.

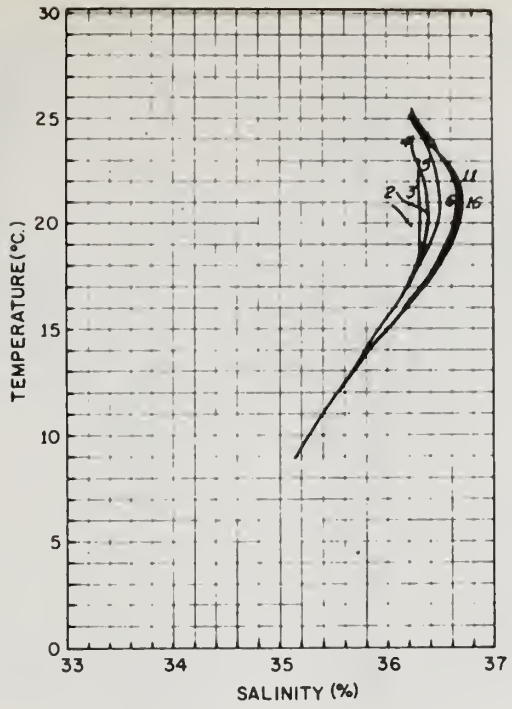

Figure 147. Mean station T/S curves, obtained by using spring data.

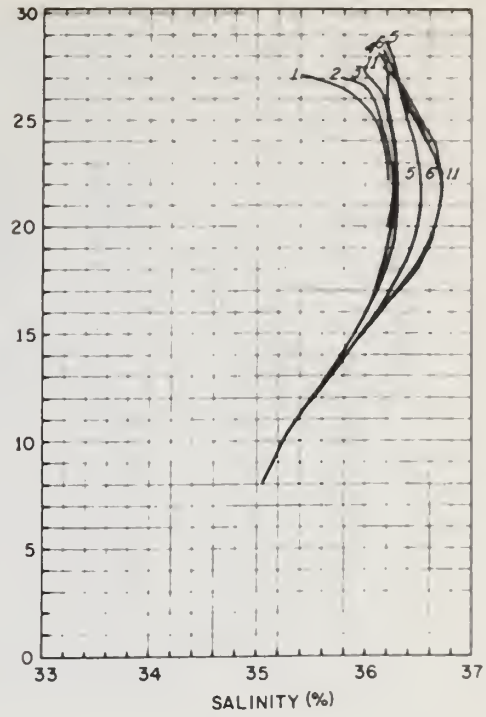

Figure 148. Mean station T/S curves, obtained by using summer data.

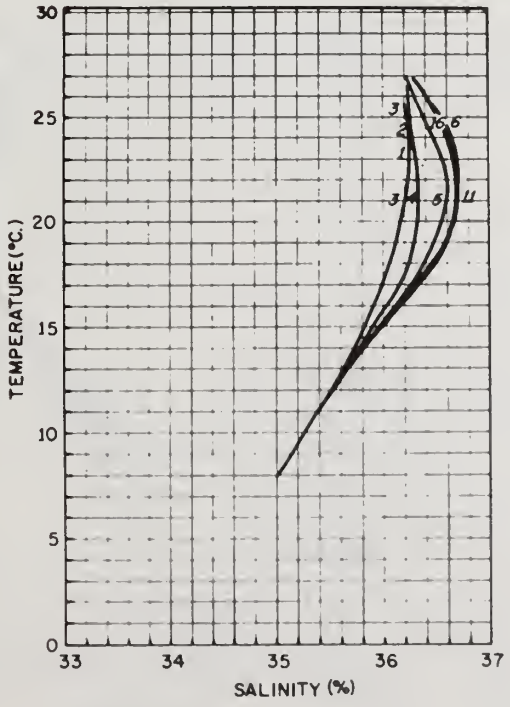

Figure 149. Mean station T/S curves, obtained by using fall data.

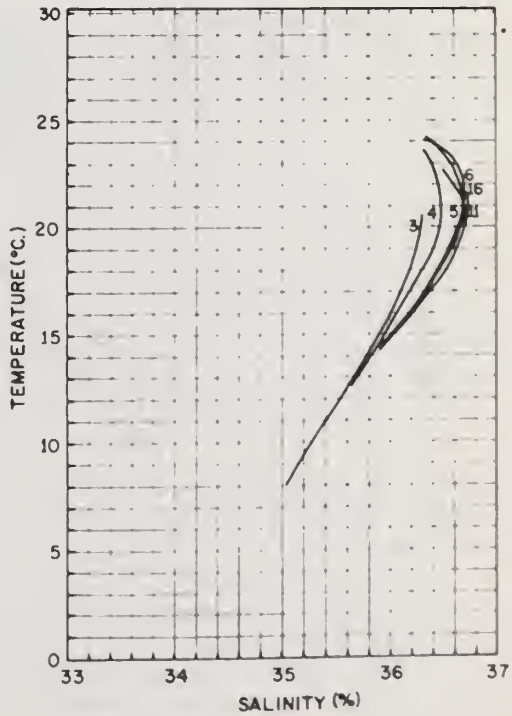

Figure 150. Mean station T/S curves, obtained by using winter data.

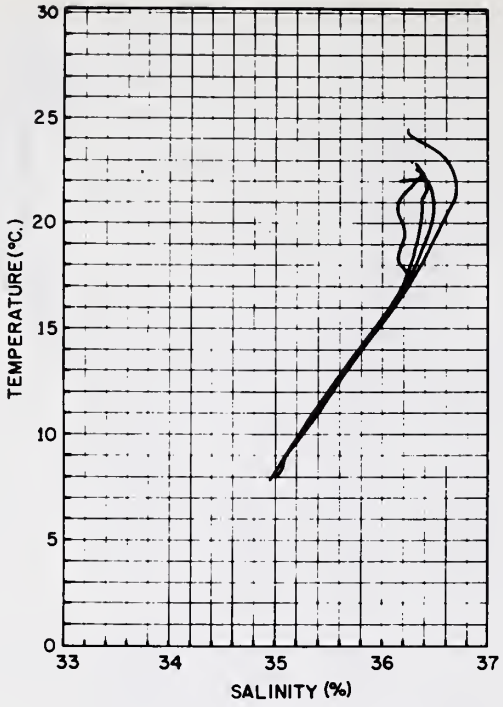

Figure 151. T/S curves for station 4 showing variation by cruise, during spring.

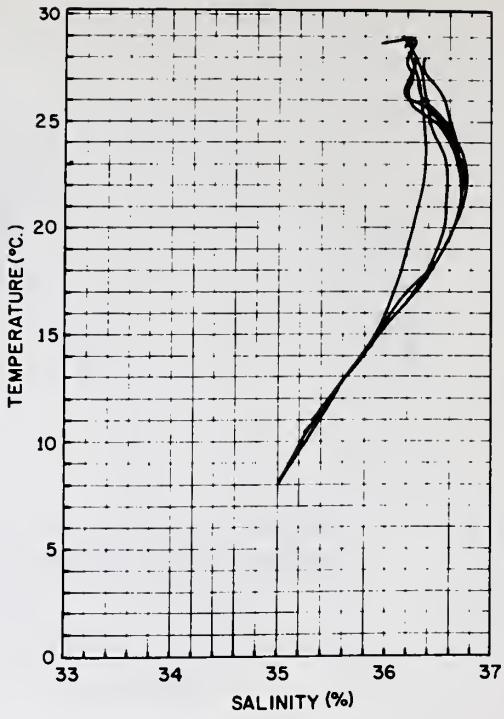

Figure 152. T/S curves for station 5 showing variation by cruise, during summer.

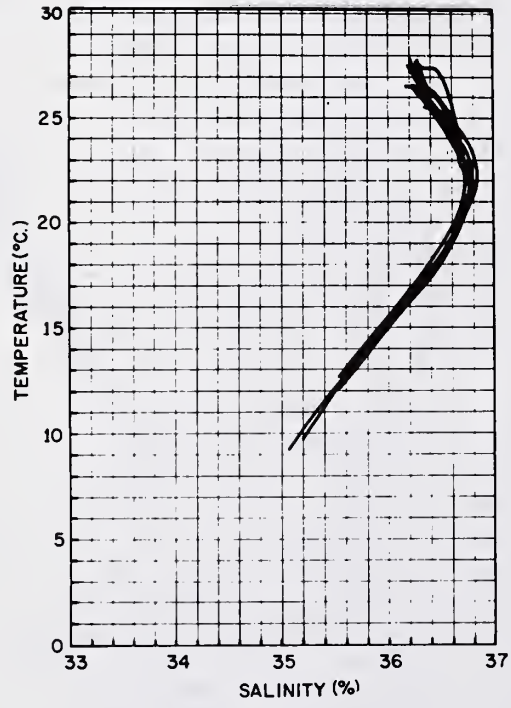

Figure 153. T/S curves for station 6 showing variation by cruise, during fall.

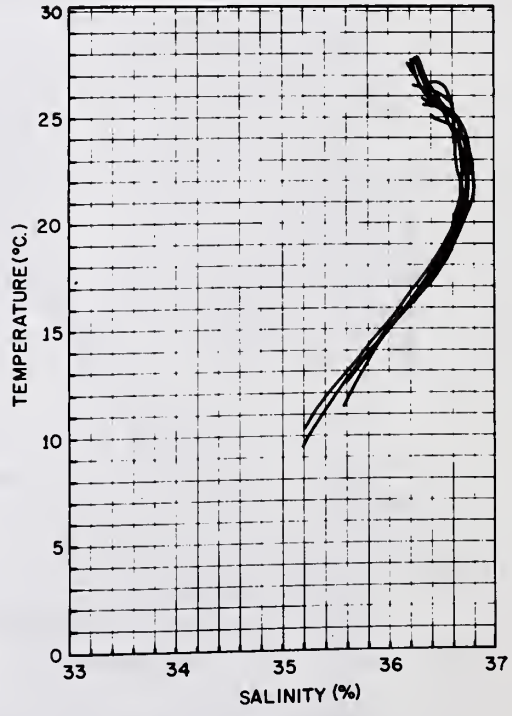

Figure 154. T/S curves for station 7 showing variation by cruise, during winter.

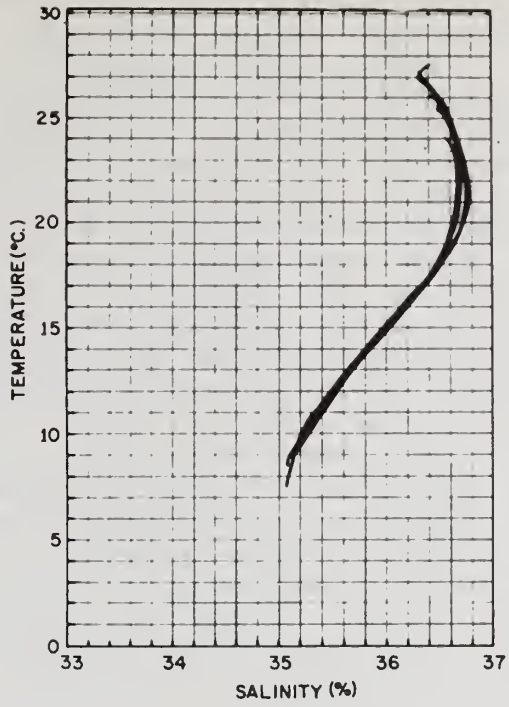

Figure 155. T/S curves for station 16 showing variation by cruise, during fall.

The transition continues at station 7 (Fig. 154). In the upper layers, Antilles Current Water predominates. Below about 20°C Yucatan Straits Water predominates, but Antilles Current Water or Sargasso Sea Water occurs above 15°C during two cruises.

By station 16, Antilles Current Water and Sargasso Sea Water completely predominate (Fig. 155). However, between 9°C and 12°C Yucatan Straits Water occurs during two cruises.

Unusually high sigma-t values occurred during cruises 2, 6, 16, and 20. Sigma-t values between 27.50 and 27.65 were associated with unusually low temperature values and unusually high salinity and oxygen values. This water can be definitely identified as Sargasso Sea Water, while the water above is definitely from the Antilles Current.

As previously mentioned, during cruise 22 the water density was unique. A relatively higher than usual density was recorded at station 5. The water at stations 4 and 6 is identified as Yucatan Straits Water, while at station 5, the surface water is a mixture of Yucatan Straits Water and Continental Edge Water. Below the surface down to at least 100 m, the water is Continental Edge Water. Apparently at some earlier time the Loop Current, west of Florida, entrained this water and carried it along without mixing.

8. OXYGEN-DENSITY RELATIONSHIP

Because use of the temperature salinity relationship was only partially successful in differentiating between the various water masses found in this area, the oxygen-density relationship was used.

Rossby (1936) found that the oxygen-salinity correlation in the Sargasso Sea is different from that in the Yucatan Channel-Florida Straits area. Lowest oxygen concentrations are found in the Straits of Florida. The oxygen-salinity values from the Antilles Current were somewhat between the other two.

To distinguish the water masses in question, Richards and Redfield (1955) defined the correlation between the oxygen concentration and each 0.1 sigma-t unit span of Sargasso Sea Water and examined the anomalies from this correlation of water samples taken across the Yucatan Channel, across the Florida Straits, and along sections across the Gulf Stream. They chose sigma-t rather than salinity because sigma-t increases with depth, so ambiguity is avoided in identifying the depth of the sample. Also surfaces of equal sigma-t are of approximately constant potential density and thus identify the paths of isentropic mixing.

As an extension of the method of Richards and Redfield (1955) oxygen sigma-t correlation curves were constructed for Sargasso Sea Water, Antilles Current Water, Continental Edge Water, and Florida Current Water.

The correlation curve for the Sargasso Sea Water was constructed from 372 observations taken at 16 stations, located 25°-30°N and 65°-72°W during the period February-July 1962.

The correlation curve for the Antilles Current Water was constructed from 679 observations taken at 32 stations during the periods February-June 1962 and May 1964. The stations were north of Hispaniola, Puerto Rico, and the American Virgin Islands and south of 24°N. Both series of observations were taken by the U.S.C.&G.S. ship Explorer.

The correlation curve for the Florida Current Water was constructed from 1443 observations at 108 stations taken during the periods July-December 1961, July-December 1962, and January-June 1963. Only stations located in the center of the Florida Straits between Miami, Florida, and Bimini, Bahama Islands, and between Palm Beach, Florida, and Settlement Point, Bahama Islands, were used. The stations were taken aboard research vessels of the Institute of Marine Science of the University of Miami.

No similar sets of control data were available to identify Continental Edge Water. According to Stefansson et al. (1971) Continental Edge Water has a more variable oxygen-density relationship than Yucatan Straits Water. Generally, it also has a higher oxygen concentration for a given sigma-t in the range 24.0-26.0. High oxygen values that did not fit any of the other oxygen-density curves regularly occurred at station 3. According to the T-S curves, this was Continental Edge Water. These values were used to construct the correlation curve.

The oxygen-sigma-t correlation curves are shown as Figure 156. In all cases, the points on the curves were computed arithmetic means of all oxygen values within a 0.25 sigma-t range.

The water layer is quite thin within certain density ranges, and the number of observations in water having these densities is small, ranging from 4 to 50 samples in each 0.25 sigma-t span. In other cases, the water thickness is considerable within the density range, and the number of observations ranges from 100 to 153.

Also shown in Figure 156 is the oxygen sigma-t correlation curve for the Sargasso Sea Water as computed by Richards and Redfield (1955). The two curves for the Sargasso Sea Water agree quite well except near a sigma-t of 26.00 ± 0.25 where they vary by 0.2 ml/l.

Figure 156 indicates that for sigma-t values greater than 24.75, Florida Current Water has a lower oxygen content than Sargasso Sea Water or Antilles Current Water. For a sigma-t between 25.00 and 27.35, Antilles Current Water has a lower oxygen content than does Sargasso Sea Water. Below a sigma-t of 27.35, oxygen values for Antilles Current Water and Sargasso Sea Water are nearly identical. Within the sigma-t range 24.00 to 24.75, the oxygen content of the three water types is very similar. But at sigma-t values less than 24.00, the oxygen values are higher for water that has passed through the Florida straits. At all sigma-t levels, Continental Edge Water exhibited highest oxygen values.

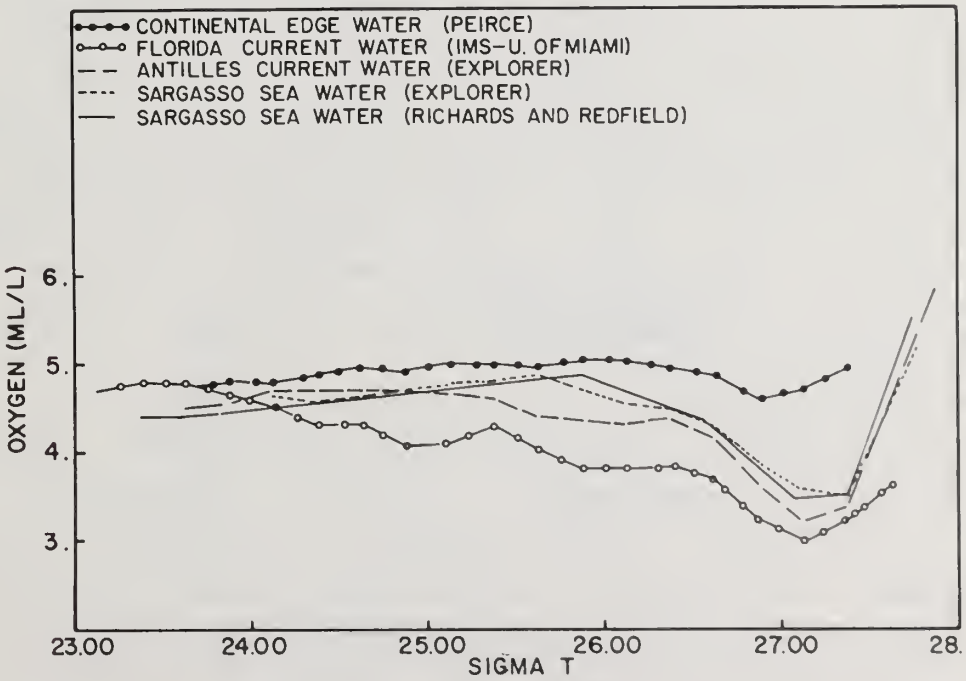

Figure 156. Oxygen-sigma-t correlation curves.

Figure 156 was designed to identify the water type at each data point. From a qualitative view, these oxygen sigma-t correlation curves do not appear to be very reliable between 23.75 and 25.00, but seem fairly reliable at greater depth.

Standard deviations and confidence limits at the 0.95% level of significance were computed for each 0.25 sigma-t group of oxygen values. The results are given in Table 3. Using the means and standard deviations and assuming Gaussian distribution, individual probability of correct identification curves were drawn. The individual values were summed and a mean computed for each water type. The probability of identifying Antilles Current Water correctly for the entire range of sigma-t values is 40%, for Sargasso Sea Water 50%, and for Florida Current Water 70%. Because of its uniqueness, Continental Edge Water was not included in these calculations.

For several reasons, these probability values are lower than the results obtained by actually using the curves to identify the water types. The distribution of the oxygen data does not fit a Gaussian distribution, but rather clusters within about two standard deviations of the mean. Also the lowest probability of correct identification occurs between 24.00 and 25.00, a region of relatively few observations. The probability of correct identification can be raised by assuming that the water type through this region is the same as the water below, which can be identified with a higher degree of reliability. Because of its position of touching only water of much lower oxygen values, Continental Edge Water could be identified with a probability of nearly 100%.

By using Figure 156, all station data were identified as to water source area. The percentage of each water type at each station was then determined. Seasonal means and total means for the entire year's observations of the percentage of each water mass at each station were calculated (Figs. 157-161).

Some identification difficulty was encountered at stations 1 to 5 mainly because information regarding nearshore water was not available. Some degree of uncertainity in identifying water masses does exist. However, the confidence limits presented in Table 3 indicate only a few cases of overlap of confidence limits. Therefore, even though there is some uncertainty in identifying individual observations, the uncertainty is greatly reduced for a mean of values.

Figures 157-161 appear to give a reliable indication of the mean of the percentage of each water mass for the year. A nearshore or coastal water mass exists at stations 1 and 2. Continental Edge Water is found at stations 2, 3, 4, and 5. In general, it extends down to about 100 m in winter and to about 60 m in summer. It is almost non-existent in fall. Florida Current Water predominates at stations 3, 4, 5, and 6 including the core of the Gulf Stream. A small amount of Antilles Current Water and Sargasso Sea Water is found at these stations. Seaward from station 5, the percentage of Florida Current Water decreases. From stations 8 to 16 the percentage varies within a narrow range of 13% to 21%. Strikingly, as elsewhere some Florida Current Water is found over 100 miles to the right of the center of the core. At the

same time, Antilles Current Water and Sargasso Sea Water move towards the core of the Gulf Stream. From station 7 to 16, the amount of Sargasso Sea Water varies from 42% to 58% of the water column. The amount of Antilles Current Water varies between 24% and 39% of the water column.

The seasonal graphs are similar to the yearly mean graph, yet considerable seasonal variation occurs. Continental Edge Water is never recorded seaward of station 5. Yet at station 3 it is 53% of the water column during winter, but only 12% during fall. This is in agreement with Wennekens (1959).

Although Florida Current Water predominates at station 4 and 5 during all seasons of the year, it varies considerably with the season. During summer and fall, it is 90% to 97% of the water column; yet during winter and spring, it is only 48% to 70% of the water column. Sargasso Sea Water is not found in any significant amount at these two stations. Antilles Current Water is found in significant amounts varying between 0 and 21% of the water column. Stations 6 and 7 occupy a transition zone. The amount of Florida Current Water is still significant but decreasing, and the amounts of Sargasso Sea Water and Antilles Current Water are increasing.

Beyond station 7, Sargasso Sea Water predominates. Florida Current Water is usually less than 30% of the water column, and Antilles Current Water was found in highly variable quantities. At times it was the least common of the three water types, yet at other times it was the most common.

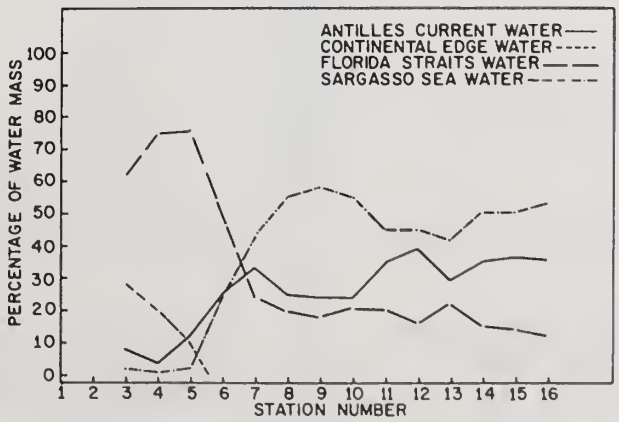

Figure 157. Percentage of each water mass type at each station - total all data.

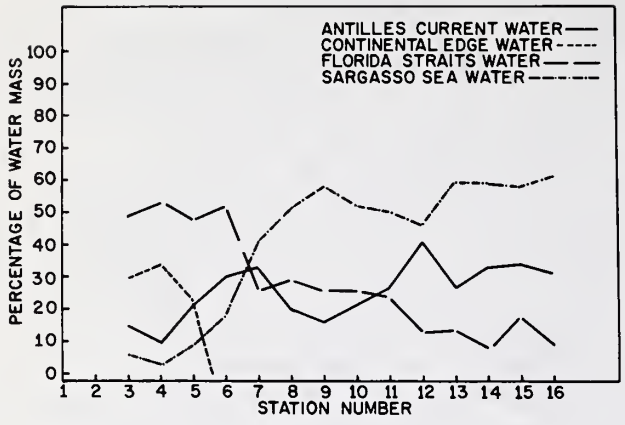

Figure 158. Percentage of each water mass type at each station - spring data.

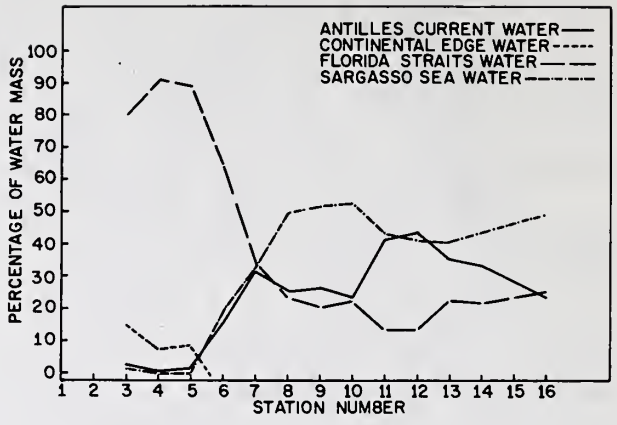

Figure 159. Percentage of each water mass type at each station - summer data.

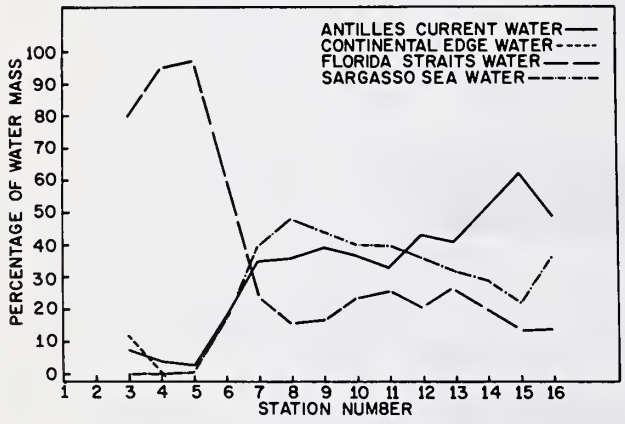

Figure 160. Percentage of each water mass type at each station - fall data.

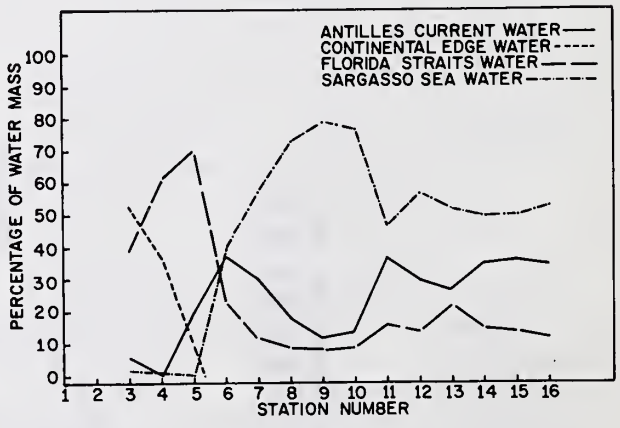

Figure 161. Percentage of each water mass type at each station - winter data.

Table 3. Means, Standard Deviations, and Confidence Limits (95%) For Sigma-t Groups of Oxygen Vaules

Sigma-t Interval	No. of Obs.	Mean Oxygen	Stand. Dev.	Conf. Limits	
		Antilles Current			
23.00-23.25					
23.25-23.50					
23.50-23.75	16	4.51	.11	4.45	4.57
23.75-24.00	43	4.54	.14	4.50	4.58
24.00-24.25	24	4.72	.11	4.67	4.77
24.25-24.50	34	4.70	.18	4.64	4.76
24.50-24.75	54	4.69	.19	4.64	4.74
24.75-25.00	36	4.69	.17	4.63	4.75
25.00-25.25	27	4.65	.16	4.59	4.71
25.25-25.50	28	4.62	.25	4.53	4.71
25.50-25.75	32	4.39	.23	4.31	4.47
25.75-26.00	29	4.34	.23	4.26	4.42
26.00-26.25	41	4.26	.22	4.19	4.33
26.25-26.50	64	4.38	.17	4.34	4.42
26.50-26.75	64	4.13	.22	4.08	4.18
26.75-27.00	69	3.57	.24	3.51	3.63
27.00-27.25	54	3.23	.16	3.19	3.27
27.25-27.50	86	3.34	.25	3.29	3.39
27.50-27.75	124	4.63	.54	4.53	4.73
27.75-28.00	141	5.84	.26	5.80	5.88
		Sargasso Sea			
23.75-24.00	5	4.48	.11	4.39	4.57
24.00-24.25	5	4.65	.11	4.56	4.74
24.25-24.50	4	4.58	. 0	4.58	4.58
24.50-24.75	5	4.64	.11	4.55	4.73
24.75-25.00	11	4.71	.10	4.65	4.77
25.00-25.25	6	4.77	. 0	4.77	4.77
25.25-25.50	46	4.81	.17	4.76	4.86
25.50-25.75	26	4.88	.14	4.83	4.93
25.75-26.00	28	4.72	.27	4.62	4.82
26.00-26.25	22	4.55	.23	4.46	4.64
26.25-26.50	50	4.48	.17	4.43	4.53
26.50-26.75	33	4.30	.20	4.23	4.37
26.75-27.00	23	3.87	.17	3.80	3.94
27.00-27.25	30	3.58	.17	3.52	3.64
27.25-27.50	29	3.49	.22	3.41	3.57
27.50-27.75	40	4.55	.40	4.43	4.67
27.75-28.00	80	5.76	.37	5.65	5.87
		Florida Current			
23.00-23.25	82	4.61	.10	4.59	4.63
23.25-23.50	36	4.73	.17	4.67	4.79
23.50-23.75	47	4.70	.10	4.67	4.73
23.75-24.00	127	4.68	.14	4.66	4.70
24.00-24.25	76	4.66	.20	4.61	4.71
24.25-24.50	105	4.67	.27	4.62	4.72
24.50-24.75	49	4.66	.31	4.57	4.75
24.75-25.00	49	4.47	.39	4.36	4.58
25.00-25.25	48	4.44	.44	4.32	4.56
25.25-25.50	47	4.43	.46	4.28	4.58
25.50-25.75	46	3.91	.48	3.77	4.05
25.75-26.00	47	4.08	.50	3.94	4.22
26.00-26.25	52	3.81	.39	3.67	3.95
26.25-26.50	82	3.84	.38	3.76	3.92
26.50-26.75	81	3.66	.38	3.58	3.74
26.75-27.00	100	3.21	.24	3.16	3.26
27.00-27.25	120	2.99	.18	2.96	3.02
27.25-27.50	153	3.18	.20	3.15	3.21
27.50-27.75	20	3.57	.13	3.51	3.63

It is significant that Antilles Current Water predominates only during the fall. Iselin (1936) noted that during February it was only a very moderate current. However, he concluded that it could be broader and swifter during the summer. Maloney (1967) observed that the Antilles Current exists as a well defined current close to the Bahama bank only during winter. During summer, a broad relatively strong flow exists. Because of travel time delay, the maximum amount of Antilles Current Water would reach this area during the fall.

The highly variable mixing characteristics of the water types are dramatically shown in Figures 162 through 168. These are oxygen sigma-t correlation cross-sections for cruises 1, 12, 14, 19, 21, 22, and 25. Oxygen anomalies were computed by subtracting the oxygen content of Antilles Current Water of the same sigma-t value as given by the correlation curve in Figure 156 from the observed data point.

High positive anomalies are recorded out as far as station 5 down to a depth of 100 m during winter and spring, yet were recorded only at station 1 or not at all during summer and fall. These large positive anomalies fit the definition given by Stefansson et al. (1971) for Continental Edge Water. But these anomalies could also indicate a nearshore water of local origin, because the solubility of oxygen in sea water increases with decreased temperature and salinity.

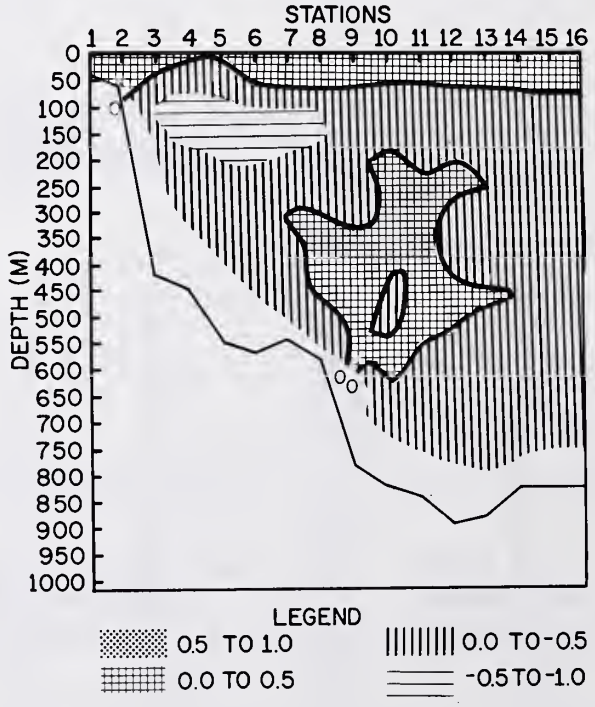

Figure 162. Cruise-1 oxygen anomaly (ml/l) cross-section.

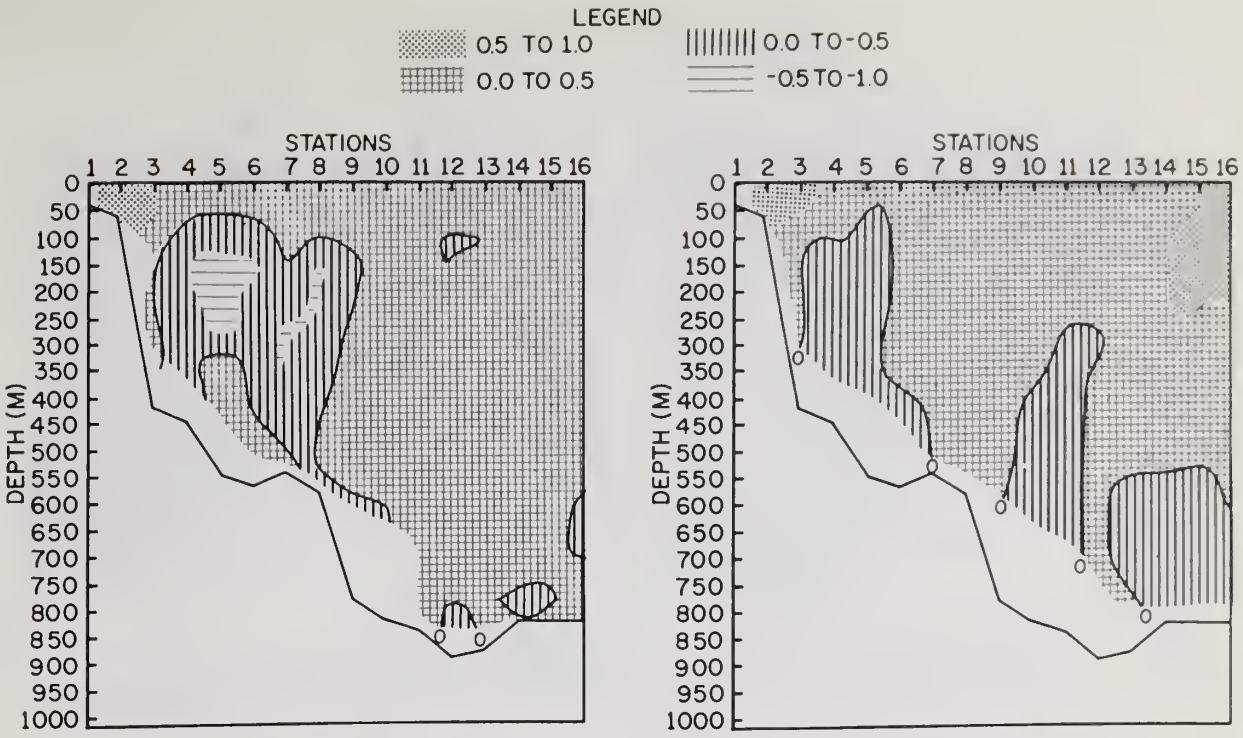

Figure 163. Cruise-12 oxygen anomaly (ml/l) cross-section.

Figure 164. Cruise-14 oxygen anomaly (ml/l) cross-section.

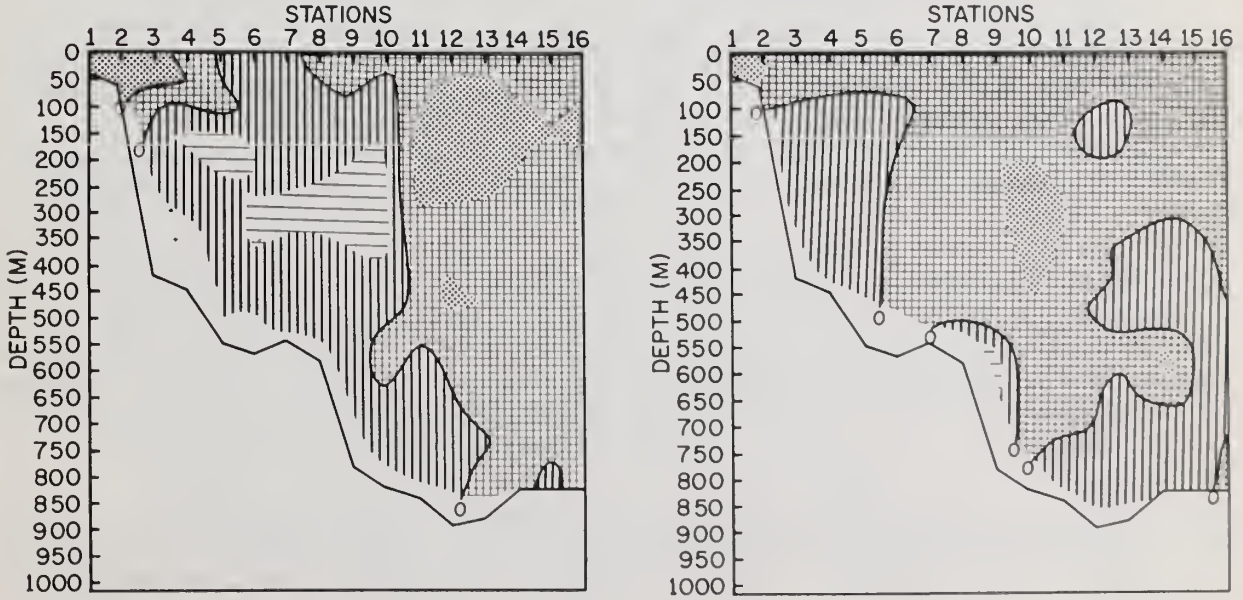

Figure 165. Cruise-19 oxygen anomaly (ml/l) cross-section.

Figure 166. Cruise-21 oxygen anomaly (ml/l) cross-section.

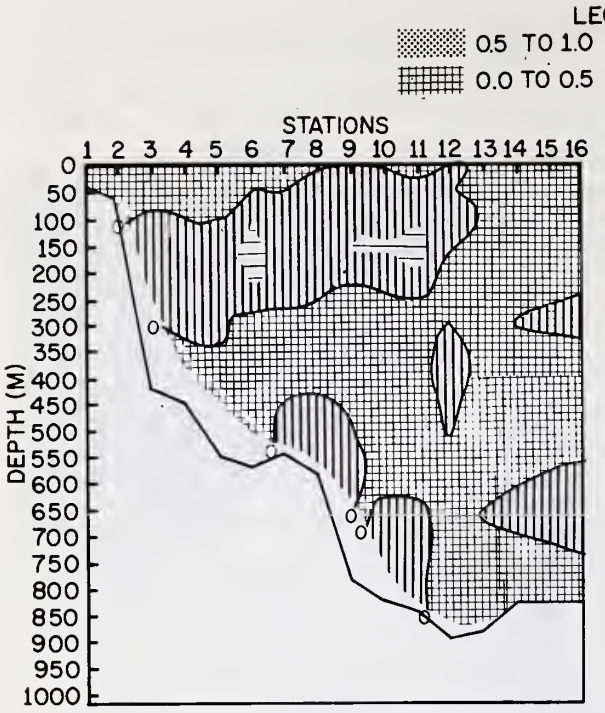

Figure 167. Cruise-22 oxygen anomaly (ml/l) cross-section.

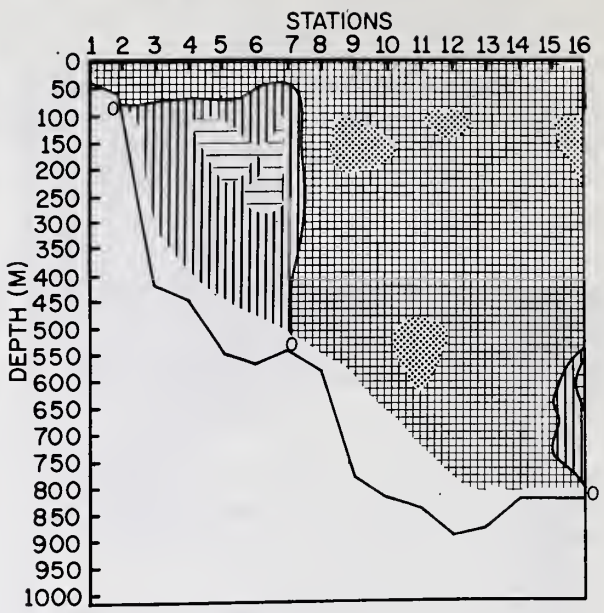

Figure 168. Cruise-25 oxygen anomaly (ml/l) cross-section.

The dramatic variations in water mass movement of the Gulf Stream are very apparent in cruises 14, 19, and 22. Large areas of negative anomalies, indicative of Florida Current Water, spread out from stations 3 to 12 during cruise 22 overriding positive anomaly water. During cruise 19, negative anomalies occur from the surface to the bottom out to station 10. On the other hand, during cruise 14, only a small area of negative anomalies occurs at station 5, the core of the Gulf Stream.

Generally, no clear cut wall of water types exist between the Florida Current Water on the left side and Antilles Current Water and Sargasso Sea Water on the right. Cross current mixing to a varying degree appeared to be the usual situation. However, during cruises 19 and 25, Florida Current Water appeared to be intact on the right side as if a vertical wall existed. Apparently Florida Current Water existed against Sargasso Sea Water and almost no mixing occurred. Only a small amount of Antilles Current Water existed near the surface and below 500 m.

9. ACKNOWLEDGMENTS

Only with the assistance of many people could this paper have been possible. I particularly wish to acknowledge the contributions of Robert B. Starr of NOAA/AOML who provided considerable guidance. David Tyler of the U.S.C&G.S., as Chief Scientist aboard the U.S.C&G.S. ship Peirce, assured consistent high quality field data. Finally, I wish to thank the officers and crew of the U.S.C&G.S. ship Peirce for the long and diligent hours they devoted to collecting the data.

10. REFERENCES

Bryson, R. A. and F. K. Hare, (1974), *Climates of North America, Vol. II of World Survey of Climatology,* Elsevier, New York, 420 p.

Bumpus, Dean F. (1955), The circulation over the continental shelf south of Cape Hatteras. *Transactions, AGU 26,* 601-611.

Defant, A. (1936), Die Troposphare des Atlantischen Ozeans. Idern, 6, I. Teil Schichtung und Zirkulation des Atlantischen Ozeans, 289-411.

Dietrich, Gunter (1937), Die Lage des Meeresoberflache im Druckfeld von Ozean und Atmosphare mit besonderer Berucksichtigung des westlichen Nordatlantischen Ozeans und des Golfs von Mexico. Veroffentlichungen des Instituts fur Meereskunde an der Universitat Berlin, Neue Folge, A, *Geogr.-Naturwiss, Heft 33,* 52 p.

Duing, Walter (1973), Some evidence for long period barotropic waves in the Florida Current. *J. of Physical Oceanography, 3,* 343-346.

Hansen, Donald V. (1970), Gulf Stream meanders between Cape Hatteras and the Grand Banks. *Deep Sea Res. 17,* 495-511.

Helland-Hansen, B. (1918), Nogen hydrografiske metoder. Forhandlinger ved de skandinaviske naturforskerer 16 de mote i. Kristiania 10-15 Juli 1916, Oslo.

Iselin, C. O'D. (1936), A study of the circulation of the western North Atlantic. Papers in Physical Oceanography and Meteorology, MIT and WHOI, 4(4), 101 p.

Iselin, C. O'D. (1940), Preliminary Report on Long-Period Variations in the Transport of the Gulf Stream System. Papers in Physical Oceanography and Meteorology, MIT and WHOI, 8(1), 39 p.

Jacobsen, J. P. (1929), Contribution to the Hydrography of the North Atlantic. Dana Exp. 1921-1922, Oceanographical reports 1(3) Copenhagen, 98 p.

Maloney, William E. (1967), A study of the Antilles Current using Moored Current Meter Arrays, TR-199, U.S. Naval Oceanographic Office, Washington, D. C., 142 p.

Montgomery, R. B. (1938), Fluctuations in Monthly Sea Level On Eastern U.S. Coast as Related to Dynamics of Western North Atlantic Ocean. *J. of Marine Research, 1,* 165-185.

Nowlin, W. D. Jr. (1971), Water Masses and General Circulation of the Gulf of Mexico, *Oceanology,* 28-33.

Parr, A. E. (1935), Report on hydrographic observations in the Gulf of Mexico and the adjacent straits made during the Yale Oceanographic Expedition on the "Mable Taylor" in 1932. *Bull. Bingham Oceanographic Coll., V*(I), 93 p.

Richards, F. A. and A. C. Redfield (1955), Oxygen-density relationships in the western North Atlantic. *Deep-Sea Res., 2,* 182-189.

Richardson, W. A. and J. R. Finlen, 1967, The transport of Northwest Providence Channel. *Deep Sea Res., 14,* 361-367.

Rossby, Carl-Gustaf (1936), Dynamics of steady ocean currents in the light of experimental fluid mechanics. *Papers in Physical Oceanogr. & Meteor., 5*(1), 43 p.

Schmitz, William J. and William S. Richardson (1968), On the transport of the Florida Current. *Deep Sea Res., 15,* 679-693.

Starr, Robert B. (1970), An Oceanographic Investigation Adjacent to Cay Sal Bank, Bahama Islands, ESSA Technical Report ERL 167-AOML 2, Washington, D. C. 52 p.

Stefansson, U., L. P. Atkinson, and D. F. Bumpus, (1971), Hydrographic properties and circulation of the North Carolina Shelf and Slope Waters. *Deep Sea Res., 18,* 383-420.

Stommel, Henry (1965), *The Gulf Stream, A Physical and Dynamical Description.* 2nd Ed., U. of Calif. Press, 248 p.

Sverdrup, H. U., M. W. Johnson, and R. H. Fleming (1946), *The Oceans, Their Physics, Chemistry, and General Biology.* Prentice Hall, Englewood Cliffs, N. J. 1087 p.

U. S. Navy Hydrographic Office (1951), Processing Oceanographic Data. By E. C. Lafond, H. O. Pub. No. 614, Washington, D.C. 114 p.

U. S. Navy Hydrographic Office (1955), Instruction Manual for Oceanographic Observations, Second Edition, H. O. Pub. No. 607, Washington, D. C., 210 p.

Von Arx, William S. (1962), *Introduction to Physical Oceanography.* Addison-Wesley, Reading, Mass. 422 p.

Weiss, R. F., (1970), The solubility of Nitrogen, Oxygen, and Argon in Water and Seawater. *Deep Sea Res., 17,* 721-735 p.

Wennekens, M. P., (1959), Water mass properties of the Straits of Florida and related waters. *Bulletin of Marine Science of the Gulf and Caribbean, 9,* 52 p.

Worthington, L. V. (1959), The 18° water in the Sargasso Sea. *Deep Sea Resc., 5,* 297-305.

Wright, W. R., and L. V. Worthington (1970), *The Water Masses of the North Atlantic Ocean, A volumetric census of temperature and salinity,* Serial Atlas of the Marine Environment, Folio 19. American Geographical Society, 5 p.

Wunsch, C., D. V. Hansen, and B. D. Zetler (1969), Fluctuations of the Florida Current inferred from sea-level records. *Deep Sea Resc, 16,* Suppl., 447-470.

Wust, Georg, (1964), *Stratification and Circulation in the Antillean-Caribbean Basins, Part One, Spreading and Mixing of the Water Types, with an Oceanographic Atlas,* Columbia University Press, New York, N. Y. 201 p.

Wust, Georg (1924), Florida und Antillenstrom, eine hydrodynamische Untersuchung. Veroff. Inst. f. Meereskunde. Berlin, N.F.A.: *Geogr.-Naturwiss, Heft 12,* 48 p.

☆ U.S. Government Printing Office: 1977-777-045/1228 Region 8

Environmental Research LABORATORIES

The mission of the Environmental Research Laboratories (ERL) is to conduct an integrated program of fundamental research, related technology development, and services to improve understanding and prediction of the geophysical environment comprising the oceans and inland waters, the lower and upper atmosphere, the space environment, and the Earth. The following participate in the ERL missions:

MESA *Marine EcoSystems Analysis Program.* Plans, directs, and coordinates the regional projects of NOAA and other federal agencies to assess the effect of ocean dumping, municipal and industrial waste discharge, deep ocean mining, and similar activities on marine ecosystems

OCSEA *Outer Continental Shelf Environmental Assessment Program* Plans, directs, and coordinates research of federal, state, and private institutions to assess the primary environmental impact of developing petroleum and other energy resources along the outer continental shelf of the United States

WM *Weather Modification Program Office.* Plans, directs, and coordinates research within ERL relating to precipitation enhancement and mitigation of severe storms. Its National Hurricane and Experimental Meteorology Laboratory (NHEML) studies hurricane and tropical cumulus systems to experiment with methods for their beneficial modification and to develop techniques for better forecasting of tropical weather. The Research Facilities Center (RFC) maintains and operates aircraft and aircraft instrumentation for research programs of ERL and other government agencies.

AOML *Atlantic Oceanographic and Meteorological Laboratories.* Studies the physical, chemical, and geological characteristics and processes of the ocean waters, the sea floor, and the atmosphere above the ocean

PMEL *Pacific Marine Environmental Laboratory* Monitors and predicts the physical and biological effects of man's activities on Pacific Coast estuarine, coastal, deep-ocean, and near-shore marine environments

GLERL *Great Lakes Environmental Research Laboratory* Studies hydrology, waves, currents, lake levels, biological and chemical processes, and lake-air interaction in the Great Lakes and their watersheds; forecasts lake ice conditions

GFDL *Geophysical Fluid Dynamics Laboratory* Studies the dynamics of geophysical fluid systems (the atmosphere, the hydrosphere, and the cryosphere) through theoretical analysis and numerical simulation using powerful high-speed digital computers

APCL *Atmospheric Physics and Chemistry Laboratory* Studies cloud and precipitation physics, chemical and particulate composition of the atmosphere, atmospheric electricity, and atmospheric heat transfer, with focus on developing methods of beneficial weather modification

NSSL *National Severe Storms Laboratory* Studies severe-storm circulation and dynamics, and develops techniques to detect and predict tornadoes, thunderstorms, and squall lines

WPL *Wave Propagation Laboratory* Studies the propagation of sound waves and electromagnetic waves at millimeter, infrared, and optical frequencies to develop new methods for remote measuring of the geophysical environment

ARL *Air Resources Laboratories* Studies the diffusion, transport, and dissipation of atmospheric pollutants, develops methods of predicting and controlling atmospheric pollution, monitors the global physical environment to detect climatic change

AL *Aeronomy Laboratory* Studies the physical and chemical processes of the stratosphere, ionosphere, and exosphere of the Earth and other planets, and their effect on high-altitude meteorological phenomena

SEL *Space Environment Laboratory* Studies solar-terrestrial physics (interplanetary, magnetospheric, and ionospheric); develops techniques for forecasting solar disturbances; provides real-time monitoring and forecasting of the space environment

U.S. DEPARTMENT OF COMMERCE
National Oceanic and Atmospheric Administration
BOULDER, COLORADO 80302